

## Chapter 3

### Synthesis and Polymerization Behavior of Asymmetric Group 4 Post-Metallocene Catalysts

*Adapted in part from:*

Klet, R. C.; VanderVelde, D. G.; Labinger, J. A.; Bercaw, J. E. *Chem. Commun.*, **2012**, 48, 6657–6659.

<http://dx.doi.org/10.1039/c2cc32806b>

© The Royal Society of Chemistry 2012

## Chapter 3

### Introduction

Polyolefins constitute one of the most important classes of commercial synthetic polymers, with annual worldwide capacity greater than 70 billion kg.<sup>1</sup> Since the discovery of Ziegler-Natta catalysts in the 1950s,<sup>2</sup>  $\alpha$ -olefin polymerization has been one of the most widely studied catalytic organometallic reactions. The past three decades have seen the development of soluble single-site olefin polymerization catalysts that span the transition metal series and allow access to previously unrealized polymer architectures.<sup>3</sup> The development of metallocene catalysts in the 1980s led to significant advances in our understanding of how catalyst structure affects the polymer microstructure.<sup>4</sup> Groundbreaking studies by Brintzinger, Bercaw and others revealed a direct correlation between metallocene catalyst symmetry and polymer tacticity; in general,  $C_2$ - and  $C_1$ -symmetric complexes produce isotactic polymers,  $C_s$ -symmetric catalysts lead to syndiotactic polymers, and  $C_{2v}$ -symmetric catalysts yield stereoirregular polymers.<sup>4</sup> More recently, “post-metallocene” olefin polymerization catalysts have emerged and have led to significant innovations in living polymerization<sup>5</sup> and the preparation of olefin block copolymers.<sup>6</sup> Our ability to develop new catalysts that produce specific polymer architectures will rely on continuing research efforts to understand and progress post-metallocene polymerization catalysts.

Our group has recently developed olefin polymerization catalysts based on early transition metals supported by symmetric, triaryl, dianionic (XLX) ligands as part of a program for developing new post-metallocene catalysts for olefin polymerization. The ligand design includes thermally robust aryl–aryl linkages, as well as versatile access to a wide variety of ligand scaffolds using cross-coupling chemistry. Additionally, these ligands can adopt various geometries when coordinated to a metal, including  $C_2$  and  $C_{2v}$ , which suggested the possibility of stereoselective polymerization, based on precedents with metallocene polymerization catalysts (Figure 3.1).

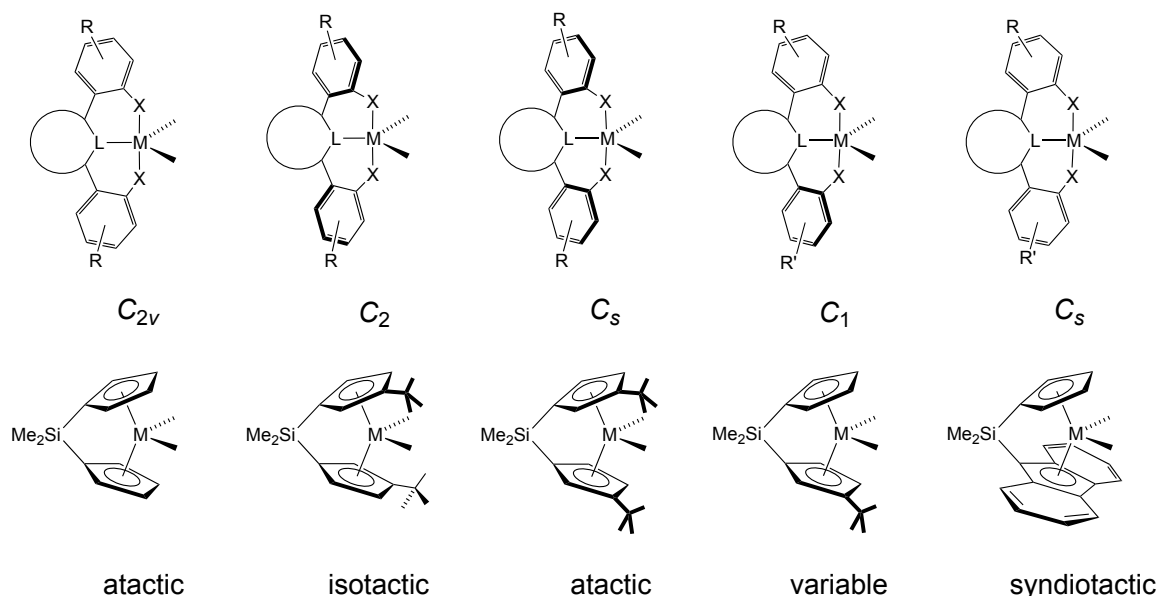
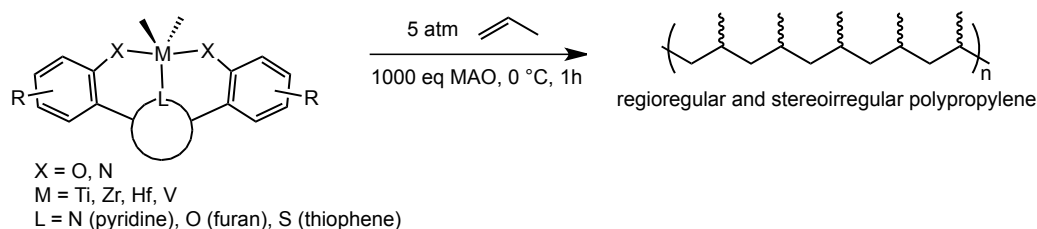


**Figure 3.1** Comparison of potential geometries of metal complexes with triaryl dianionic ligands and metallocene catalysts and polymer tacticity.

We have reported a series of heterocycle-linked bis(phenolate) ligands, where the heterocycle is pyridine (ONO), furan (OOO), or thiophene (OSO), which upon complexation with titanium, zirconium, hafnium, and vanadium can give propylene polymerization precatalysts that exhibit good to excellent activities

upon activation with methylaluminoxane (MAO).<sup>7</sup> (We have also reported bis(anilide)pyridyl ligands (NNN),<sup>8</sup> but their group 4 metal complexes exhibit poor activity for polymerization.) Despite the promising polymerization activity of these catalysts, we have thus far observed disappointing stereocontrol; we have generally produced stereoirregular polypropylene (Scheme 3.1).



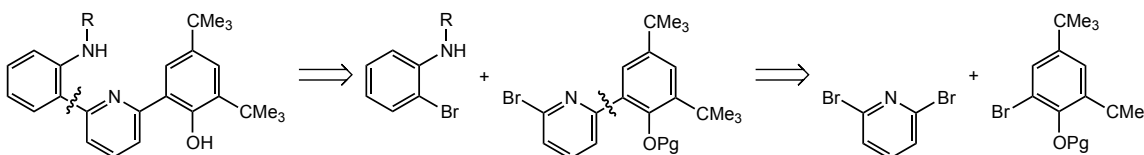
**Scheme 3.1** Propylene polymerization with post-metallocene complexes of triaryl dianionic ligands.

## Results and Discussion

### *NNO Ligand: Design and Synthesis*

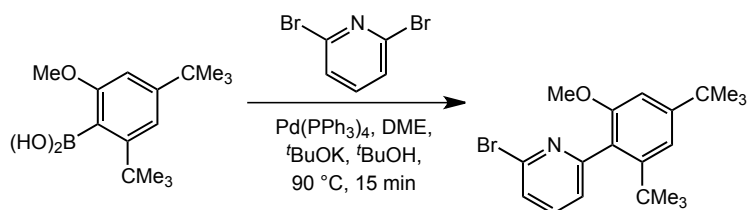
In order to further our understanding of the fundamental processes governing stereocontrol in these post-metallocene complexes, we decided to examine the effect of an asymmetric ligand. As a first target, we designed an anilide(pyridine)phenoxide (NNO) ligand. The modular design of the NNO ligand allows for facile variation of substituents using cross-coupling reactions, including access to enantiopure catalysts (which can be difficult to access with metallocene frameworks) for potential asymmetric applications by incorporation of a chiral group into the ligand. For our first asymmetric NNO ligand, we selected a ligand containing a chiral (1-phenylethyl)amine group.

The synthesis of the ligand was envisioned through a series of cross coupling reactions (Scheme 3.2). We planned for a common intermediate (pyridine-phenoxide) in the ligand design that we could couple with different anilines to give access to various frameworks through systematic changes.



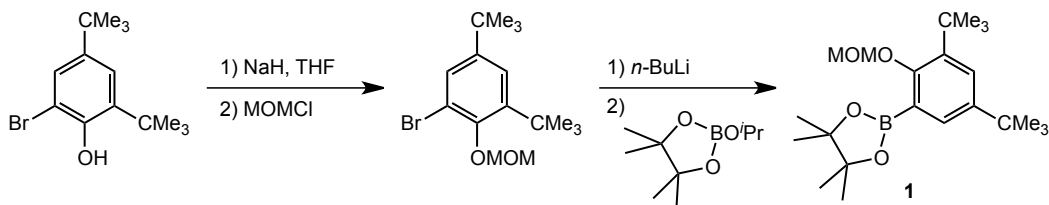
**Scheme 3.2** Retrosynthetic scheme for anilide(pyridine)phenoxide ligands.

The first obstacle in our synthesis was to find a methodology for selective monoarylation of 2,6-dibromopyridine. Although the asymmetrically substituted 2-bromo-6-iodopyridine is commercially available, it is prohibitively expensive, especially compared to 2,6-dibromopyridine: Alfa Aesar lists 2-bromo-6-iodopyridine at \$544/5g (~\$109/1g),<sup>9</sup> while 2,6-dibromopyridine is \$50/25g (\$2/1g).<sup>10</sup> 2-bromo-6-chloropyridine, a less desirable substrate for cross coupling, is even more costly: \$278/1g.<sup>11</sup> The synthesis of 2-bromo-6-iodopyridine is also non trivial, with most reported syntheses suffering from low yield and poor regioselectivity.<sup>12</sup> We were encouraged, however, by a report from Chan and co-workers that described monoarylation of 2,6-dibromopyridine with a protected phenol substrate using a Suzuki coupling (Scheme 3.3).<sup>13</sup> Based on this report, we predicted that conditions to achieve monoarylation of 2,6-dibromopyridine with our substrate could be discovered.



**Scheme 3.3** Literature precedent for monoarylation of 2,6-dibromopyridine using a Suzuki coupling. (Adapted from ref. 14).

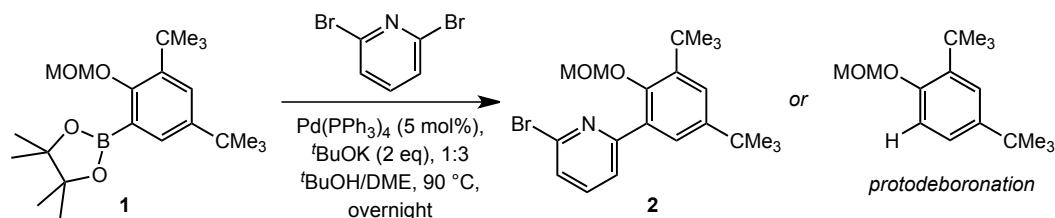
As a first step, we needed to synthesize the boronic ester coupling partner of 2,6-dibromopyridine: (3,5-di-*t*-butyl-2-(methoxymethoxy)phenyl)pinacolborane. Deprotonation of commercially available 2-bromo-4,6-di-*t*-butylphenol with NaH, followed by treatment with chloromethyl methyl ether (MOMCl) led to the MOM-protected bromo-phenol intermediate.<sup>14</sup> Lithium halogen exchange of this intermediate with *n*-butyl lithium, followed by reaction with 2-isopropoxy-4,4,5,5-tetramethyl-1,3,2-dioxaborolane yielded the desired boronic ester **1** in good yield after recrystallization from hot methanol (Scheme 3.4).



**Scheme 3.4** Synthesis of boronic ester **1**.

Initial small-scale reactions of **1** with 2,6-dibromopyridine following the Suzuki coupling reaction conditions employed by Chan et al. (cat.: 5 mol % Pd(PPh<sub>3</sub>)<sub>4</sub>, base: 2 equiv KO<sup>*t*</sup>Bu, solvent: DME/<sup>*t*</sup>BuOH 3:1; DME = dimethoxymethane)<sup>13</sup> yielded the desired monoarylated pyridine intermediate **2** in acceptable yields. Repeated reactions and attempts to scale the coupling reaction up, however, revealed very inconsistent and unpredictable yields, with

some reactions resulting in exclusive formation of the protodeboronated product of the boronic ester **1** and no pyridine-phenoxide coupled product **2** (Scheme 3.5).



**Scheme 3.5** Suzuki coupling **1** and 2,6-dibromopyridine led to inconsistent product formation with complete conversion of **1** to the protodeboronated product without any formation of **2** occurring in many instances.

Despite careful investigation of each component of the reaction, we were ultimately unable to determine what led to protodeboronation over C–C bond formation (Table 3.1). One potential culprit could be the solvent DME, as DME is prone to develop peroxides over time, which could react unfavorably with the Pd(0) catalyst; however, we still observed significant protodeboronation when using a brand new bottle of DME, DME passed through alumina prior to use (to remove peroxide impurities), and DME collected from drying columns and kept 100% air-free. We also considered that water or protic solvents, although commonly employed in Suzuki reactions, could facilitate protodeboronation. Ultimately, after screening many reaction conditions, we found that non-aqueous conditions with Pd(PPh<sub>3</sub>)<sub>4</sub>, K<sub>3</sub>PO<sub>4</sub>, and toluene gave consistent yields for the coupled product **2** with no protodeboronated product observed to form in the reaction (Table 3.1). The bis-arylated pyridine product **3** was observed to form in small quantities under these reaction conditions; however, it could mostly be separated from the monoarylated product **2** via column chromatography.

Alternatively, we later discovered that this minor impurity could be carried on and easily separated in later synthetic steps without affecting product yields. Finally, achieving monoarylation under our optimized conditions requires long reaction times of nearly 7 d; employing a more efficient catalyst, such as Pd<sub>2</sub>(dba)<sub>3</sub>/SPhos (dba = dibenzylideneacetone, SPhos = 2-dicyclohexylphosphino-2',6'-dimethoxybiphenyl), results in faster reaction times, but exclusive formation of the bis-arylated product **3** without formation of any monoarylated product **2**.

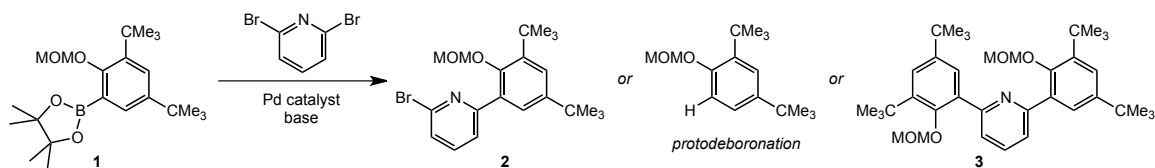
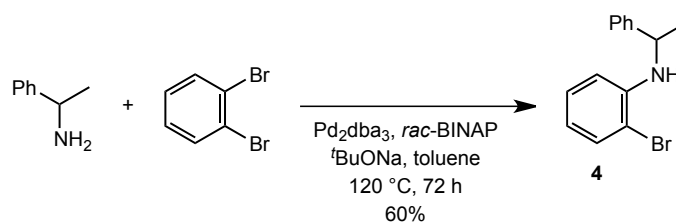


**Table 3.1** Conditions screened for Suzuki coupling to achieve monoarylation of 2,6-dibromopyridine.

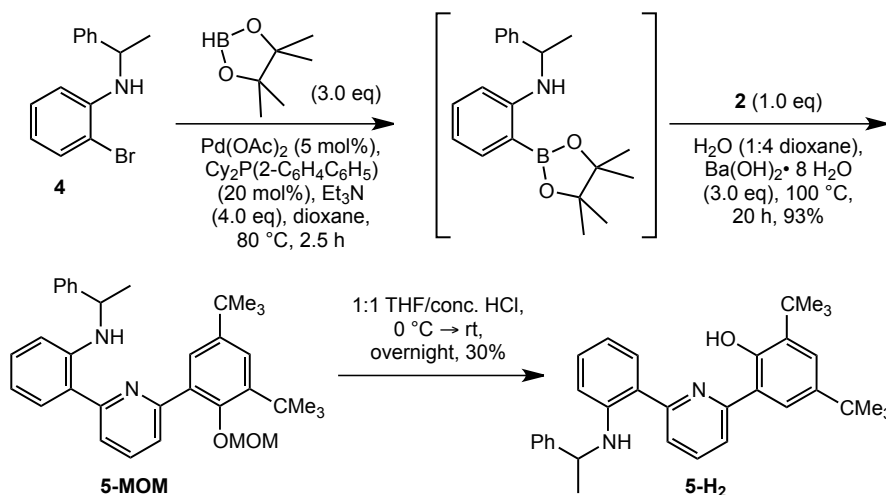
Catalyst	Base	Solvent	% Yield of 2	% Yield of proto-deboronated	% Yield of 3	Scale	Comments
Pd(PPh <sub>3</sub> ) <sub>4</sub>	KO <sup>t</sup> Bu	DME/BuOH (3:1)	57	43	0	0.500 g	
Pd(PPh <sub>3</sub> ) <sub>4</sub>	KO <sup>t</sup> Bu	DME/BuOH (3:1)	0	100	0	1.5 g	
Pd(PPh <sub>3</sub> ) <sub>4</sub>	KO <sup>t</sup> Bu	DME/BuOH (3:1)	0	100	0	100 mg	
Pd(PPh <sub>3</sub> ) <sub>4</sub>	KO <sup>t</sup> Bu	DME/BuOH (3:1)	40	13	47	100 mg	DME through alumina to remove peroxides
Pd(PPh <sub>3</sub> ) <sub>4</sub>	KO <sup>t</sup> Bu	DME/BuOH (3:1)	0	100	0	2 g	DME through alumina to remove peroxides
Pd(PPh <sub>3</sub> ) <sub>4</sub>	KO <sup>t</sup> Bu	DME/BuOH (3:1)	0	100	0	200 mg	DME from columns
Pd(PPh <sub>3</sub> ) <sub>4</sub>	KO <sup>t</sup> Bu	dioxane/BuOH (3:1)	69	6	25	50 mg	Dioxane dried over mol sieves
Pd(PPh <sub>3</sub> ) <sub>4</sub>	KO <sup>t</sup> Bu	dioxane/BuOH (3:1)	0	100	0	250 mg	
Pd(PPh <sub>3</sub> ) <sub>4</sub>	KO <sup>t</sup> Bu	toluene/BuOH (3:1)	68	21	11	50 mg	Toluene from columns
Pd(PPh <sub>3</sub> ) <sub>4</sub>	KO <sup>t</sup> Bu	toluene/BuOH (3:1)	0	100	0	250 mg	
Pd(OAc) <sub>2</sub> /SPhos	K <sub>3</sub> PO <sub>4</sub>	toluene	0	69	31	50 mg	SPhos added
Pd <sub>2</sub> (dba) <sub>3</sub> /SPhos	K <sub>3</sub> PO <sub>4</sub>	toluene	0	0	100	50 mg	
Pd(PPh <sub>3</sub> ) <sub>4</sub>	K <sub>3</sub> PO <sub>4</sub>	toluene	84	0	16	50 mg	Very slow (5 d v. overnight)

Synthesis of the anilide portion of the ligand was significantly more straightforward than monoarylation of 2,6-dibromopyridine. Chiral 2-bromo-N-(1-phenylethyl)aniline **4** was prepared according to a reported synthesis utilizing a Buchwald-Hartwig coupling (Scheme 3.6).<sup>15</sup> **4** was then coupled to **2** with a Suzuki coupling using a modified literature procedure reported for coupling pyridines and anilines.<sup>16</sup> Finally, deprotection with acidic THF afforded the

desired asymmetric NNO ligand **5** (Scheme 3.7).



**Scheme 3.6** Buchwald-Hartwig coupling to yield 2-bromo-N-(1-phenylethyl)aniline **4**.

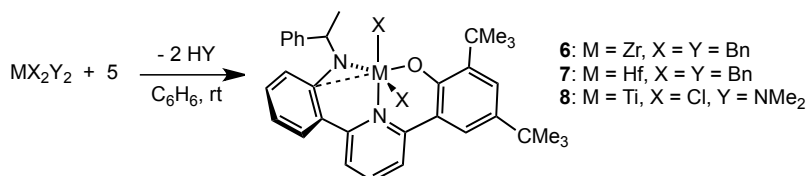


**Scheme 3.7** Synthesis of ligand **5** from coupling **4** and **2**.

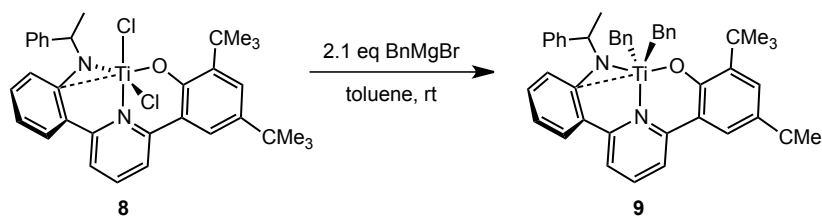
### NNO Ligand: Metalation

Metalation of NNO ligand **5** was achieved by protonolysis of suitable group **4** starting materials. Reaction of **5** with tetrabenzylzirconium and tetrabenzylhafnium gave (NNO)ZrBn<sub>2</sub> **6** and (NNO)HfBn<sub>2</sub> **7**, respectively. The analogous reaction of **5** with tetrabenzyltitanium led to an inseparable mixture; however, reaction of **2** with TiCl<sub>2</sub>(NMe<sub>2</sub>)<sub>2</sub> yielded a related titanium complex, (NNO)TiCl<sub>2</sub> **8** (Scheme 3.8). **8** could be converted into (NNO)TiBn<sub>2</sub> **9** by treating **8** with 2.1 equiv of BnMgCl; however, we found that working with (NNO)TiCl<sub>2</sub> was sufficient

for our purposes, and, in fact, easier to purify compared to the highly soluble dibenzyl species (Scheme 3.9).



**Scheme 3.8** Synthesis of anilide(pyridine)phenoxide Zr, Hf, and Ti complexes.



**Scheme 3.9** Synthesis of (NNO)TiBn<sub>2</sub> complex **9** from (NNO)TiCl<sub>2</sub> complex **8**.

The <sup>1</sup>H NMR spectrum of the Ti complex **8** gives sharp signals at room temperature; in contrast, the resonances of the Zr complex **6** are broad at room temperature, suggestive of fluxional behavior on the NMR time scale. Upon lowering the temperature to –30 °C, the resonances for **6** were observed to sharpen and give the expected number of peaks for the complex **6** (Figure 3.2). As expected, increasing the temperature above room temperature led to further broadening of the resonances for **6**. Surprisingly, the benzylic protons (4 doublets integrating to 1H each for the C<sub>1</sub> symmetric complex **6**) broadened at different rates; in particular, one benzylic proton remained a sharp doublet, while the three other benzylic protons broadened. This behavior is especially unexpected for protons on the same carbon, which would be predicted to have the same temperature dependent fluxionality. Additionally, the temperature dependence of the chemical shifts of the two sets of benzylic protons is different, with the more

downfield set of benzylic protons shifting approximately 0.5 ppm over a 130 degree temperature range, while the more upfield protons shift only about 0.25 ppm over the same temperature range (Figure 3.3). Unfortunately, we do not have a good explanation for this observed fluxionality at this time, but notably, a large temperature dependence on Zr benzylic protons has been observed previously.<sup>17</sup>

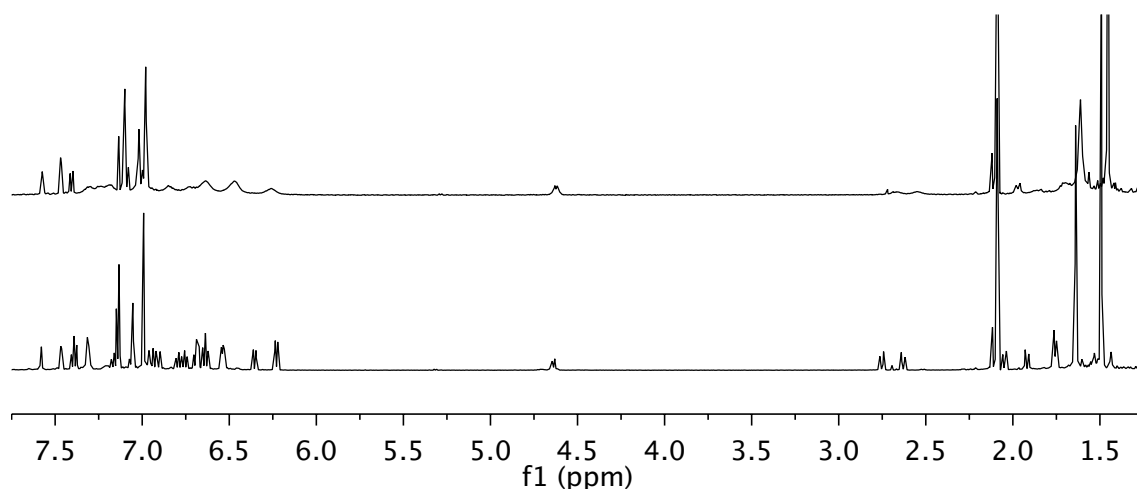


**Figure 3.2**  $^1\text{H}$  NMR spectra of **6** at 25 °C (top) and -30 °C (bottom) in toluene- $d_8$ .

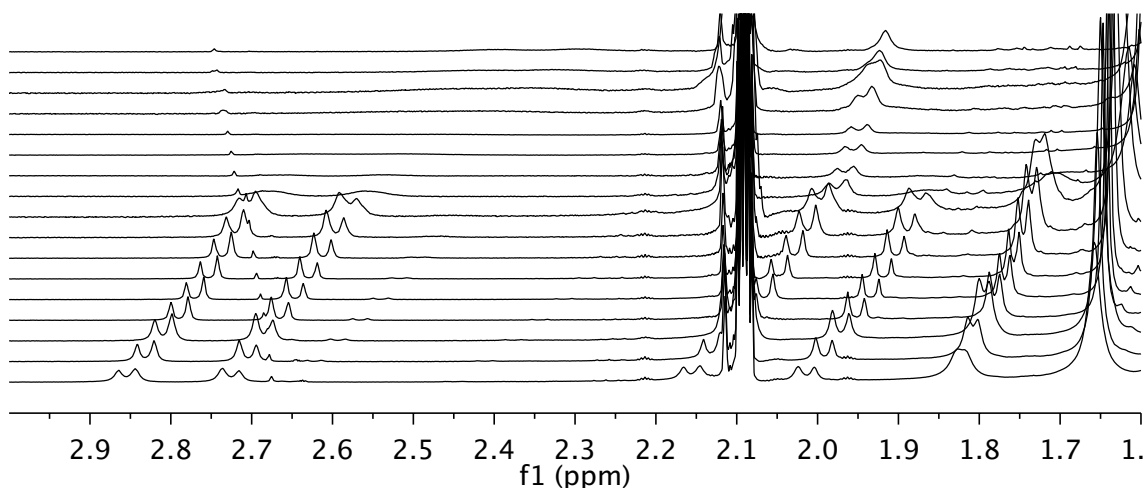


**Figure 3.3** Close-up of Zr-benzylic proton resonances of **6** in  $^1\text{H}$  NMR spectra from -80 °C to 90 °C in toluene- $d_8$  (temperature increases up y-axis).

Crystals of **8** suitable for X-ray diffraction were grown by slow vapor diffusion of pentane into a concentrated ether/dichloromethane solution; the X-ray structure reveals distorted trigonal bipyramidal geometry about titanium (Fig 3.4). The bond lengths and angles for **8** are similar to other five-coordinate Ti(IV) complexes.<sup>7a,18</sup> Notably, the Ti(1)–C(1)<sub>ipso</sub> distance is quite contracted at 2.61 Å, with a Ti(1)–N(1)–C(1)<sub>ipso</sub> angle of 104.05°, suggestive of an *ipso* interaction, which may help stabilize the highly electrophilic Ti center. We have observed a similar *ipso* interaction in a related anilide-containing metal complex (NNN)TiCl<sub>2</sub>.<sup>8</sup>

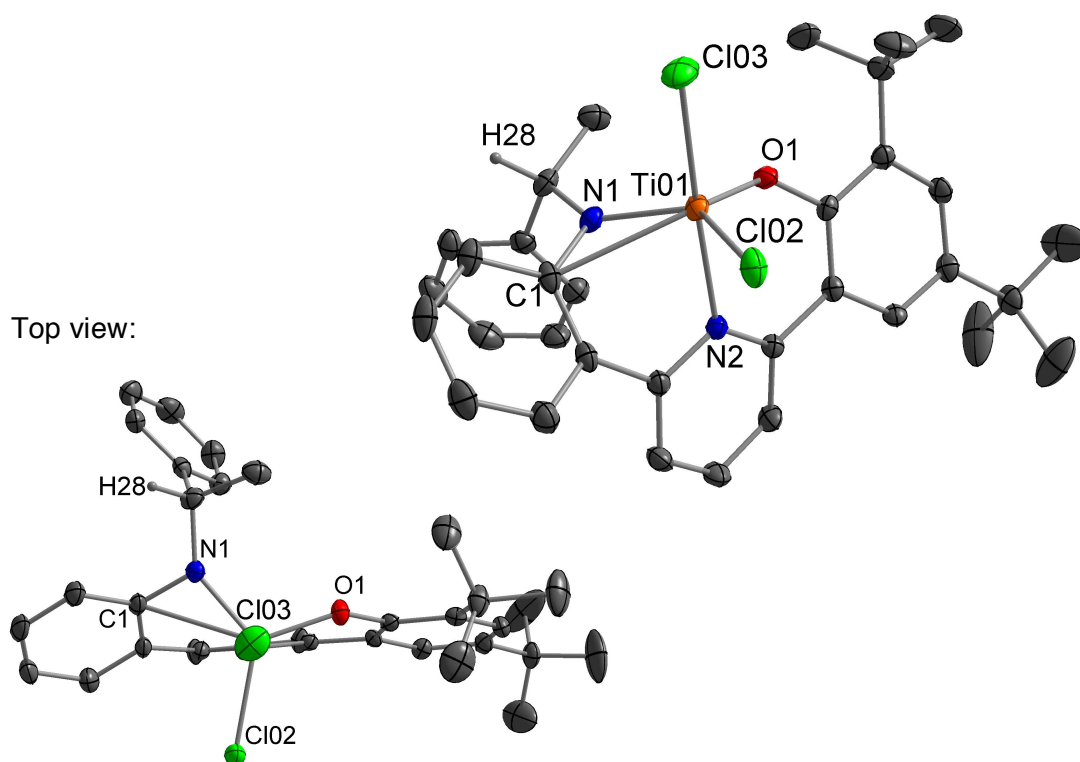
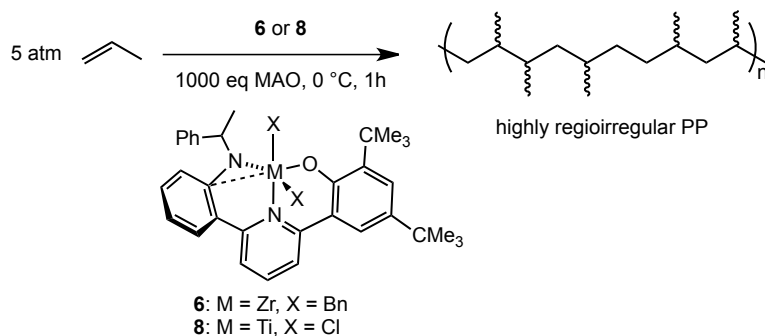


**Figure 3.4** Probability ellipsoid diagram (50%) of the X-ray structure **8**. Selected bond lengths (Å) and angles (°): Ti(1)–O(1) = 1.8040(17), Ti(1)–N(1) = 1.879(2), Ti(1)–N(2) = 2.153(2), Ti(1)–Cl(2) = 2.3161(8), Ti(1)–Cl(3) = 2.3285(8), Ti(1)–C(1) = 2.609(2); O(1)–Ti(1)–N(1) = 110.87(8), O(1)–Ti(1)–Cl(2) = 118.49(6), N(1)–Ti(1)–Cl(2) = 127.68(7), Cl(3)–Ti(1)–N(2) = 175.84(6), C(1)–N(1)–Ti(1) = 104.05(15).

### *NNO Complexes: Polymerization Behavior*

Activation of complexes **6** and **8** in toluene or chlorobenzene solution, respectively, resulted in formation of polypropylene (PP) under 5 atm propylene at 0 °C (Scheme 3.10). Somewhat surprisingly, the Hf analogue **7** showed no activity under these conditions; Hf is the most active group 4 metal for some types of post-metallocene catalysts.<sup>19</sup> The PP obtained from both **6** and **8** was a solid, nonsticky, elastomeric polymer.



**Scheme 3.10** Polymerization of propylene with complex **6** or **8**.

The activity of **6** was  $1.7 \times 10^4$  g PP (mol cat)<sup>-1</sup> h<sup>-1</sup>, while the Ti complex **8** was approximately an order of magnitude more active, at  $1.5 \times 10^5$  g PP (mol cat)<sup>-1</sup> h<sup>-1</sup>. The activity of **8** remains the same after 3 h as after 30 min at 0 °C, suggesting that the active species is relatively stable under polymerization conditions.

Gel permeation chromatograms (GPC) on the polymers obtained from **6** and **8** show narrow molecular weight distributions, with  $M_w/M_n$  of 1.8 and 1.5, respectively, suggesting catalysis occurs at a single site. The  $M_n$  values are higher for **8** than **6**: 147,000 and 26,000 g/mol, respectively. Thus with this ligand framework, Ti gives a better polymerization catalyst than Zr, in terms of activity

and polymer molecular weight (Table 3.2, below). The polymers from **6** and **8** were not observed to have melting points ( $T_m$ ), but the glass transition temperatures ( $T_g$ ) of the polymers were determined to be  $-8.8$  °C and  $-14.4$  °C, respectively, which is approximately the expected  $T_g$  of stereoirregular PP.<sup>20</sup>

$^{13}\text{C}$  NMR spectroscopy was carried out to determine whether these  $C_1$ -symmetric precatalysts led to any degree of stereocontrol. Unexpectedly, we instead found that these catalysts make PP with low regio- and stereocontrol. The  $^{13}\text{C}$  NMR spectra of polypropylene obtained from **6** and **8** reveal a large number of 2,1-insertions; as many as *30-40% of insertions may be inverted* (Figure 3.5). In contrast, primarily regioregular (and stereoirregular) polypropylene was obtained using the related bis(phenoxide)pyridyl (ONO) and bis(anilide)pyridyl (NNN) complexes previously reported by our group.<sup>7,8</sup>

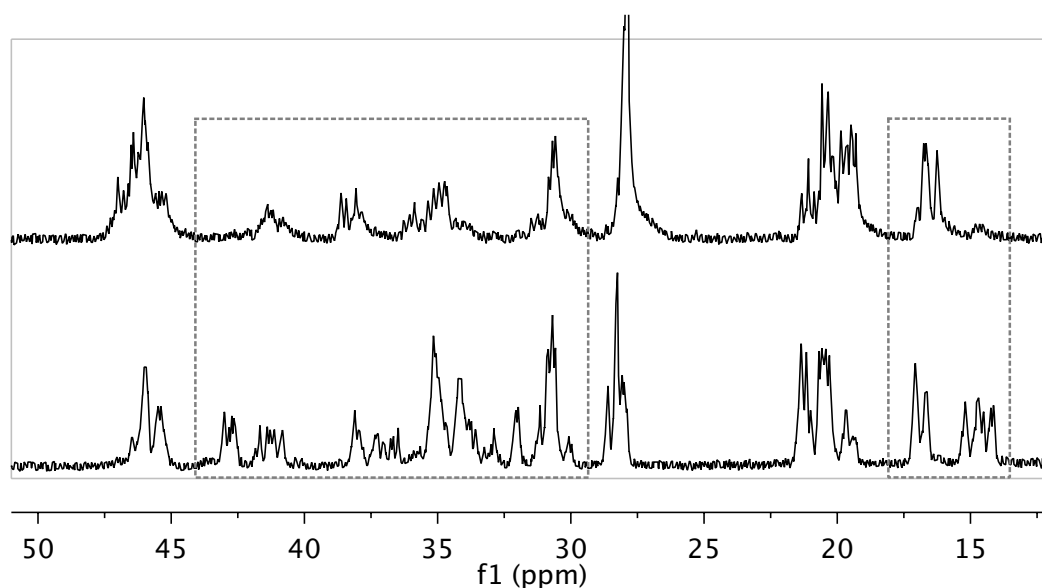
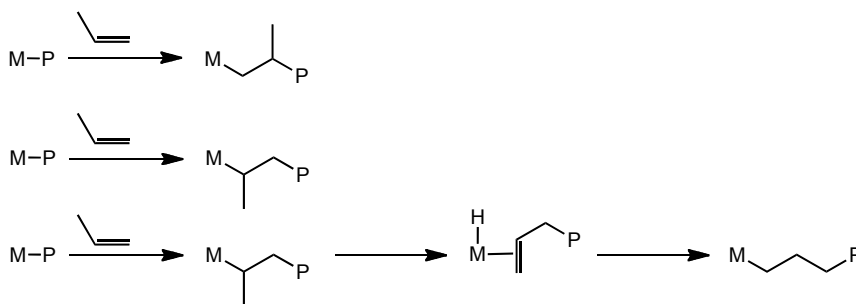


**Figure 3.5**  $^{13}\text{C}$  NMR spectra of PP from **6** (top) and **8** (bottom) at 120 °C in  $\text{TCE-}d_2$ . Regions indicating 2,1-insertions are highlighted.

We also sought to determine the presence of “3,1-insertions” —  $-(CH_2)_3-$  groupings — which can result from  $\beta$ -hydride elimination and re-insertion in the opposite sense following a 2,1-insertion (Scheme 3.11). Such a process would result in an excess of methylene groups; in its absence the ratio of  $CH:CH_2:CH_3$  groups would be 1:1:1.  $^{13}C$  NMR spectroscopy alone is not able to determine the ratio, as the regions containing the signals for methine and methylene carbons are known to overlap; the methyl carbons are well separated and upfield of both methine and methylene carbons (see Appendix B for detailed  $^{13}C$  NMR assignments of PP).<sup>21</sup> We performed 2D  $^1H$ - $^{13}C$  HSQC NMR spectroscopy on the PP obtained from **6** and **8**; such experiments determine the proton connectivity of each  $^{13}C$  signal, as well as the  $^1H$  chemical shift of the associated protons. Although the methine and methylene signals do indeed overlap in the  $^{13}C$  NMR spectra, all three types ( $CH$ ,  $CH_2$  and  $CH_3$ ) are sufficiently separated in the  $^1H$  NMR spectra to allow their relative abundance to be determined by integration. In fact, we observe a 1:1:1 ratio for  $CH:CH_2:CH_3$ , which suggests that there is little or no 3,1-insertion, only 1,2- and 2,1-, during propylene polymerization (Figure 3.6).



**Scheme 3.11** Propylene insertion modes: 1,2-insertion (top), 2,1-insertion (middle), 3,1-insertion (bottom).

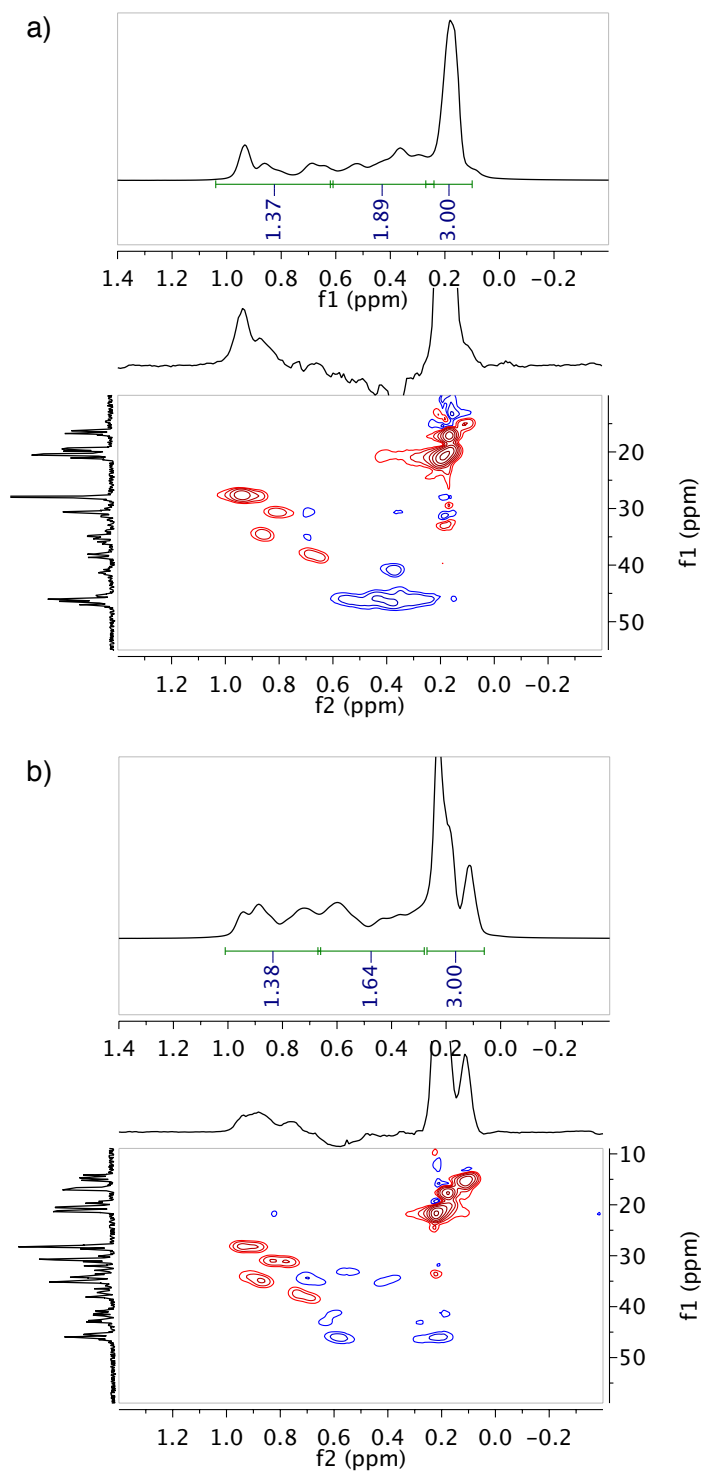


**Figure 3.6** <sup>1</sup>H NMR and 2D <sup>1</sup>H-<sup>13</sup>C HSQC NMR spectra for PP from **6** (a) and **8** (b). Red or positive peaks indicate odd numbers of protons on carbon, and blue or negative peaks indicate even numbers of protons on carbon.

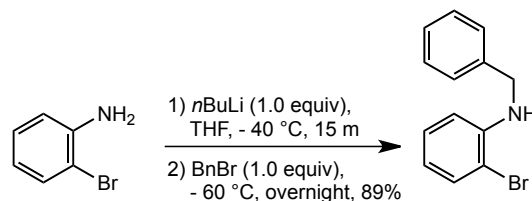
For early transition metal metallocene catalysts 1,2-insertion is typically

avored by both electronic and steric factors; competing 2,1-insertion is usually quite rare, on the order of <1 mol%.<sup>22</sup> There are examples of post-metallocene catalysts that appear to propagate exclusively via a 2,1-insertion mechanism,<sup>23</sup> but to the best of our knowledge, this is the only early metal catalyst that shows so little apparent preference for 1,2- vs. 2,1-insertions;<sup>24</sup> such low regiocontrol is more commonly observed with late metal polymerization catalysts that can undergo “chain running” and incorporate 3,1-insertions.<sup>25</sup> A half-metallocene system has been reported that incorporates 2,1-insertions on the order of 10% at 25 °C, but the percentage decreased at lower temperatures – our polymerizations are run at 0 °C. The relative steric openness of the half-metallocene system was offered as a possible explanation for the higher frequency of inversion relative to metallocene polymerization catalysts.<sup>26</sup> In our case, the (NNO) catalysts **6** and **8** are sterically very similar to their symmetric (ONO) and (NNN) analogues, which exhibit no such regioirregularity,<sup>7,8</sup> suggesting that some factor other than simple sterics may control regioselectivity in these post-metallocene polymerization catalysts.

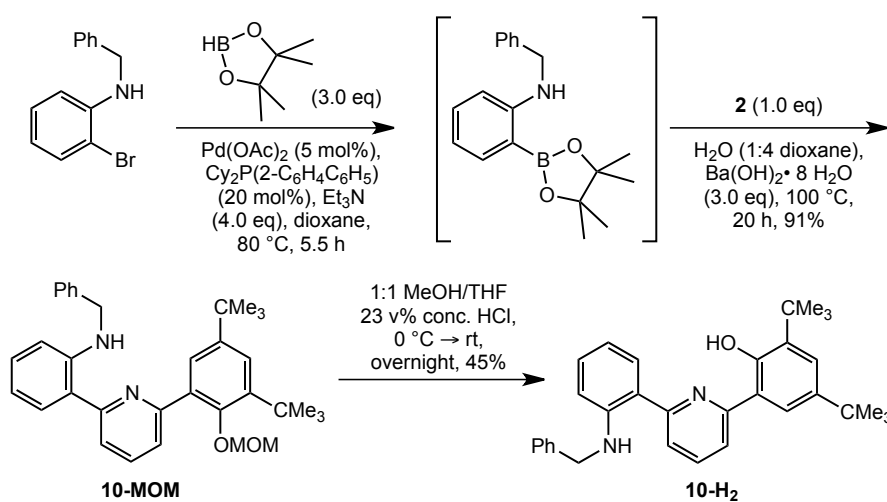
#### *Modification of the Amine R-group: <sup>R</sup>NNO Ligand Synthesis*

The initial ligand design **5** included a chiral 1-phenylethyl group on the anilide arm resulting in a *C*<sub>1</sub>-symmetric ligand and precatalyst. The NNO ligand was designed to be easily variable at the anilide R-group, and given the proximity of this group to the metal center, it was expected to have some influence on

incoming monomers. We reasoned one potential source of regioerrors could be the chiral group on the ligand arm. To probe the effect of this group on regiocontrol, we sought to make  $C_s$ -symmetric ligands. Ligands **10** and **11**, with benzyl and adamantyl groups, respectively, were synthesized using synthetic procedures similar to that reported for the synthesis of **5**. *N*-benzyl-2-bromoaniline was synthesized following the procedure of Glorius et al., by treating 2-bromoaniline with *n*-butyl lithium then benzyl bromide (Scheme 3.12).<sup>27</sup> This aniline could then be coupled to **2** with a Suzuki coupling using the same procedures employed for the synthesis of **5**. Deprotection with an acidic THF/MeOH solution led to the benzyl-substituted NNO ligand **10** (Scheme 3.13).

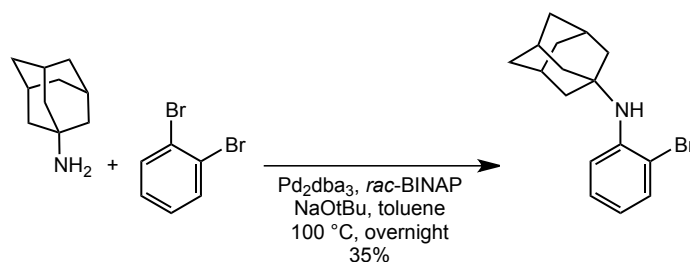


**Scheme 3.12** Synthesis of *N*-benzyl-2-bromoaniline.

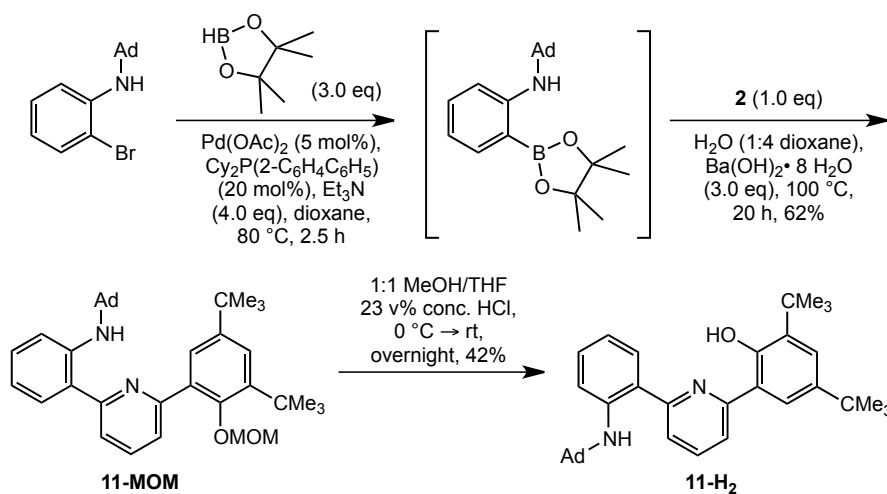


**Scheme 3.13** Synthesis of ligand **10** from *N*-benzyl-2-bromoaniline.

A Buchwald-Hartwig coupling was used to access *N*-adamant-1-yl-2-bromoaniline from 1-adamantylamine and 1,2-dibromobenzene (Scheme 3.14).<sup>28</sup> Coupling this aniline with **2** via a Suzuki reaction, followed by deprotection of the MOM group with an acidic THF/MeOH solution led to the adamantyl-substituted NNO ligand **11** (Scheme 3.15).



**Scheme 3.14** Synthesis of *N*-adamant-1-yl-2-bromoaniline via a Buchwald-Hartwig reaction.

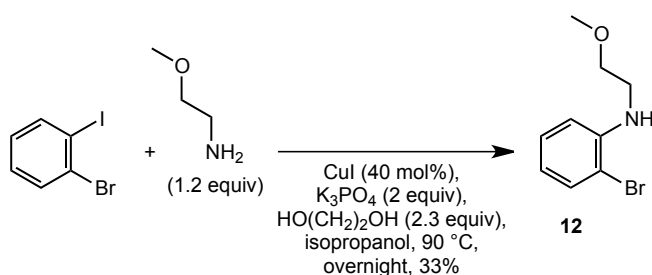


**Scheme 3.15** Synthesis of ligand **11** from *N*-adamant-1-yl-2-bromoaniline.

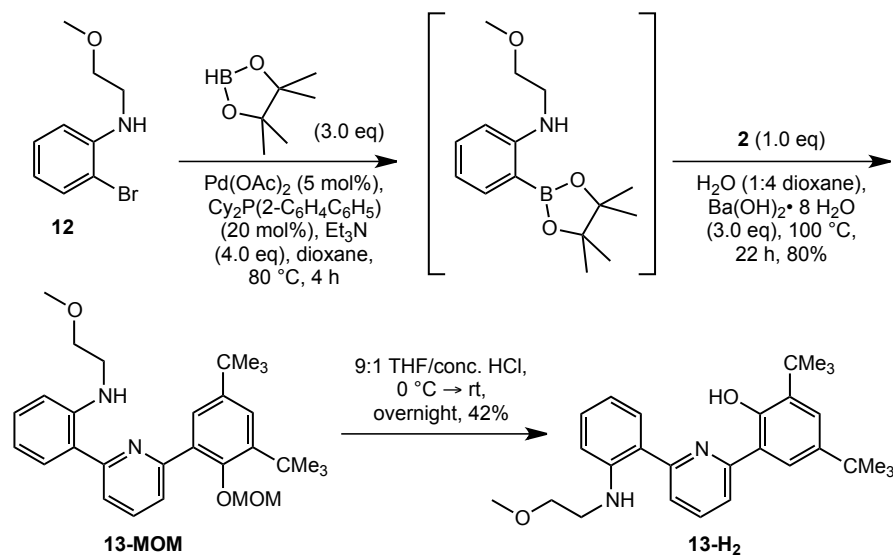
In addition to ligands **10** and **11**, we sought to make a new  $\text{L}_2\text{X}_2$  ligand based on the success of polymerization catalysts pioneered by Mosche Kol and co-workers. Kol has developed post-metallocene polymerization catalysts based on Ti and Zr supported by amine bis(phenolate) and diamine bis(phenolate) ligands. These precatalysts, upon activation with  $\text{B}(\text{C}_6\text{F}_5)_3$ , polymerize 1-hexene

with excellent activities<sup>29</sup> and can produce high molecular weight stereocontrolled poly-1-hexene.<sup>30</sup> For some catalysts, living polymerization was achieved.<sup>31</sup> In any case, all of the ligands employed were tetradentate  $L_2X_2$ . This led us to hypothesize that perhaps increasing the coordination number of our ligands (from  $XLX$  to  $L_2X_2$ ) would lead to more stable and more active polymerization catalysts. We saw an opportunity to test this hypothesis with the NNO ligands since this ligand could be easily modified to include a pendant L-donor on the anilide arm.

Our target for an  $L_2X_2$  ligand was methoxyethyl-NNO with a pendant methoxy group. The substituted aniline precursor 2-bromo-*N*-methoxyethylaniline **12** was synthesized using a Cu-catalyzed Goldberg-modified Ullman reaction to couple 1-bromo-2-iodobenzene and 2-methoxyethylamine by adapting a procedure reported by Buchwald et al. (Scheme 3.16).<sup>32</sup> Suzuki coupling with **2** and deprotection following our standard conditions led to the methoxyethyl-NNO ligand **13** (Scheme 3.17).



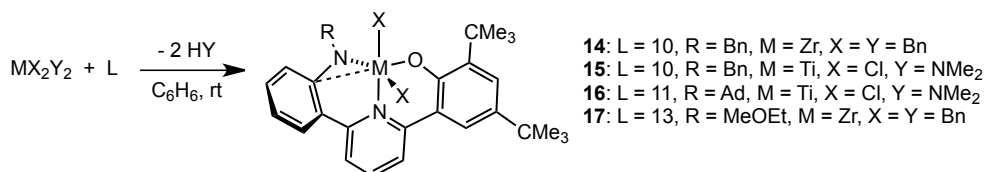
**Scheme 3.16.** Synthesis of 2-bromo-*N*-methoxyethylaniline via a Goldberg-modified Ullman reaction.



**Scheme 3.17** Synthesis of ligand **13** from **12**.

### *R*NNO Ligands: Metalation

Metalation of the NNO variant ligands **10**, **11** and **13** was achieved through either protonolysis with tetrabenzylzirconium or reaction with  $\text{TiCl}_2(\text{NMe}_2)_2$  to yield  $(\mathbf{10})\text{ZrBn}_2$  **14**,  $(\mathbf{10})\text{TiCl}_2$  **15**,  $(\mathbf{11})\text{TiCl}_2$  **16** and  $(\mathbf{13})\text{ZrBn}_2$  **17** (Scheme 3.18). As Hf complexes did not produce polymer in our initial report, we did not pursue any Hf complexes for the new ligands.



**Scheme 3.18** Synthesis of metal complexes **14-17**.

Notably, unlike the Zr dibenzyl complex with the 1-phenylethyl NNO ligand **5** (**6**), the Zr dibenzyl complex with the benzyl ligand **10** (**14**) has sharp resonances in the  $^1\text{H}$  NMR spectrum at room temperature (Figure 3.7).

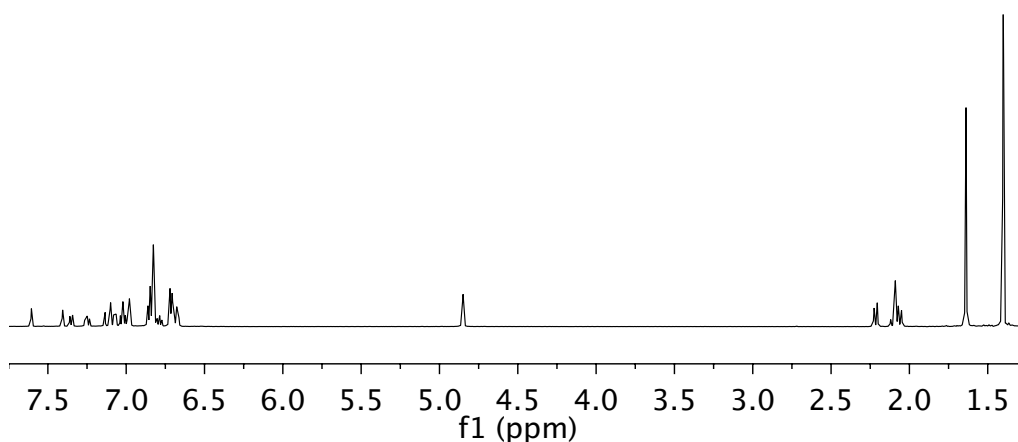


**Figure 3.7** Room temperature  $^1\text{H}$  NMR spectrum of Zr complex **14** in toluene- $d_8$ .

Crystals of **14** suitable for X-Ray diffraction were grown from a concentrated pentane solution at 35 °C (Figure 3.8). The crystal structure of **14** is similar to the structure of (5)TiCl<sub>2</sub> **8**. Both complexes have distorted trigonal bipyramidal geometry and the anilide arm is noticeably distorted out of the O–N(pyridine)–M plane. In the case of **8**, the anilide and phenoxide arms of the meridional ligand **5** coordinate in the equatorial plane to put the most  $\pi$ -donating ligand (Cl) in the axial position to maximize the potential for  $\pi$ -donation. In contrast, **14** has the anilide and phenoxide arms in axial positions, since the other ancillary ligands (benzyl groups) cannot participate in  $\pi$ -bonding (Figure 3.9).

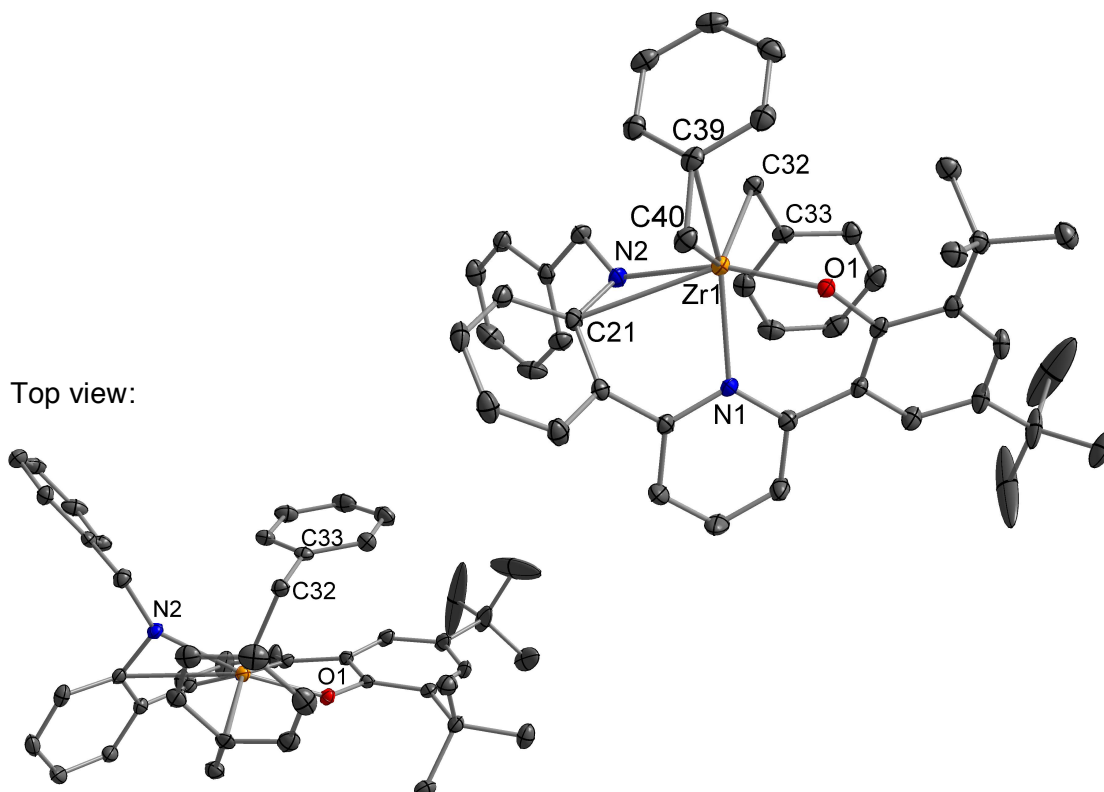


**Figure 3.8** Probability ellipsoid diagram (50%) of the X-ray structure **14**. Selected bond lengths (Å) and angles (°): Zr(1)–O(1) = 1.9917(7), Zr(1)–N(1) = 2.2911(2), Zr(1)–N(2) = 2.1482(8), Zr(1)–C(21) = 2.8470(9), Zr(1)–C(40) = 2.2913(10), Zr(1)–C(39) = 2.5765(9), Zr(1)–C(32) = 2.2851(9); O(1)–Zr(1)–N(2) = 157.17(3), N(1)–Zr(1)–C(40) = 96.19(3), C(40)–Zr(1)–C(32) = 126.48(3), C(32)–Zr(1)–N(1) = 120.71(3), Zr(1)–C(40)–C(39) = 83.53(5), C(21)–N(2)–Zr(1) = 104.95(6).

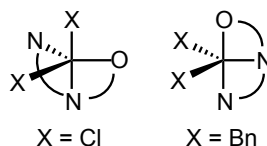


**Figure 3.9** Different binding modes of NNO ligands in trigonal bipyramidal metal complexes depending on the identity of the X-type ligands.

As has been observed for other early metal dibenzyl complexes,<sup>7a,29a,33,34</sup>

one of the benzyl groups in **14** strongly interacts with Zr and is significantly bent toward the metal center to give a Zr–C–C<sub>ipso</sub> angle of 83.5° and a short Zr–C<sub>ipso</sub> distance of 2.58 Å.

The molecular structure of **16** was also determined by single crystal X-Ray diffraction of crystals grown from slow vapor diffusion of pentane into a concentrated dichloromethane solution of **16** (Figure 3.10). The structure of **16** is very similar to that obtained for **8** with distorted trigonal bipyramidal geometry about titanium, and very similar bond lengths and angles. Similar to **8**, **16** appears to have an *ipso* interaction with a short  $\text{Ti}(1)\text{--C}(1)_{ipso}$  distance of 2.54 Å, and a  $\text{Ti}(1)\text{--N}(2)\text{--C}(1)_{ipso}$  angle of  $100.2^\circ$ .

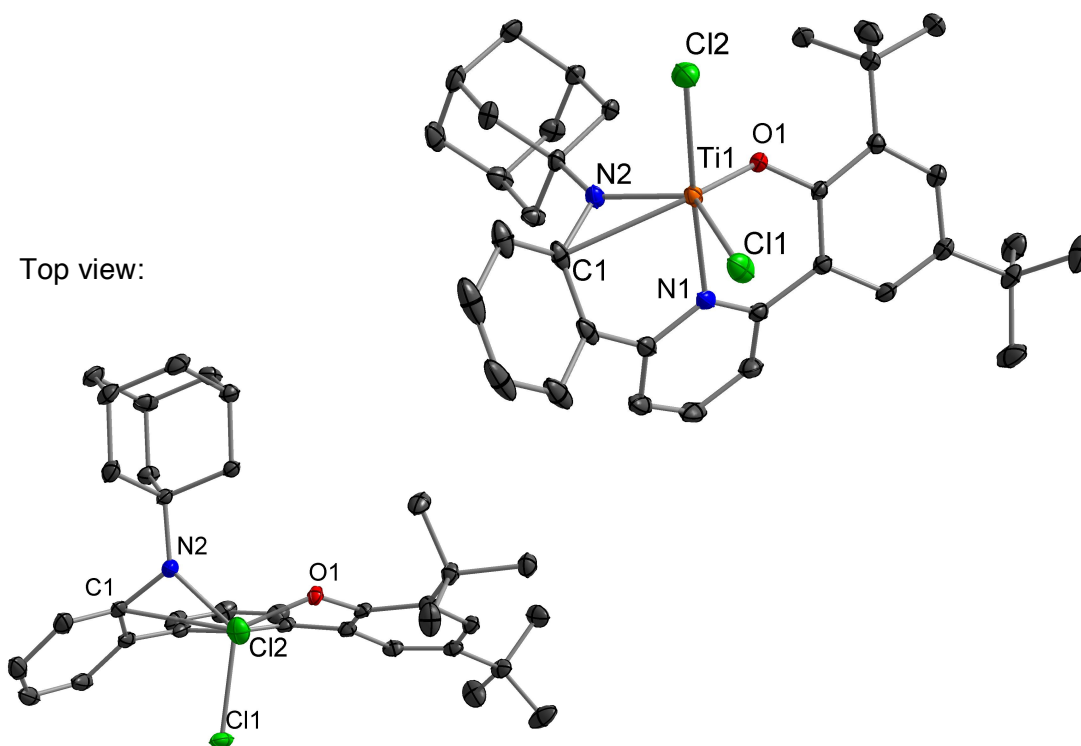


**Figure 3.10** Probability ellipsoid diagram (50%) of the X-ray structure **16**. Selected bond lengths (Å) and angles ( $^\circ$ ):  $\text{Ti}(1)\text{--O}(1) = 1.8170(10)$ ,  $\text{Ti}(1)\text{--N}(1) = 2.1879(13)$ ,  $\text{Ti}(1)\text{--N}(2) = 1.8570(12)$ ,  $\text{Ti}(1)\text{--Cl}(2) = 2.3531(6)$ ,  $\text{Ti}(1)\text{--Cl}(1) = 2.2966(6)$ ,  $\text{Ti}(1)\text{--C}(1) = 2.5354(15)$ ;  $\text{O}(1)\text{--Ti}(1)\text{--N}(2) = 112.36(5)$ ,  $\text{O}(1)\text{--Ti}(1)\text{--Cl}(1) = 119.28(4)$ ,  $\text{N}(2)\text{--Ti}(1)\text{--Cl}(1) = 125.62(4)$ ,  $\text{Cl}(2)\text{--Ti}(1)\text{--N}(1) = 177.32(3)$ ,  $\text{C}(1)\text{--N}(2)\text{--Ti}(1) = 100.15(8)$ .

*R*NNO Ligands: Polymerization Behavior

Activation of complexes **14–16** with MAO in toluene or chlorobenzene resulted in formation of PP under 5 atm of propylene at 0 °C; complex **17** was not active for polymerization. The activity, molecular weight, and polydispersity index (PDI) (when available) are shown in Table 3.2. Data for **6** and **8** is included for comparison. As was observed previously for complexes supported by ligand **5**, Ti complexes are more active than their Zr congeners for the NNO ligand system. In comparing the Ti catalysts with three different amine R-groups (1-phenylethyl (**8**), benzyl (**15**), and adamantyl (**16**)), **8** was observed to be the most active catalyst and gave the highest molecular weight polymer; overall, however, the activities are not significantly different. Additionally, no obvious trend between R-group and molecular weight is apparent for this small data set. Notably, all of the polymers obtained have narrow PDIs ( $M_w/M_n$ ) suggesting single-site catalysis. The PP from complexes **15** and **16** had no melting points, as expected for stereoirregular PP, and had similar  $T_g$  values to those measured for the PP from complexes **6** and **8**.

**Table 3.2** Propylene polymerization data for complexes **6**, **8**, **14–16**.

Precatalyst	Precatalyst (mmol)	Time (h)	Yield PP (mg) <sup>a</sup>	Activity (g PP (mol cat) <sup>-1</sup> h <sup>-1</sup> )	T <sub>g</sub> (°C)	M <sub>w</sub> (g/mol)	M <sub>w</sub> /M <sub>n</sub>
<b>6</b>	0.0076	1	130.8	1.6 × 10 <sup>4</sup>	-8.77	26000	1.8
<b>8</b>	0.0092	0.5	553.7	1.2 × 10 <sup>5</sup>	-15.25	93190	1.50
<b>8</b>	0.0096	1	2412	2.5 × 10 <sup>5</sup>	-14.40	147000	1.5
<b>8</b>	0.0091	3	3963	1.5 × 10 <sup>5</sup>	-12.76	400810	1.99
<b>14</b>	0.0081	1	609.8	3.8 × 10 <sup>4</sup>			
<b>15</b>	0.0093	0.5	384.2	8.3 × 10 <sup>4</sup>	-13.66	80192	1.47
<b>15</b>	0.0098	1	839.3	8.6 × 10 <sup>4</sup>	-13.54	133384	1.55
<b>15</b>	0.0100	3	2504	8.4 × 10 <sup>4</sup>	-13.22	196942	2.38
<b>16</b>	0.0102	1	589.3	5.8 × 10 <sup>4</sup>	-15.36	91529	1.35

<sup>a</sup>Polymerizations were carried out in 30 mL liquid propylene with 1000 eq dry MAO in 3 mL of toluene or PhCl at 0 °C for the time indicated.

$^{13}\text{C}$  NMR spectroscopy was carried out on the polymers obtained from complexes **15–16**. We were particularly interested in comparing the microstructure of the PP for the Ti catalysts with three different amine R-groups (**8**, **15** and **16**). Surprisingly, we observed nearly no difference between the polymer microstructures as determined by  $^{13}\text{C}$  NMR spectroscopy (Figure 3.11).

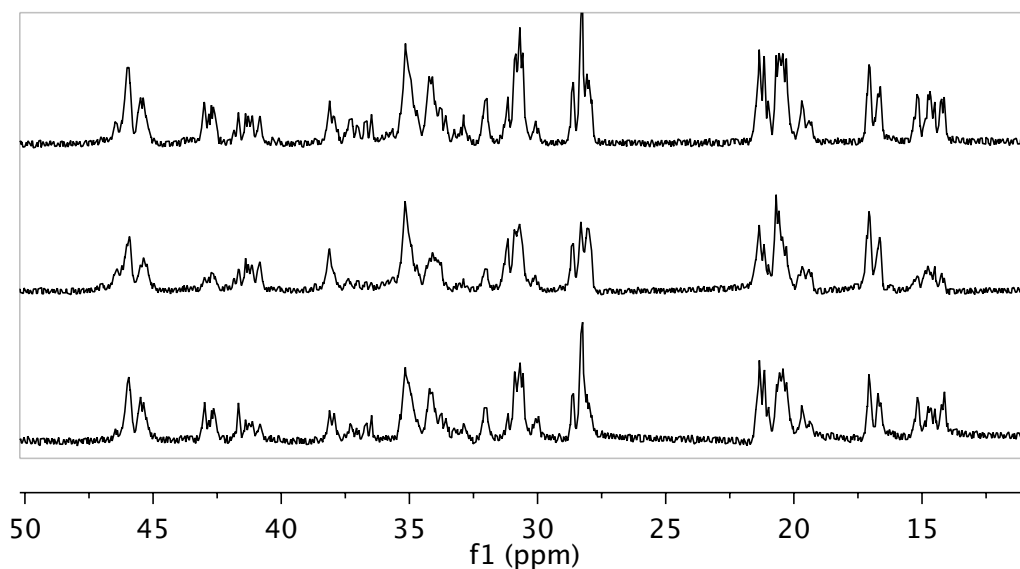


**Figure 3.11**  $^{13}\text{C}$  NMR spectra of PP from complex **8** (top), **15** (middle), and **16** (bottom) at 120 °C in  $\text{TCE-}d_2$ .

These results suggest that – contrary to our original hypothesis – the amine R-group does not seem to affect the stereo- or regiocontrol of the active polymerization catalyst. Although it is possible that the R-group is just an observer to the polymerization reaction in terms of monomer selectivity, we also considered catalyst modification pathways to explain the identical regioselectivity for different precatalysts, especially considering how unusual this type of PP is for an early metal polymerization catalyst. In fact, no other early metal

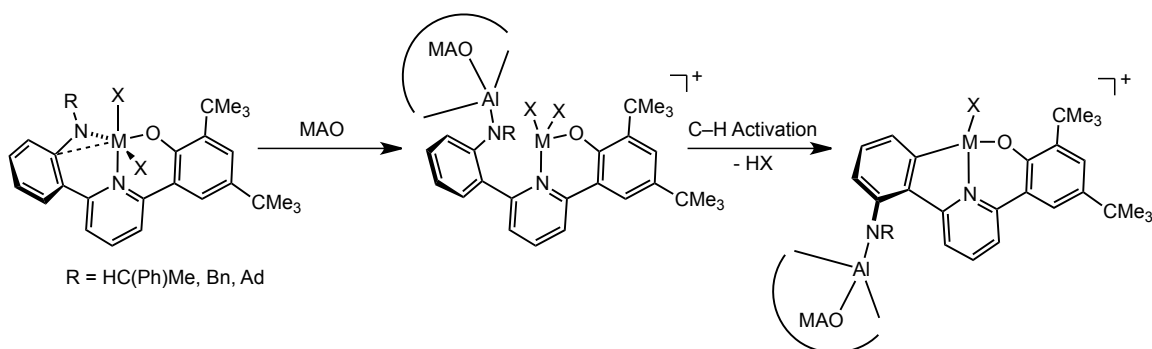
polymerization catalysts are known that make the same type of regioirregular PP as the Ti and Zr NNO-type catalysts described here.

One hypothesis for catalyst modification that may explain the identical regioselectivity for the Ti catalysts **8**, **15** and **16** is anilide arm dissociation under polymerization conditions, which would perhaps prevent the amine R-group from having any influence on the catalyst stereo- or regioselectivity. Notably, bis(anilide)pyridyl polymerization catalysts reported by our group, have very large PDIs for propylene polymerization (4.9-31.2),<sup>8</sup> which may indicate the instability of the Ti-(anilide)N linkages under polymerization conditions; if the Ti-N bonds are susceptible to cleavage, multiple active species may be obtained leading to a broad molecular weight distribution and large PDIs. In contrast, the NNO polymerization catalysts reported here exhibit narrow PDIs indicative of primarily one active species (Table 3.2); thus, even if the Ti-(anilide)N bonds of the NNO ligand are unstable, the active polymerization catalysts appear to be stabilized by having a phenoxide moiety in the ligand framework.

### *CNO Ligand: Design and Synthesis*

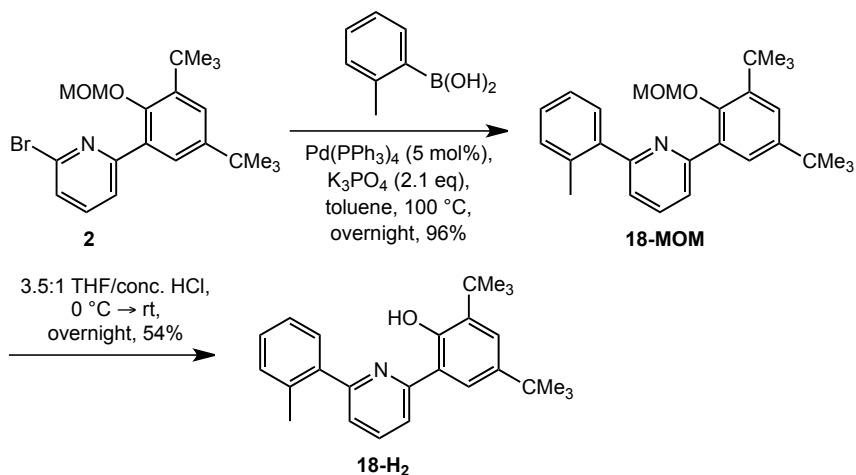
In considering the possibility of anilide arm dissociation – perhaps facilitated by MAO – we postulated that the arm could remain uncoordinated, or could rotate along the C<sub>aryl</sub>-C<sub>aryl</sub> bond and possibly C-H activate *meta* to the C<sub>aryl</sub>-N<sub>anilide</sub> bond (Scheme 3.19). Since studying the active catalyst in solution was not feasible, we sought to synthesize model complexes that upon activation

with MAO would be analogous to either a (perhaps) fluxional dissociated anilide arm or a C–H-activated anilide arm. Group 4 orthometalated aryl(pyridine)phenoxide (CNO) complexes are well known and, in fact, have been used in polymerizations with ethylene as well as ethylene/propylene copolymerizations, thus a CNO-ligated group 4 complex was our first target.<sup>35</sup>



**Scheme 3.19** Potential pathways for NNO catalyst modification upon activation with MAO.

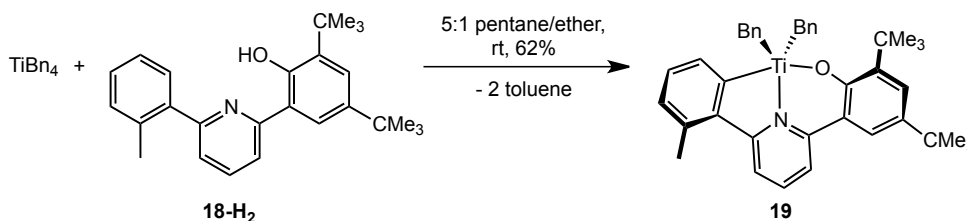
Ligand **18** was synthesized as shown in Scheme 3.20. The 2-bromo-6-(3,5-di-*t*-butyl-2-(methoxymethoxy)phenyl)pyridine synthon **2** underwent Suzuki coupling with commercially available *o*-tolyl-boronic acid. Deprotection of this intermediate with acidic THF afforded the desired CNO ligand **18**.



**Scheme 3.20** Synthesis of ligand **18** from synthon **2**.

### CNO Ligand: Metalation

Metalation of **18** was achieved by reaction with tetrabenzyltitanium to yield orthometalated (**18**)TiBn<sub>2</sub> **19** (Scheme 3.21). An X-Ray quality crystal of **19** was grown from a 5:1 pentane/ether solution at room temperature, which shows the expected distorted trigonal bipyramidal structure and bond lengths and angles similar to those reported for crystal structures of other (CNO)TiBn<sub>2</sub> complexes (Figure 3.12).<sup>35a</sup> Notably, the Ti–C–C<sub>ipso</sub> angle for one of the benzyl groups is slightly distorted at 93.7° and has a shortened Ti–C<sub>ipso</sub> distance of 2.64 Å (compare to 123.3° and 3.18 Å for the other benzyl group) suggesting a weak η<sup>2</sup>-*ipso* interaction between the benzyl group and Ti.



**Scheme 3.21** Synthesis of Ti complex **19**.

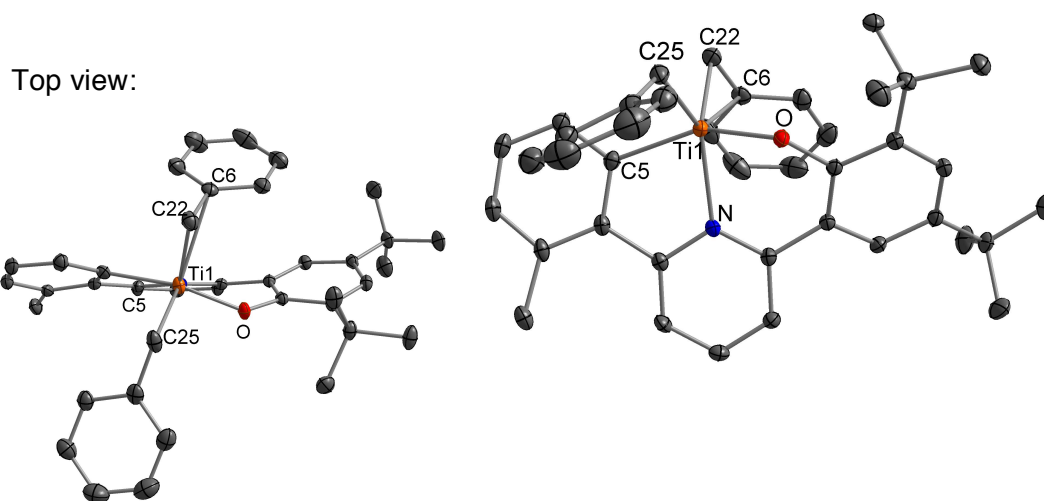


**Figure 3.12** Probability ellipsoid diagram (50%) of the X-ray structure **17**. Selected bond lengths (Å) and angles (°): Ti(1)–O(1) = 1.8649(4), Ti(1)–N(1) = 2.2132(4), Ti(1)–C(5) = 2.1352(5), Ti(1)–C(22) = 2.1037(6), Ti(1)–C(6) = 2.6385(6), Ti(1)–C(25) = 2.1135(6); O(1)–Ti(1)–C(5) = 153.81(2), C(25)–Ti(1)–C(22) = 97.60(3), C(22)–Ti(1)–N(1) = 126.85(2), C(25)–Ti(1)–N(1) = 134.79(2), Ti(1)–C(22)–C(6) = 93.46(4).

### *CNO Ligand: Polymerization Behavior*

Activation of **19** with MAO in toluene under 5 atm propylene at 0 °C yielded PP. The activity of the complex was measured to be  $1.5 \times 10^4$  g PP (mol cat)<sup>-1</sup> h<sup>-1</sup>, which is an order of magnitude less active than the NNO-type Ti polymerization catalysts **8**, **15**, and **16**. Importantly, investigation of the PP from **19** with <sup>13</sup>C NMR spectroscopy revealed stereoirregular and regioregular PP (Figure 3.13). This result tentatively suggests that the NNO complexes do not C–H activate to form CNO polymerization catalysts.

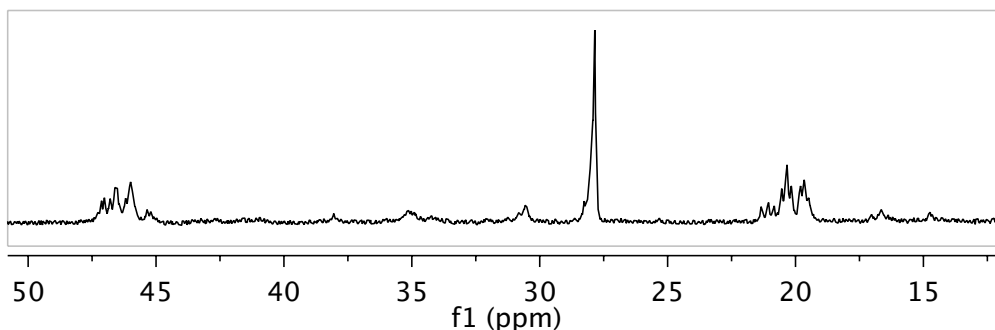


**Figure 3.13**  $^{13}\text{C}$  NMR spectrum of stereoirregular regioirregular PP from complex **19** at 120 °C in  $\text{TCE-}d_2$ .

To further investigate the possibility of C–H activation, a solution of **8** in chlorobenzene was activated with 50 equiv of MAO in the presence of 1-hexene; we have separately demonstrated that **8** polymerizes 1-hexene to make stereoirregular and regioirregular poly-1-hexene (Figure 3.14).<sup>36</sup>

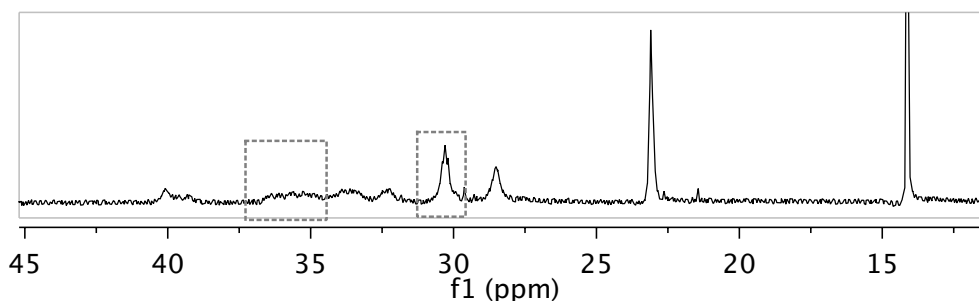
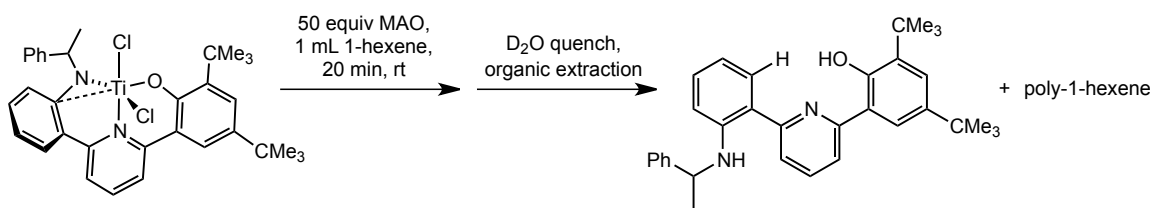


**Figure 3.14**  $^{13}\text{C}$  NMR spectrum of stereoirregular regioirregular poly-1-hexene from complex **8**. Regions indicating regioerrors are highlighted.

The solution of precatalyst **8**, MAO, and 1-hexene was stirred for 20 min and then quenched with  $\text{D}_2\text{O}$ . The organic layer was extracted and analyzed by  $^1\text{H}$  NMR spectroscopy, which revealed the formation of poly-1-hexene and recovery of the intact ligand **5** (Scheme 3.22). If C–H activation occurred with MAO, we would expect to see deuterium incorporation into the aryl ring of the ligand; however, the ligand isolated from the reaction of **8**/MAO did not show

deuterium incorporation into the aryl ring by either HRMS or  $^1\text{H}$  NMR spectroscopy. Additionally, the 1-phenylethyl R-group on the NNO ligand **5** was intact, ruling out N–C bond cleavage by MAO as another potential pathway for catalyst modification to make identical  $\{(\text{NNO})\text{Ti}\}$  active species. Finally, monomer was not incorporated into the isolated ligand, as has been observed for Hf pyridyl–amide catalysts discovered by Dow and Symyx (these catalysts are modified by insertion of a monomer into a M–C bond, which admittedly is far more likely than insertion into M–O or M–N bonds).<sup>37</sup> Based on these experiments, we have tentatively ruled out (1) C–H activation of the anilide arm to form a  $\{(\text{CNO})\text{Ti}\}$  complex (2) N–C bond cleavage of the anilide R-group and (3) monomer insertion into M–ligand bonds to explain the identical regiocontrol observed for NNO-type polymerization catalysts.

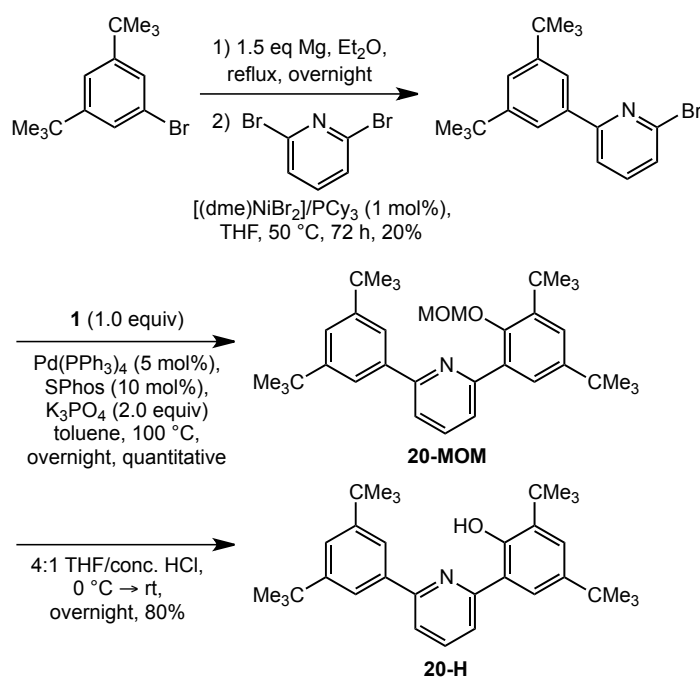


**Scheme 3.22** Recovery of ligand **5** after activation and polymerization of 1-hexene with complex **8**.

### *ArNO Ligand: Synthesis*

Synthesizing a model complex for anilide arm dissociation to make a pyridine(phenoxide) catalyst has, unfortunately, proven challenging (Scheme 3.19, middle complex). We designed a bulky aryl(pyridine)phenoxide (ArNO) ligand that we anticipated would resist aryl C–H activation, and might allow for formation of mono-ligated metal complexes (rather than homoleptic bis-ligated

complexes) despite being a bidentate coordinating ligand. Coupling 3,5-di-*t*-butylbromobenzene with 2,6-dibromopyridine via a Kumada coupling following a literature procedure led to the monoarylated pyridine intermediate 2-bromo-6-(3,5-di-*t*-butylphenyl)pyridine.<sup>38</sup> A Suzuki coupling reaction between 2-bromo-6-(3,5-di-*t*-butylphenyl)pyridine and the boronic ester **1**, followed by deprotection with acidic THF led to the target ArNO ligand **20** (Scheme 3.22).



**Scheme 3.22** Synthesis of ligand **20** via Kumada and Suzuki coupling reactions.

### *ArNO Ligand: Metalation*

Although we were able to synthesize the desired ligand, we were unable to obtain clean Ti complexes to test for polymerization, possibly because the pyridine(phenoxy) ligand **20** leads to metal complexes that are too electron poor to be stable.

Reaction of **20** with  $\text{TiCl}_2(\text{NMe}_2)_2$  led to a species we have tentatively assigned as  $(\mathbf{20})\text{TiCl}_2(\text{NMe}_2)$ , however, clean isolation of this species was complicated by residual  $\text{HNMe}_2$  in the reaction mixture. Alternatively, reaction of **20** with  $\text{TiBn}_4$  initially yielded the complex  $(\mathbf{20})\text{TiBn}_3$  with concomitant formation of 1 equiv of toluene; however, over time or upon removal of solvent this species was observed to decompose to a new unidentifiable – albeit clean – product perhaps resulting from dimerization of Ti species (Figure 3.15). Synthesis of  $(\mathbf{20})\text{TiCl}_3$  was also attempted by reaction of **20** with  $\text{TiCl}_4$ , but formation of  $\text{HCl}$  was unobserved and the product of the reaction appears to be  $(\mathbf{20-H})\text{TiCl}_4$  with a diagnostic downfield resonance at 12.31 ppm indicative of an O–H group. Although other metal starting materials or synthetic routes might have yielded an appropriate Ti complex, we ultimately decided to not pursue this ligand framework for polymerization studies.

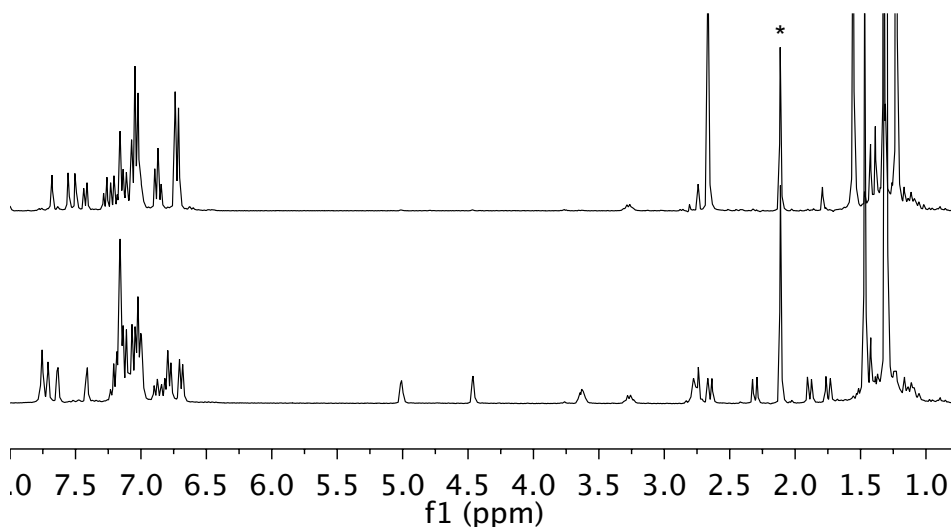


**Figure 3.15**  $^1\text{H}$  NMR spectrum of crude reaction between  $\text{TiBn}_4$  and **20** in  $\text{C}_6\text{D}_6$  after 10 min (top) and after sitting in a J. Young NMR tube at rt overnight (bottom). Toluene formed in the reaction is indicated by an asterisk.

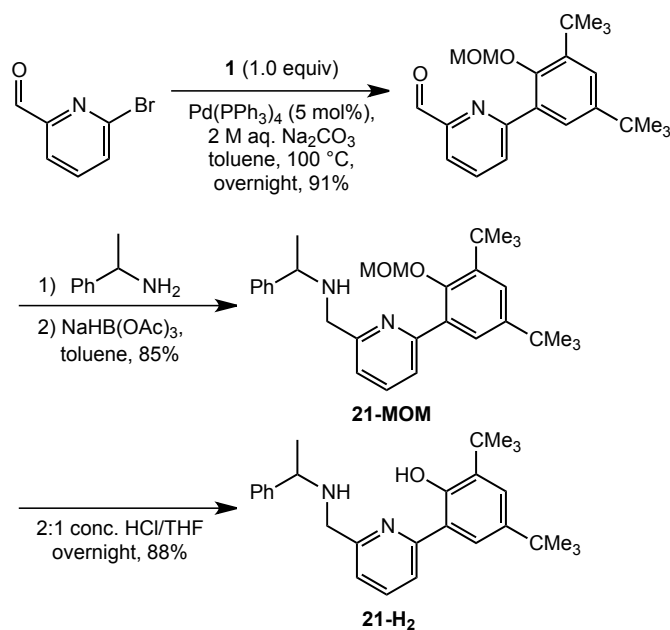
Nonetheless, our studies up to this point with the CNO–Ti complex **19**, as well as our activation study with the NNO–Ti complex **8** in the presence of monomer seem to disfavor a catalyst modification hypothesis and, in fact, provide no evidence for anilide arm dissociation under polymerization conditions. Despite the proximity of the R-group on the anilide arm to the metal center (Figures 3.4, 3.8, and 3.10), it appears to have no (or at a minimum very little) influence on monomer selectivity. Thus, while an explanation for the unique regioselectivity of NNO-type polymerization catalysts remains, as yet, out of reach, based on the data presented here, we suspect that the active species involves the intact anilide(pyridine)phenoxide ligand bound to the metal center.

#### *amido* NNO Ligand: Design and Synthesis

Our group has demonstrated that bis(phenoxide)pyridyl complexes<sup>7</sup> and bis(anilide)pyridyl complexes<sup>8</sup> produce regioregular (and stereoirregular) polypropylene; a related aryl(pyridine)phenoxide complex (**19**) presented here also polymerizes propylene in a regioregular sense. These data perhaps suggest that incorporation of an anionic nitrogen donor into an asymmetric ligand framework impacts the regioselectivity of the resulting catalytic species; thus, we were interested in investigating the polymerization behavior of metal complexes with other dianionic asymmetric NNO-coordinating ligands. For a first target, we selected an amido(pyridine)phenoxide ligand due to its straightforward synthesis and literature precedent for this framework supporting a Hf propylene

polymerization catalyst; unfortunately, the microstructure of the PP produced by the known Hf catalyst was only probed by FT-IR, which does not allow for analysis of the regiostructure of the polymer.<sup>39</sup>

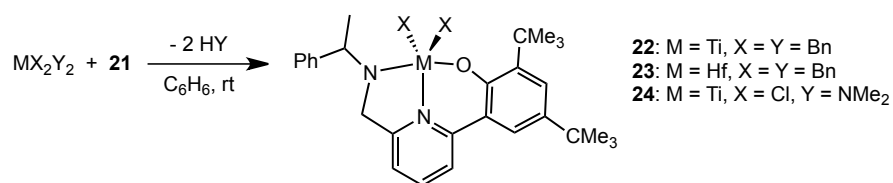
The amido(pyridine)phenoxide ligand **21** was synthesized using protocols similar to those reported for other 2-phenoxy-6-(methanamino)pyridines.<sup>40</sup> A Suzuki coupling reaction between boronic ester **1** and 6-bromo-2-pyridinecarboxaldehyde yielded 6-(3,5-di-*t*-butyl-2-(methoxymethoxy)phenyl)-picolinaldehyde. A condensation reaction with the desired amine, 1-phenylethylamine, generated a 2-phenoxy-6-iminopyridine intermediate, which underwent a one-pot reduction with sodium triacetoxyborohydride to yield the MOM-protected amido(pyridine)ligand **21-MOM**. Deprotection with acidic MeOH gave the desired ligand **21** in good yield (Scheme 3.23).



**Scheme 3.23** Synthesis of amido(pyridine)phenoxide ligand **21**.

*amido* NNO Ligand: Metalation

Reaction of the amido(pyridine)phenoxide ligand **21** with tetrabenzyltitanium and tetrabenzylhafnium led to clean (by  $^1\text{H}$  NMR spectroscopy) dibenzyl Ti and Hf complexes **22** and **23** (Scheme 3.24); the related reaction with tetrabenzylzirconium did not yield a clean product. Although the crude reaction mixtures of **22** and **23** appear to be very clean, we have been unable to isolate solids of the complexes; solutions of **22** and **23** decompose when concentrated by removal of solvent in vacuo, potentially because of the highly electrophilic nature of these metal complexes. We were able to obtain the molecular structure of a related Ti complex (**21**)TiCl<sub>2</sub> **24**, synthesized by reaction of ligand **21** with TiCl<sub>2</sub>(NMe<sub>2</sub>)<sub>2</sub>, by single crystal X-ray diffraction (Scheme 3.24). **24** was crystallized as the THF adduct from slow vapor diffusion of pentane into a concentrated THF solution. The X-ray structure of **24** reveals pseudo-octahedral geometry around the Ti metal center and a typical Ti–(amido)N bond length, as well as other standard bond lengths and angles for an octahedral Ti(IV) complex (Figure 3.16).



**Scheme 3.24** Synthesis of amido(pyridine)phenoxide complexes **23-24**.

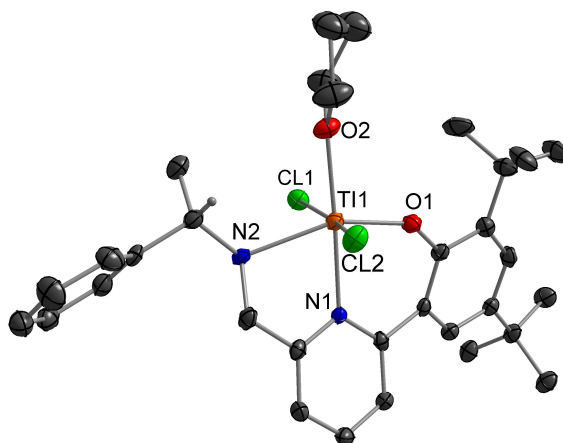


**Figure 3.16** Probability ellipsoid diagram (50%) of the X-ray structure of the THF adduct of **24**. Selected bond lengths (Å) and angles (°): Ti(1)–Cl(1) = 2.4135(12), Ti(1)–Cl(2) = 2.4167(12), Ti(1)–O(1) = 1.852(2), Ti(1)–O(2) = 2.133(3), Ti(1)–N(1) = 2.183(3), Ti(1)–N(2) = 2.272(3); Cl(1)–Ti(1)–Cl(2) = 167.97(4), O(1)–Ti(1)–N(2) = 156.94(11), O(2)–Ti(1)–N(1) = 176.38(11), N(1)–Ti(1)–N(2) = 74.16(10), O(1)–Ti(1)–N(1) = 83.06(10).

#### *amido* NNO Ligand: Polymerization Behavior

Since we were unable to isolate clean metal complexes containing the amido(pyridine)phenoxide ligand **21**, we tested the polymerization activity of **22** and **23** by preparing the catalysts in situ; a freshly prepared solution of **21** and either tetrabenzyltitanium or tetrabenzylhafnium was loaded into a syringe and injected directly into the polymerization vessel. The in situ prepared hafnium complex **22** did not yield any polymer; however, recall that in our hands the anilide(pyridine)phenoxide Hf complex **7** also did not polymerize propylene. The Ti complex **23**, however, did yield PP and the activity at 0 °C was determined to be  $1.6 \times 10^4$  g PP (mol cat)<sup>-1</sup> h<sup>-1</sup>. Investigation of the polymer with <sup>13</sup>C NMR spectroscopy revealed regioregular stereoirregular polypropylene, identical to that obtained from the (CNO)TiBn<sub>2</sub> catalyst **19** (Figure 3.17, see Figure 3.13).

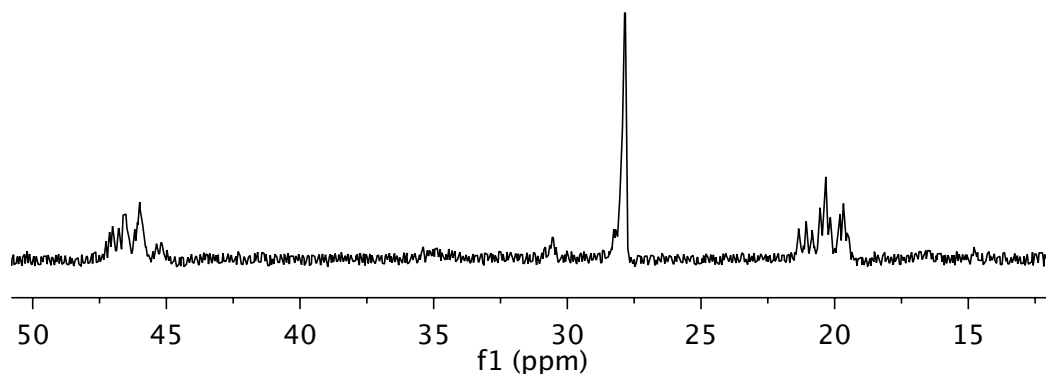


**Figure 3.17**  $^{13}\text{C}$  NMR spectrum of stereoirregular regioregular PP from in situ formed Ti complex **23** at 120 °C in TCE- $d_2$ .

This preliminary polymerization data suggests that a group 4 polymerization catalysts with a dianionic NNO ligand motif is not enough to give regioregular PP. We recognize that the anionic nitrogen donor in the amido(pyridine)phenoxide ligand is in a 5-membered ring compared to a 6-membered ring in the anilide(pyridine)phenoxide ligands. Additionally, by incorporating a dialkyl amido donor, the ligand motif is no longer a triaryl pincer framework, and the potential impact of these changes alone on polymerization behavior should be noted. Nevertheless, our polymerization results taken together clearly indicate that only the tridentate anilide(pyridine)phenoxide ligands **5**, **10**, and **11** support group 4 catalysts that exhibit nearly random regioselectivity for propylene polymerization. Furthermore, closely related tridentate dianionic ligand frameworks, whether incorporating symmetric anilide groups or pyridine(phenoxide) moieties, all lead to catalysts that produce regioregular PP, such that only the specific combination of an anilide, pyridine and a phenoxide together seems to result in regiorandom polymerization activity.

*(NNO)TiCl<sub>2</sub>: Further Polymerization Studies*

Our studies with various post-metallocene polymerization catalysts up to this point suggest that anilide(pyridine)phenoxide catalysts are quite unique in their regioselectivity and that this regioselectivity may somehow be inherent in the catalyst structure; however, we thought it worthwhile to test these catalysts under different polymerization reaction conditions to investigate whether temperature or co-catalyst/activator had any effect on regioselectivity. With help from our collaborators at King Fahd University of Petroleum and Minerals (KFUPM) and Dow Chemical, we were able to test propylene polymerization with precatalyst **8** under different sets of conditions.

*Polymerization with (NNO)TiCl<sub>2</sub> **8** at (KFUPM)*

Ti complex **8** was tested in a 1 L glass reactor, which allowed for testing propylene polymerization at higher temperatures (22-25 °C) and higher pressures of propylene (8-9 atm) compared to the Fisher–Porter setup employed in the Bercaw laboratories (0 °C, 5 atm). A polymerization reaction using complex **8** as a catalyst, along with triisobutyl aluminum (TIBA) and MAO in toluene at room temperature yielded very sticky non-solid PP (Figure 3.17). We were not able to calculate an accurate activity for the reaction, but we estimate the activity to be on the order of  $\sim 9 \times 10^5$  g PP (mol cat)<sup>-1</sup> h<sup>-1</sup>.



**Figure 3.17** Sticky non-solid PP produced at KFUPM (rt, 8–9 atm propylene) with precatalyst **8** (left) and nonsticky solid PP produced at Caltech (0 °C, 5 atm propylene) also with precatalyst **8** (right).

Investigation of the PP with  $^{13}\text{C}$  NMR spectroscopy revealed stereoirregular and regioirregular PP (Figure 3.18). Notably, this sample of PP had a slightly different microstructure than the PP obtained from **8** in our reactor at 0 °C with 5 atm of propylene and dry MAO as the co-catalyst. We thought that the addition of free aluminum (TIBA) to the polymerization might affect the speciation of the catalyst and subsequently the polymer microstructure; the MAO used in our polymerizations is dried in vacuo to remove free trimethylaluminum (TMA). To test the possibility of TIBA affecting the polymerization, we set up a polymerization reaction with **8** in chlorobenzene using MMAO at 0 °C in our reactor. MMAO or modified MAO is a more stable version of MAO made from careful hydrolysis of TIBA. As we used the solution directly, it presumably contained free TIBA. Polymerization with MMAO as a co-catalyst yielded sticky non-solid PP; the activity was determined to be  $1.0 \times 10^5 \text{ g PP (mol cat)}^{-1} \text{ h}^{-1}$ .  $^{13}\text{C}$  NMR spectroscopy on the PP from the reaction of **8**/MMAO revealed a microstructure identical to that from the PP synthesized at KFUPM with

**8**/MAO/TIBA (Figure 3.18). These results suggest that the polymerization reaction is very sensitive to free aluminum, but importantly shows that the regiorandom behavior of catalyst **8** is not affected by reaction temperatures between 0 and 22 °C.

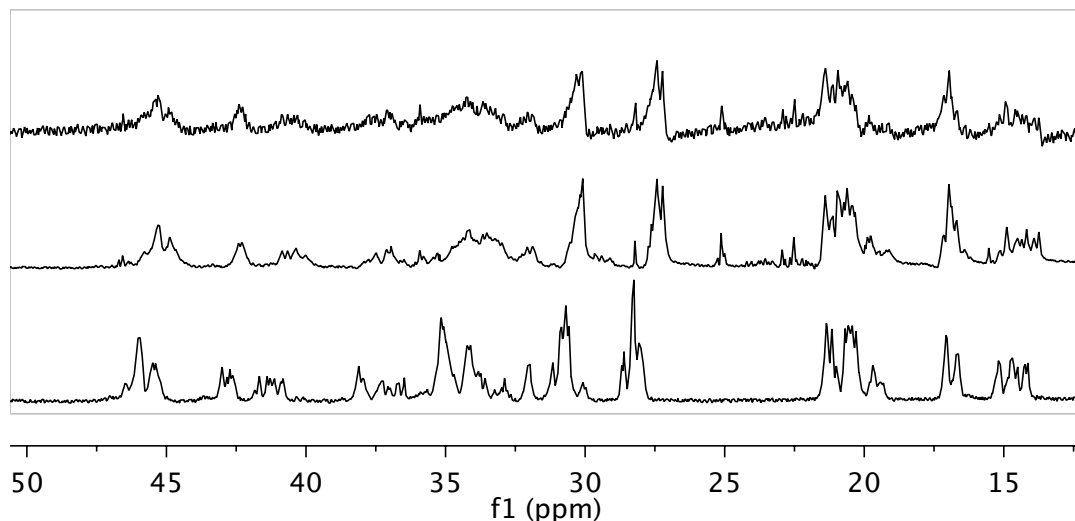


**Figure 3.18**  $^{13}\text{C}$  NMR spectra of PP from complex **8**/MAO/TIBA run at rt at KFUPM (top), PP from **8**/MMAO run at 0 °C at Caltech (middle), and PP from **8**/dry MAO run at 0 °C at Caltech (bottom). Spectra were taken at 120 °C in  $\text{TCE-}d_2$ .

Notably, GPC on the polymer obtained from **8**/MAO/TIBA at KFUPM revealed lower molecular weight PP compared to the polymers obtained at Caltech with the same precatalyst under different polymerization conditions; the PP from **8**/MAO/TIBA has a  $M_w$  value of only 4,076 g/mol, while the molecular weights of PP from **8**/dry MAO ranged from 93,190 g/mol to 400,810 g/mol (see Table 3.2). The molecular weight distribution for the polymer was still rather narrow with a  $M_w/M_n$  of 2.45. As expected, the PP had no observable  $T_m$  and a  $T_g$  of  $-26.11$  °C. The GPC of PP from **8**/MMAO run at 0 °C showed a bimodal distribution with a low molecular weight peak of 3,975 g/mol and a high molecular weight peak of 195,372 g/mol. The low molecular weight polymers observed in

polymerizations with **8**/MAO/TIBA and **8**/MMAO may be a result of free aluminum present in the reaction, as aluminum alkyls are known to act as chain-transfer agents;<sup>41</sup> only higher molecular weight PP was obtained when dry MAO with minimal free TMA was used (Table 3.2).

*Polymerization with (NNO)TiCl<sub>2</sub> **8** at Dow Chemical Company.*

Ti complex **8** was tested for propylene polymerization in a 1.8 L SS batch reactor. Polymerizations were run at 70 °C with 700 g of IsoparE, 150 g of propylene, 50 psi of hydrogen for 15 min. PMAO-IP or MAO were used as co-catalysts. These polymerizations yielded solid PP with excellent activities of  $2.1 \times 10^6$  g PP (mol cat)<sup>-1</sup> h<sup>-1</sup> (**8**/PMAO-IP) and  $9.6 \times 10^5$  g PP (mol cat)<sup>-1</sup> h<sup>-1</sup> (**8**/MAO) (Table 3.3), and broad molecular weight distributions,  $M_w/M_n$ , of 18.55 and 20.86, respectively; however, the GPC traces show trimodal distributions. Deconvolution of the GPC data for the PP from **8**/PMAO-IP reveals two low  $M_w$  peaks of 319 and 1,864 g/mol and a high  $M_w$  peak of 85,883 g/mol. Similarly, the deconvoluted GPC data for **8**/MAO has two low  $M_w$  peaks of 315 and 2,355 g/mol and a high  $M_w$  peak of 82,256 g/mol. Most interestingly, unlike the PP produced by our catalysts under any other condition, the PP produced with **8**/PMAO-IP or **8**/MAO at Dow had melting points of 158.2 °C and 155.3 °C, which is in the range expected for isotactic PP (Table 3.3). Indeed, <sup>13</sup>C NMR spectroscopy on the polymers revealed peaks indicative of stereocontrolled isotactic PP (iPP), as well as peaks for stereoirregular and regioirregular PP (Figure 3.19 and Figure 3.20);

significantly, these results provide the first example of isotactic PP from a NNO-type catalyst. Consistent with the GPC data, the  $^{13}\text{C}$  NMR spectra suggest that more than one type of polymer was made (presumably by different active species). Comparison of the  $^{13}\text{C}$  NMR spectra for PP from **8**/PMAO-IP or **8**/MAO to the PP from **8**, **15**, or **16** activated with dry MAO shows identical regioirregular microstructures (Figure 3.21 and Figure 3.11).

**Table 3.3** Propylene polymerization data for **8**/PMAO-IP and **8**/MAO.

Precatalyst	Precatalyst (mmol)	Time (h)	MAO (equiv)	PMAO-IP (equiv)	Yield PP (g) <sup>a</sup>	Activity (g PP (mol cat) <sup>-1</sup> h <sup>-1</sup> )	T <sub>g</sub> (°C)	T <sub>m</sub> (°C)	M <sub>w</sub> (g/mol)	M <sub>w</sub> /M <sub>n</sub>
<b>8</b>	0.010	0.25	-	10000	5.3	2.1 × 10 <sup>6</sup>	-12.8	158.2	65599	18.55
<b>8</b>	0.010	0.25	10000	-	2.4	9.6 × 10 <sup>6</sup>	-31.0	155.3	50041	20.86

<sup>a</sup>Polymerizations were carried out with 700 g of IsoparE, 150 g of propylene, 50 psi of hydrogen at 70 °C for the time indicated.

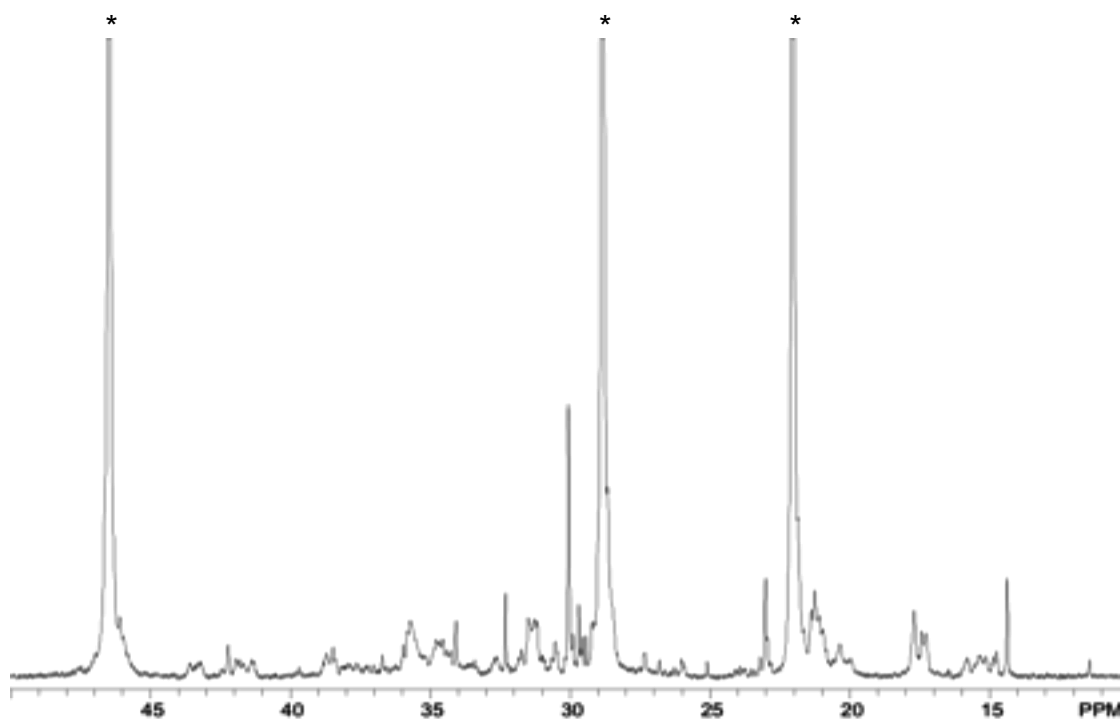


**Figure 3.19**  $^{13}\text{C}$  NMR spectrum of PP from **8**/PMAO-IP at 115 °C in TCE- $d_2$ . Resonances for iPP are indicated with asterisks.

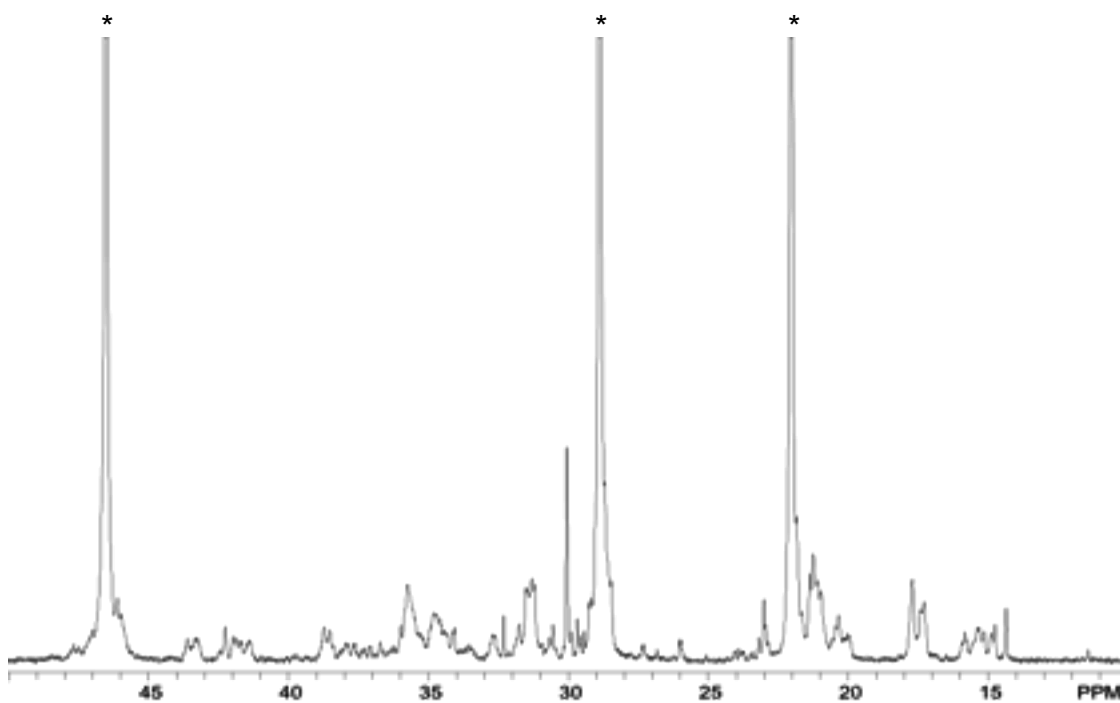


**Figure 3.20**  $^{13}\text{C}$  NMR spectrum of PP from **8**/MAO at 115 °C in  $\text{TCE-}d_2$ . Resonances for iPP are indicated with asterisks.

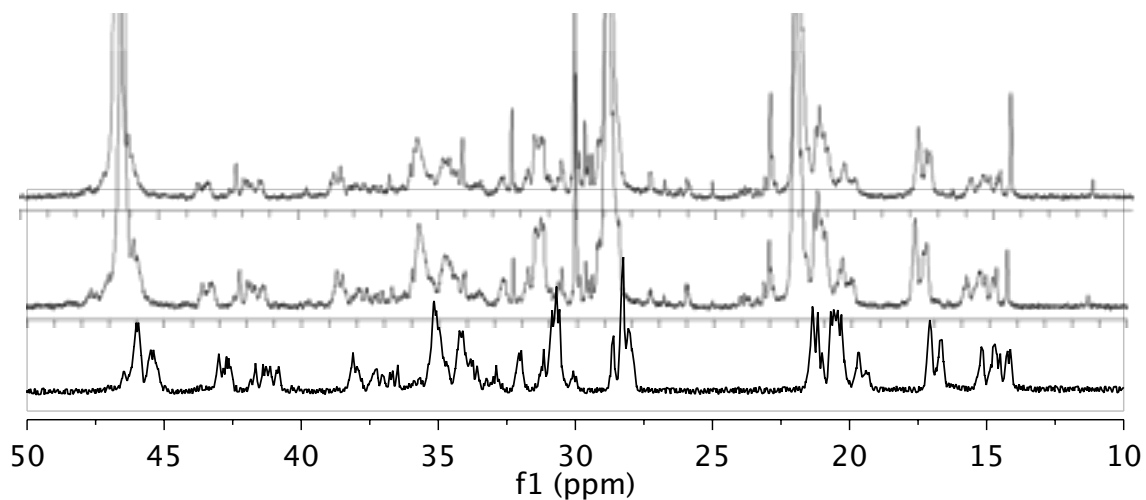


**Figure 3.21**  $^{13}\text{C}$  NMR spectra of PP from complex **8**/PMAO-IP (top), **8**/MAO (middle), and **8**/dry MAO/0 °C (bottom) at 115 or 120 °C in  $\text{TCE-}d_2$ .

These results seem to indicate that at least one new species is obtained from **8** under these polymerization conditions, which polymerizes propylene with

high stereo- and regioselectivity to yield iPP. At the same time, however, the species which was observed to yield regioirregular and stereoirregular PP at 0 or 22 °C is still active. Further studies are needed to separate the different types of PP in order to determine the yields of each polymer and to confirm that the isotactic fraction does not contain any regioerrors.

### Conclusions and Future Work

A series of asymmetric post-metallocene group 4 complexes have been synthesized and tested for propylene polymerization activity. In most cases, the complexes were found to polymerize propylene upon activation with MAO with moderate to good activities. Interestingly, group 4 complexes based on a modular anilide(pyridine)phenoxide framework were discovered to produce highly regioirregular (and stereoirregular) polypropylene resulting from little apparent preference by these catalysts for 1,2- or 2,1-insertions of propylene; importantly, near regiorandom behavior is a new discovery for early metal polymerization catalysts, which typically polymerize propylene with a very high degree of regiocontrol. Furthermore, these NNO complexes feature a variable R-group on the anilide arm (R = 1-phenylethyl, benzyl, or adamantyl) close to the metal center (see Figures 3.4, 3.8, and 3.10 for X-ray structures), which has apparently no influence on monomer selectivity based on analysis of the PP obtained from different NNO catalysts by  $^{13}\text{C}$  NMR spectroscopy (Figure 3.11). Subjecting the anilide(pyridine)phenoxide catalyst **8** to different polymerization conditions,

namely, higher pressures of propylene and higher reaction temperatures, revealed that the catalytically active species that produces regioirregular PP operates regardless of temperature or pressure, but also that at least one new polymerization species is formed at higher temperatures and pressures, which, surprisingly, produces apparently stereo- and regiocontrolled isotactic PP.

Catalyst modification pathways to explain the unusual regioselectivity of NNO-type catalysts were investigated through the synthesis of model complexes, as well as stoichiometric activation studies. These experiments seem to suggest that catalyst modification by dissociation of the anilide arm and subsequent C–H activation of an aryl C–H group, monomer insertion into a metal–ligand bond, or cleavage of the anilide arm R-group are unlikely under standard polymerization conditions. In fact, these studies imply that having an intact anilide(pyridine)phenoxide ligand is critical for regioirregular propylene polymerization and that the active species is coordinated to the NNO ligand. Unfortunately, the underlying factors influencing and ultimately leading to the unique regioselectivity of these interesting post-metallocene polymerization catalysts remain, at this time, a mystery, but perhaps future studies could lead to a better understanding of these complexes. For example, one path of inquiry that has not yet been explored is stoichiometric activations. If clean species could be obtained upon activation with typical stoichiometric activators (boranes, trityl or borate salts), then these studies could be carefully studied by NMR spectroscopy, which could perhaps lead to insights into the speciation of the

active catalyst, as well as the first insertions. Another potentially interesting future study would be to investigate anilide(pyridine)phenoxide species with aryl R-groups, as all of the NNO ligands described here had alkyl groups. Notably, the bis(anilide)pyridyl complexes investigated by our group for propylene polymerization had aryl groups.<sup>8</sup> Although this seemingly small change is unlikely to be the cause of regioirregular polymerizations, it would be worth confirming that, indeed, the anilide R-group has no impact on regioselectivity whether it is a 1°, 2°, or 3° alkyl group or an aryl group.

Although these experiments together do not provide a satisfying explanation of the unusual polymerization behavior of group 4 anilide(pyridine)phenoxide complexes, they represent a small contribution to our understanding of the complex behavior of post-metallocene catalysts. As recently noted by Busico, “the common belief that ‘single-site’ olefin polymerization catalysis is easily amenable to rational understanding” does not hold true for post-metallocene catalysts and in fact, “it is clear that molecular catalysts are not necessarily simple nor foreseeable.”<sup>42</sup> Nonetheless, these results importantly show that new discoveries are still possible in established fields like early metal  $\alpha$ -olefin polymerization catalysis. Continued work in this area will undoubtedly lead to new breakthroughs in post-metallocene catalysts for olefin polymerization.

## Acknowledgements

We thank Tonia Ahmed (SURF), Dr. Jerzy Klosin (Dow), and Professor John Bercaw for contributing experimental data to this chapter.

## Experimental Section

### *General Considerations*

All air- and moisture-sensitive compounds were manipulated using standard high-vacuum and Schlenk techniques or manipulated in a glovebox under a nitrogen atmosphere. Solvents for air- and moisture-sensitive reactions were dried over sodium benzophenone ketyl and stored over titanocene where compatible, or dried by the method of Grubbs.<sup>43</sup>  $\text{TiCl}_2(\text{NMe})_2$ <sup>44</sup>,  $\text{ZrBn}_4$ ,  $\text{HfBn}_4$ <sup>45</sup>, 2-bromo-N-(1-phenylethyl)aniline (**4**)<sup>15</sup>, N-benzyl-2-bromoaniline,<sup>27</sup> N-Adamant-1-yl-2-bromoaniline<sup>28</sup>, and 2-bromo-6-(3,5-di-t-butylphenyl)pyridine<sup>38</sup> were prepared following literature procedures. 2-isopropoxy-4,4,5,5-tetramethyl-1,3,2-dioxaborolane was purchased from Sigma Aldrich and distilled prior to use. Butyllithium solution, potassium phosphate tribasic, barium hydroxide octahydrate and palladium(II)acetate were purchased from Sigma Aldrich and used as received.  $\text{Pd}(\text{PPh}_3)_4$  and 2-(dicyclohexylphosphino)biphenyl were purchased from Strem and used as received. Pinacolborane was purchased from Alfa Aesar. 1,4-dioxane and pinacolborane were dried over 3 Å molecular sieves prior to use. Methylaluminoxane (MAO) was purchased as a toluene solution from Albemarle and was dried in vacuo at 150 °C overnight to remove free

trimethylaluminum before use. Propylene was dried by passage through a column of activated alumina and molecular sieves. Benzene-d<sub>6</sub>, toluene-d<sub>8</sub>, C<sub>6</sub>D<sub>5</sub>Cl, CDCl<sub>3</sub> and 1,1,2,2-tetrachloroethane-d<sub>2</sub> (TCE-d<sub>2</sub>) were purchased from Cambridge Isotopes. Benzene-d<sub>6</sub> and toluene-d<sub>8</sub> were dried over sodium benzophenone ketyl then over titanocene. C<sub>6</sub>D<sub>5</sub>Cl was distilled from CaH<sub>2</sub> and passed through a plug of activated alumina prior to use. NMR spectra were recorded on Varian Mercury 300, Varian INOVA 500 or Varian INOVA 600 spectrometers and referenced to the solvent residual peak. High resolution mass spectra (HRMS) were obtained at the California Institute of Technology Mass Spectral Facility using a JEOL JMS-600H magnetic sector mass spectrometer. Elemental analyses were performed by Midwest Microlab LLC, Indianapolis, IN 46250. X-ray quality crystals were grown as indicated in the experimental procedures for each complex. The crystals were mounted on a glass fiber with Paratone-N oil. Data collection was carried out on a Bruker KAPPA APEX II diffractometer with a 0.71073 Å MoKα source. Structures were determined using direct methods with standard Fourier techniques using the Bruker AXS software package. In some cases, Patterson maps were used in place of the direct methods procedure. Some details regarding crystal data and structure refinement are available in Tables 3.3 and 3.4. Selected bond lengths and angles are supplied in the corresponding figures.

**2-(3,5-di-*tert*-butyl-2-(methoxymethoxy)phenyl)-4,4,5,5-tetramethyl-1,3,2-dioxaborolane** **1**. 26.20 g (0.0796 mol) of 1-bromo-3,5-di-*tert*-butyl-2-(methoxymethoxy)benzene was placed in a 250 mL Schlenk flask charged with a stir bar. The vessel was evacuated and refilled with Ar three times, and then 200 mL of dry Et<sub>2</sub>O was added via cannula to the flask. The reaction solution was cooled to -78 °C in a dry ice/acetone bath, and 46.5 mL (1.5 eq) of *n*-BuLi (2.5 M in hexanes) was added dropwise using an addition funnel. The solution was stirred at -78 °C for 30 min, then 26.0 mL (1.6 eq) of 2-isopropoxy-4,4,5,5-tetramethyl-1,3,2-dioxaborolane was added via syringe. After 30 min at -78 °C, the flask was removed from the cooling bath and allowed to warm to room temperature while stirring; stirring was continued for an additional 2 hours. The reaction was quenched with saturated aqueous ammonium chloride and extracted with Et<sub>2</sub>O (3 × 70 mL). The combined organics were dried over magnesium sulfate and rotovapped to yield a yellow white solid, which was further dried under vacuum. Recrystallization from hot MeOH yielded white microcrystals. 21.38 g, (0.0568 mol, 71% yield). <sup>1</sup>H NMR (500 MHz, CDCl<sub>3</sub>) δ 1.31 (s, 9H, C(CH<sub>3</sub>)<sub>3</sub>), 1.36 (s, 12H, BOC(CH<sub>3</sub>)<sub>2</sub>), 1.44 (s, 9H, C(CH<sub>3</sub>)<sub>3</sub>), 3.57 (s, 3H, CH<sub>2</sub>OCH<sub>3</sub>), 5.16 (s, 2H, CH<sub>2</sub>OCH<sub>3</sub>), 7.47 (d, *J* = 2.6 Hz, 1H, aryl-CH), 7.53 (d, *J* = 2.6 Hz, 1H, aryl-CH). <sup>13</sup>C NMR (126 MHz, CDCl<sub>3</sub>) δ 25.00 (C(CH<sub>3</sub>)<sub>2</sub>), 30.91 (BOC(CH<sub>3</sub>)<sub>2</sub>), 31.68 (C(CH<sub>3</sub>)<sub>2</sub>), 34.54 (C(CH<sub>3</sub>)<sub>2</sub>), 35.34 (BOC(CH<sub>3</sub>)<sub>2</sub>), 57.58 (CH<sub>2</sub>OCH<sub>3</sub>), 83.72 (C(CH<sub>3</sub>)<sub>2</sub>), 100.59 (CH<sub>2</sub>OCH<sub>3</sub>), 120.98,

127.75, 130.97, 140.53, 144.58, 159.34 (aryl-C). HRMS (FAB+)  $m/z$ : calcd for  $C_{22}H_{37}O_4B$   $[M]^+$  376.2785; found 376.2776.

**2-bromo-6-(3,5-di-*tert*-butyl-2-(methoxymethoxy)phenyl)pyridine 2.** An oven-dried 350 mL Schlenk bomb was charged with a stirbar, evacuated and refilled with Ar. Under positive Ar pressure, 6.88 g (0.0292 mol) of 2,6-dimethylpyridine, 10.02 g (0.0266 mol) of 2-(3,5-di-*tert*-butyl-2-(methoxymethoxy)phenyl)-4,4,5,5-tetramethyl-1,3,2-dioxaborolane, 1.55 g (0.00134 mol) of  $Pd(PPh_3)_4$  and 11.33 g (0.0534 mol) of  $K_3PO_4$  crushed with a mortar and pestle were added and the vessel was sealed with a septum. The vessel was evacuated and refilled with Ar three times. 100 mL of dry toluene was added via syringe and the vessel was sealed with a Kontes valve. The reaction mixture was stirred at room temperature for 25 min, during which time the bright yellow color faded to pale yellow (with insoluble white  $K_3PO_4$ ). The vessel was placed in a 115 °C oil bath for 7 days, then cooled to room temperature, and the suspension filtered through celite with the aid of  $Et_2O$ . Solvent was removed in vacuo and the resulting residue was purified by column chromatography on  $SiO_2$  using 1:3  $Et_2O$ /hexanes ( $R_f = 0.625$ ). 9.52 g (82% yield). (This product contains 7% of the bis-arylated pyridine product 2,6-bis(3,5-di-*tert*-butyl-2-(methoxymethoxy)phenyl)pyridine reported previously<sup>7a</sup>, but we have found that we can carry this product on and remove the impurity completely during a later purification step.)  $^1H$  NMR (500 MHz,  $CDCl_3$ )  $\delta$  1.33 (s, 9H,  $C(CH_3)_3$ ), 1.46 (s, 9H,  $C(CH_3)_3$ ), 3.32 (s, 3H,  $CH_2OCH_3$ ), 4.56 (s, 2H,

$\text{CH}_2\text{OCH}_3$ ), 7.39 (d,  $J = 2.5$  Hz, 1H, aryl-CH), 7.47 – 7.41 (m, 2H, aryl-CH), 7.56 (t,  $J = 7.7$  Hz, 1H, aryl-CH), 7.66 (d,  $J = 7.7$  Hz, 1H, aryl-CH).  $^{13}\text{C}$  NMR (126 MHz,  $\text{CDCl}_3$ )  $\delta$  31.05 ( $\text{C}(\text{CH}_3)_3$ ), 31.61 ( $\text{C}(\text{CH}_3)_3$ ), 34.80 ( $\text{C}(\text{CH}_3)_2$ ), 35.58 ( $\text{C}(\text{CH}_3)_2$ ), 57.51 ( $\text{CH}_2\text{OCH}_3$ ), 99.85 ( $\text{CH}_2\text{OCH}_3$ ), 124.11, 125.69, 126.12, 126.48, 132.68, 138.28, 141.90, 142.63, 146.34, 151.40, 159.83 (aryl-C). HRMS (FAB+)  $m/z$ : calcd for  $\text{C}_{21}\text{H}_{29}\text{O}_2\text{NBr}$  [ $\text{M} + \text{H}$ ] $^+$  406.1382; found 406.1385.

**2-(6-(3,5-di-*tert*-butyl-2-(methoxymethoxy)phenyl)pyridin-2-yl)-*N*-(1-phenylethyl)aniline NNO-MOM 5-MOM.** This synthesis is based on reported procedures.<sup>16</sup> To a 350 mL Schlenk bomb charged with a stirbar was added 1.50 g (0.00544 mol) of 2-bromo-*N*-(1-phenylethyl)aniline, and the bomb was evacuated and refilled with Ar. Under positive Ar pressure, 0.0611 g (0.272 mmol) of  $\text{Pd}(\text{OAc})_2$  and 0.382 g (1.09 mmol) of 2-(dicyclohexylphosphino)biphenyl were added and the vessel was sealed with a septum. The reaction vessel was then evacuated and refilled with Ar three times and 15 mL of dry dioxane was added via syringe, followed by 3.79 mL triethylamine (0.0272 mol) and 2.37 mL pinacolborane (0.0163 mol). The reaction vessel was sealed with a Kontes valve and placed in an 80 °C oil bath for 1.5 h, during which time the color changed to olive green, then cooled to room temperature and 3.75 mL of  $\text{H}_2\text{O}$  was added via syringe. Under positive Ar pressure, 5.15 g of  $\text{Ba}(\text{OH})_2 \cdot 8 \text{H}_2\text{O}$  (0.0163 mol) and 2.38 g (1 eq) **2** were added successively. The reaction vessel was sealed with a Kontes valve and placed in

a 90 °C oil bath overnight (~16 h), then cooled to room temperature and the mixture filtered through celite with the aid of Et<sub>2</sub>O. Brine was added to the filtrate, which was extracted with additional Et<sub>2</sub>O (3 × 50 mL). The combined extracts were dried over magnesium sulfate and rotovapped to yield a brown oil, which was further purified by passage through SiO<sub>2</sub> with dichloromethane to yield a yellow oil. (2.6558 g, 0.00508 mol, crude yield 93%; some impurities were subsequently removed following deprotection). <sup>1</sup>H NMR (500 MHz, CDCl<sub>3</sub>) δ 1.33 (s, 9H, C(CH<sub>3</sub>)<sub>3</sub>), 1.43 (d, *J* = 6.7 Hz, 3H, CH(CH<sub>3</sub>)), 1.51 (s, 9H, C(CH<sub>3</sub>)<sub>3</sub>), 3.27 (s, 3H, CH<sub>2</sub>OCH<sub>3</sub>), 4.61 – 4.52 (m, 3H, CH(CH<sub>3</sub>), CH<sub>2</sub>OCH<sub>3</sub>), 6.55 (d, *J* = 8.4 Hz, 1H, aryl-CH), 6.70 (t, *J* = 7.5 Hz, 1H, aryl-CH), 7.14 – 7.09 (m, 1H, aryl-CH), 7.16 (d, *J* = 7.1 Hz, 1H, aryl-CH), 7.19 (t, *J* = 7.1 Hz, 2H, aryl-CH), 7.33 (d, *J* = 6.9 Hz, 2H, aryl-CH), 7.49 – 7.46 (m, 2H, aryl-CH), 7.53 (dd, *J* = 7.7, 0.9 Hz, 1H, aryl-CH), 7.68 (dd, *J* = 7.9, 1.4 Hz, 1H, aryl-CH), 7.73 (d, *J* = 8.1 Hz, 1H, aryl-CH), 7.83 (t, *J* = 7.9 Hz, 1H, aryl-CH), 9.37 (d, *J* = 6.0 Hz, 1H, NH). <sup>13</sup>C NMR (126 MHz, CDCl<sub>3</sub>) δ 25.37 (CH(CH<sub>3</sub>)), 31.11 (C(CH<sub>3</sub>)<sub>3</sub>), 31.68 (C(CH<sub>3</sub>)<sub>3</sub>), 34.78 (C(CH<sub>3</sub>)<sub>3</sub>), 35.62 (C(CH<sub>3</sub>)<sub>3</sub>), 53.15 (CH(CH<sub>3</sub>)), 57.57 (CH<sub>2</sub>OCH<sub>3</sub>), 99.69 (CH<sub>2</sub>OCH<sub>3</sub>), 112.96, 115.61, 119.96, 120.60, 122.21, 124.95, 125.99, 126.28, 126.62, 128.58, 129.23, 130.36, 134.32, 136.99, 142.36, 145.86, 145.96, 147.33, 151.52, 156.55, 159.70 (aryl-C). HRMS (FAB+) *m/z*: calcd for C<sub>35</sub>H<sub>43</sub>O<sub>2</sub>N<sub>2</sub> [M + H]<sup>+</sup> 523.3325; found 523.3299.

**2,4-di-*tert*-butyl-6-(6-(2-((1-phenylethyl)amino)phenyl)pyridin-2-yl)phenol 5-H<sub>2</sub>.** 3.150 g of **5-MOM** was placed in a 250 mL round bottom flask charged with a stir bar, and 30-mL of THF was added to give a yellow solution. The flask was cooled to 0 °C using a water-ice bath; a 30 mL solution of 2:1 conc. HCl/THF was added dropwise; the reaction mixture was stirred for 30 minutes at 0 °C, then removed from the ice bath and allowed to reach room temperature while stirring was continued overnight. The reaction was re-cooled again to 0 °C and quenched with a 2 M aq. NaOH solution to give a solution with neutral pH. The organic layer was extracted with Et<sub>2</sub>O (3 × 50 mL) and the combined organics were dried over magnesium sulfate and rotovapped to yield a yellow-white solid, which was redissolved and passed through a SiO<sub>2</sub> plug, using 10% Et<sub>2</sub>O/hexanes as an eluent, to give an off-white solid. Recrystallization by dissolving in hot hexanes followed by cooling in the freezer yielded a clean off-white powder (868.4 mg, 0.00181 mol, yield: 34%). <sup>1</sup>H NMR (500 MHz, CDCl<sub>3</sub>) δ 1.40 (s, 9H, C(CH<sub>3</sub>)<sub>3</sub>), 1.45 (d, *J* = 6.7 Hz, 3H, CH(CH<sub>3</sub>)), 1.50 (s, 9H C(CH<sub>3</sub>)<sub>3</sub>), 4.57 – 4.47 (m, 1H, CH(CH<sub>3</sub>)), 6.00 (d, *J* = 4.6 Hz, 1H, NH), 6.51 (d, *J* = 8.3 Hz, 1H, aryl-CH), 6.78 – 6.69 (m, 1H, aryl-CH), 7.13 (t, *J* = 7.8 Hz, 1H, aryl-CH), 7.22 (t, *J* = 7.3 Hz, 1H, aryl-CH), 7.31 (t, *J* = 7.6 Hz, 2H, aryl-CH), 7.36 (dd, *J* = 7.6, 1.5 Hz, 1H, aryl-CH), 7.44 (d, *J* = 2.3 Hz, 1H, aryl-CH), 7.51 – 7.46 (m, 3H, aryl-CH), 7.73 (d, *J* = 2.3 Hz, 1H, aryl-CH), 7.89 (d, *J* = 8.2 Hz, 1H, aryl-CH), 7.96 (t, *J* = 8.0 Hz, 1H, aryl-CH), 14.03 (s, 1H, OH). <sup>13</sup>C NMR (126 MHz, CDCl<sub>3</sub>) δ 25.43 (CH(CH<sub>3</sub>)), 29.81 (C(CH<sub>3</sub>)<sub>3</sub>), 31.80 (C(CH<sub>3</sub>)<sub>3</sub>), 34.55 (C(CH<sub>3</sub>)<sub>3</sub>), 35.46 (C(CH<sub>3</sub>)<sub>3</sub>), 53.89 (CH(CH<sub>3</sub>)),

112.58, 116.56, 118.13, 118.41, 121.38, 121.69, 123.05, 126.07, 126.47, 126.89, 128.79, 130.44, 130.61, 137.85, 139.09, 140.16, 145.09, 145.55, 156.31, 156.41, 158.24 (aryl-C). HRMS (FAB+)  $m/z$ : calcd for  $C_{33}H_{38}N_2O$   $[M]^+$  478.2984; found 478.2993.

**(5)ZrBn<sub>2</sub> 6.** A 2 mL benzene solution of **5-H<sub>2</sub>** (95.0 mg, 0.198 mmol) was added to a 2 mL benzene solution of ZrBn<sub>4</sub> (91.0 mg, 0.200 mmol) and stirred for ten minutes under inert atmosphere in the glovebox. Benzene was removed in vacuo from the resulting yellow-brown solution to yield a yellow-brown oil, which was redissolved in pentane and pumped dry several times to remove residual toluene, before being filtered through celite with pentane. The resulting solution was cooled to -30 °C resulting in precipitation of bright yellow solid. (131.2 mg, 0.174 mmol, yield: 88%.) <sup>1</sup>H NMR (500 MHz, toluene-*d*<sub>8</sub>, -20 °C) δ 1.48 (s, 9H, C(CH<sub>3</sub>)<sub>3</sub>), 1.63 (s, 9H, C(CH<sub>3</sub>)<sub>3</sub>), 1.74 (d,  $J = 6.5$  Hz, 3H, CH(CH<sub>3</sub>)), 1.90 (d,  $J = 10.3$  Hz, 1H, ZrCH<sub>2</sub>), 2.02 (d,  $J = 10.3$  Hz, 1H, ZrCH<sub>2</sub>), 2.61 (d,  $J = 10.7$  Hz, 1H, ZrCH<sub>2</sub>), 2.73 (d,  $J = 10.7$  Hz, 1H, ZrCH<sub>2</sub>), 4.63 (q,  $J = 6.4$  Hz, 1H, CH(CH<sub>3</sub>)), 6.23 (d,  $J = 7.4$  Hz, 2H, aryl-CH), 6.37 (d,  $J = 7.7$  Hz, 1H, aryl-CH), 6.52 (t,  $J = 6.5$  Hz, 3H, aryl-CH), 6.63 (t,  $J = 7.6$  Hz, 2H, aryl-CH), 6.68 (t,  $J = 7.6$  Hz, 2H, aryl-CH), 6.75 (t,  $J = 7.3$  Hz, 1H, aryl-CH), 6.80 (t,  $J = 7.5$  Hz, 1H, aryl-CH), 7.22 – 7.11 (m, 3H, aryl-CH), 7.29 (d,  $J = 7.3$  Hz, 2H, aryl-CH), 7.33 (d,  $J = 8.2$  Hz, 1H, aryl-CH), 7.37 (t,  $J = 7.6$  Hz, 2H, aryl-CH), 7.46 (d,  $J = 2.1$  Hz, 1H, aryl-CH), 7.57 (d,  $J = 2.2$  Hz, 1H, aryl-CH). <sup>13</sup>C NMR (126 MHz, toluene-*d*<sub>8</sub>, -20 °C) δ 24.87

(CH(CH<sub>3</sub>)), 30.46 (C(CH<sub>3</sub>)<sub>3</sub>), 32.26 (C(CH<sub>3</sub>)<sub>3</sub>), 34.97 (C(CH<sub>3</sub>)<sub>3</sub>), 36.15 (C(CH<sub>3</sub>)<sub>3</sub>), 64.06 (ZrCH<sub>2</sub>), 65.45 (CH(CH<sub>3</sub>)), 66.19 (ZrCH<sub>2</sub>), 120.07, 121.83, 122.40, 124.02, 124.52, 124.82, 126.35, 126.65, 126.77, 126.86, 127.14, 128.40, 128.61, 128.90, 129.55, 129.75, 130.42, 132.52, 132.75, 134.95, 138.65, 138.87, 142.00, 144.56, 145.89, 149.79, 155.00, 155.11, 158.71 (aryl-C). Anal. Calcd for C<sub>47</sub>H<sub>50</sub>N<sub>2</sub>OZr (%): C, 75.25; H, 6.72; N, 3.73. Found (1): C, 73.39; H, 6.72; N, 3.68. (2): C, 73.62; H, 6.50; N, 3.68. (This compound is air- and moisture-sensitive and despite repeated attempts satisfactory %C analysis could not be obtained.)

**(5)HfBn<sub>2</sub> 7.** A 2 mL benzene solution of **5-H<sub>2</sub>** (54.6 mg, 0.114 mmol) was added to a 2 mL benzene solution of HfBn<sub>4</sub> (62.5 mg, 0.115 mmol) and stirred for ten minutes under inert atmosphere in the glovebox. Benzene was removed in vacuo from the resulting yellow solution to yield a yellow solid, which was redissolved in pentane and pumped dry several times to remove residual toluene to give a fine pale yellow powder (62.7 mg, 0.075 mmol, yield: 66%). <sup>1</sup>H NMR (500 MHz, toluene-*d*<sub>8</sub>, -20 °C) δ 1.48 (s, 9H, C(CH<sub>3</sub>)<sub>3</sub>), 1.64 (s, 9H, C(CH<sub>3</sub>)<sub>3</sub>), 1.67 (d, *J* = 11.3 Hz, 1H, HfCH<sub>2</sub>), 1.80 – 1.74 (m, 4H, HfCH<sub>2</sub>, CH(CH<sub>3</sub>)), 2.40 (d, *J* = 11.5 Hz, 1H, HfCH<sub>2</sub>), 2.55 (d, *J* = 11.5 Hz, 1H, HfCH<sub>2</sub>), 4.79 (q, *J* = 6.4 Hz, 1H, CH(CH<sub>3</sub>)), 6.27 (d, *J* = 7.4 Hz, 2H, aryl-CH), 6.42 (d, *J* = 7.7 Hz, 1H, aryl-CH), 6.53 – 6.45 (m, 3H, aryl-CH), 6.67 (dd, *J* = 17.0, 7.7 Hz, 4H, aryl-CH), 6.76 (dd, *J* = 13.9, 7.1 Hz, 2H, aryl-CH), 6.88 (d, *J* = 8.2 Hz, 1H, aryl-CH), 6.93 (d, *J* = 7.7 Hz, 1H, aryl-CH), 7.16 – 7.11 (m, 3H, aryl-CH), 7.30 (d, *J* = 7.5 Hz, 2H, aryl-CH), 7.35 (d, *J* =

8.2 Hz, 1H, aryl-CH), 7.39 (d,  $J = 7.5$  Hz, 2H, aryl-CH), 7.43 (d,  $J = 2.2$  Hz, 1H, aryl-CH), 7.60 (d,  $J = 2.2$  Hz, 1H, aryl-CH).  $^{13}\text{C}$  NMR (126 MHz, toluene- $d_8$ ,  $-20$  C°)  $\delta$  25.13 (CH(CH<sub>3</sub>)), 30.43 (C(CH<sub>3</sub>)<sub>3</sub>), 32.25 (C(CH<sub>3</sub>)<sub>3</sub>), 34.95 (C(CH<sub>3</sub>)<sub>3</sub>), 36.07 (C(CH<sub>3</sub>)<sub>3</sub>), 64.57 (CH(CH<sub>3</sub>)), 71.19 (HfCH<sub>2</sub>), 72.13 (HfCH<sub>2</sub>), 120.55, 121.76, 122.37, 124.41, 124.62, 124.86, 125.57, 125.78, 126.73, 126.85, 126.92, 127.16, 128.41, 128.63, 128.94, 129.56, 129.60, 129.66, 131.56, 132.55, 135.73, 138.97, 139.02, 142.12, 145.14, 146.61, 149.61, 154.94, 155.12, 158.14 (aryl-C). Anal. Calcd for C<sub>47</sub>H<sub>50</sub>HfN<sub>2</sub>O (%): C, 67.41; H, 6.02; N, 3.35. Found (1): C, 61.82; H, 5.65; N, 3.55. (2): C, 59.22; H, 5.68; N, 3.55. (This compound is air- and moisture-sensitive and despite repeated attempts satisfactory %C analysis could not be obtained.)

**(5)TiCl<sub>2</sub> 8.** A 4 mL benzene solution of **5-H<sub>2</sub>** (301.1 mg, 0.629 mmol) was added to a 4 mL benzene solution of TiCl<sub>2</sub>(NMe<sub>2</sub>)<sub>2</sub> (130.8 mg, 0.632 mmol) and stirred for ten minutes under inert atmosphere in the glovebox. Benzene was removed in vacuo from the resulting dark red solution to yield a dark orange solid, which was triturated several times with pentane to remove free dimethylamine (373.6 mg, 0.627 mmol, quantitative yield).  $^1\text{H}$  NMR (500 MHz, C<sub>5</sub>D<sub>5</sub>Cl)  $\delta$  1.34 (s, 9H, C(CH<sub>3</sub>)<sub>3</sub>), 1.78 (s, 9H, C(CH<sub>3</sub>)<sub>3</sub>), 2.31 (d,  $J = 6.7$  Hz, 3H, CH(CH<sub>3</sub>)), 5.12 – 5.06 (m, 1H, CH(CH<sub>3</sub>)), 6.36 (dd,  $J = 7.7, 1.7$  Hz, 2H, aryl-CH), 6.77 – 6.72 (m, 2H, aryl-CH), 7.04 – 7.00 (m, 1H, aryl-CH), 7.06 (d,  $J = 7.7$  Hz, 1H, aryl-CH), 7.23 – 7.19 (m, 4H, aryl-CH), 7.39 (d,  $J = 7.5$  Hz, 1H, aryl-CH), 7.51 (t,  $J = 8.0$  Hz, 1H,

aryl-CH), 7.79 – 7.72 (m, 3H, aryl-CH).  $^{13}\text{C}$  NMR (126 MHz,  $\text{C}_5\text{D}_5\text{Cl}$ )  $\delta$  25.20 (CH(CH<sub>3</sub>)), 30.50 (C(CH<sub>3</sub>)<sub>3</sub>), 31.44 (C(CH<sub>3</sub>)<sub>3</sub>), 34.78 (C(CH<sub>3</sub>)<sub>3</sub>), 35.80 (C(CH<sub>3</sub>)<sub>3</sub>), 72.23 (CH(CH<sub>3</sub>)), 121.70, 123.57, 123.77, 124.01, 126.20, 127.03, 128.11, 128.33, 128.53, 128.62, 129.53, 132.94, 133.91, 135.26, 137.92, 139.03, 144.16, 145.45, 151.46, 152.70, 158.24 (aryl-C). Anal. Calcd for  $\text{C}_{33}\text{H}_{36}\text{Cl}_2\text{N}_2\text{OTi}$  (%): C, 66.57; H, 6.09; N, 4.70. Found: C, 66.43; H, 5.93; N, 4.78.

**(5)TiBn<sub>2</sub> 9.** To a 5 mL toluene solution of **8** (12.0 mg, 0.020 mmol) was added 42.3  $\mu\text{L}$  of a BnMgCl solution (2.1 equiv) via syringe and the resulting orange solution stirred for ten minutes under inert atmosphere in the glovebox. The reaction mixture was filtered through a plug of celite with the aid of toluene and then toluene was removed in vacuo to yield a red solid. The red solid was triturated several times with pentane.  $^1\text{H}$  NMR (300 MHz,  $\text{C}_6\text{D}_6$ )  $\delta$  1.48 (s, 9H, C(CH<sub>3</sub>)<sub>3</sub>), 1.76 (s, 9H, C(CH<sub>3</sub>)<sub>3</sub>), 1.80 (d,  $J = 6.6$  Hz, 3H, CH(CH<sub>3</sub>)), 2.40 (d,  $J = 9.0$  Hz, 1H, ZrCH<sub>2</sub>), 2.86 (d,  $J = 8.7$  Hz, 1H, ZrCH<sub>2</sub>), 3.15 (d,  $J = 9.8$  Hz, 1H, ZrCH<sub>2</sub>), 3.25 (d,  $J = 9.9$  Hz, 1H, ZrCH<sub>2</sub>), 4.85 (q,  $J = 6.6$  Hz, 1H, CH(CH<sub>3</sub>)), 6.12 (d,  $J = 7.1$  Hz, 2H, aryl-CH), 6.41 (d,  $J = 7.3$  Hz, 2H, aryl-CH), 6.45 – 6.62 (m, 4H, aryl-CH), 6.69 (t,  $J = 7.3$  Hz, 3H, aryl-CH), 6.82 (t,  $J = 7.0$  Hz, 1H, aryl-CH), 6.97 – 7.04 (m, 2H, aryl-CH), 7.10 (dd,  $J = 10.2, 6.2$  Hz, 2H, aryl-CH), 7.22 (td,  $J = 7.6, 7.0, 1.6$  Hz, 1H, aryl-CH), 7.38 (dd,  $J = 8.8, 6.0$  Hz, 5H, aryl-CH), 7.52 (d,  $J = 1.9$  Hz, 1H, aryl-CH), 7.67 (d,  $J = 2.2$  Hz, 1H, aryl-CH).

**<sup>Bn</sup>NNO-MOM 10-MOM**. Followed the same procedure as **5-MOM** starting from *N*-benzyl-2-bromoaniline. Crude yield: 91% yellow oil; some impurities were subsequently removed following deprotection. <sup>1</sup>H NMR (500 MHz, CDCl<sub>3</sub>) δ 1.33 (s, 9H, C(CH<sub>3</sub>)<sub>3</sub>), 1.50 (s, 9H, C(CH<sub>3</sub>)<sub>3</sub>), 3.23 (s, 3H, CH<sub>2</sub>OCH<sub>3</sub>), 4.49 (s, 2H, CH<sub>2</sub>OCH<sub>3</sub>), 4.50 (d, *J* = 4.3 Hz, 2H, benzyl-CH<sub>2</sub>), 6.69 (dd, *J* = 8.3, 1.2 Hz, 1H, aryl-CH), 6.76 (ddd, *J* = 8.2, 7.3, 1.1 Hz, 1H, aryl-CH), 7.14 – 7.17 (m, 2H, aryl-CH), 7.20 – 7.24 (m, 1H, aryl-CH), 7.29 – 7.33 (m, 1H, aryl-CH), 7.42 (d, *J* = 2.5 Hz, 1H, aryl-CH), 7.47 (d, *J* = 2.6 Hz, 1H, aryl-CH), 7.54 (dd, *J* = 7.7, 0.9 Hz, 1H, aryl-CH), 7.69 – 7.74 (m, 2H, aryl-CH), 7.84 (t, *J* = 7.9 Hz, 1H, aryl-CH), 9.44 (s, 1H, NH). <sup>13</sup>C NMR (126 MHz, CDCl<sub>3</sub>) δ 31.02 (C(CH<sub>3</sub>)<sub>3</sub>), 31.63 (C(CH<sub>3</sub>)<sub>3</sub>), 34.71 (C(CH<sub>3</sub>)<sub>3</sub>), 35.58 (C(CH<sub>3</sub>)<sub>3</sub>), 47.39 (benzyl-CH<sub>2</sub>), 57.56 (CH<sub>2</sub>OCH<sub>3</sub>), 99.73 (CH<sub>2</sub>OCH<sub>3</sub>), 112.07, 112.94, 115.80, 119.92, 121.57, 124.86, 126.35, 126.62, 126.88, 128.41, 129.25, 130.50, 134.14, 137.27, 139.93, 142.45, 145.99, 148.16, 151.72, 156.54, 159.50 (aryl-C). HRMS (FAB+) *m/z*: calcd for C<sub>34</sub>H<sub>40</sub>N<sub>2</sub>O<sub>2</sub> [M + H]<sup>+</sup> 508.3090; found 508.3081.

**<sup>Bn</sup>NNO-H<sub>2</sub> 10-H<sub>2</sub>**. 1.0010 g of **10-MOM** was placed in a 100 mL round bottom flask charged with a stirbar and 5 mL of THF and 2 mL of MeOH were added to give a yellow solution. The flask was cooled to 0 °C with a water-ice bath; a 6 mL solution of 1:1 MeOH/conc. HCl was added dropwise resulting in the solution turning brighter yellow. The reaction was stirred for 30 min at 0 °C, then removed from the ice bath and allowed to reach room temperature while stirring was

continued overnight. The solution was then quenched with 2 M aq. NaOH to give a solution with neutral pH. The organic layer was extracted with diethyl ether (3 × 70 mL) and the combined organics were dried over magnesium sulfate and rotovapped to reveal a yellow oil, which was redissolved in dichloromethane and passed through a SiO<sub>2</sub> plug to give an orange oil. Recrystallization by dissolving in hot hexanes followed by cooling in the freezer yielded bright yellow crystals. 412.7 mg (45% yield). <sup>1</sup>H NMR (500 MHz, CDCl<sub>3</sub>) δ 1.40 (s, 9H, C(CH<sub>3</sub>)<sub>3</sub>), 1.49 (s, 9H, C(CH<sub>3</sub>)<sub>3</sub>), 4.42 (s, 2H, benzyl-CH<sub>2</sub>), 6.08 (s, 1H, NH), 6.70 (dd, *J* = 8.3, 1.0 Hz, 1H, aryl-CH), 6.80 (td, *J* = 7.4, 1.1 Hz, 1H, aryl-CH), 7.18 – 7.32 (m, 4H, aryl-CH), 7.40 (dd, *J* = 7.6, 1.6 Hz, 1H, aryl-CH), 7.42 – 7.46 (m, 3H, aryl-CH), 7.48 (dd, *J* = 7.7, 0.9 Hz, 1H, aryl-CH), 7.69 (d, *J* = 2.4 Hz, 1H, aryl-CH), 7.85 (d, *J* = 7.7 Hz, 1H, aryl-CH), 7.95 (t, *J* = 8.0 Hz, 1H, aryl-CH), 13.88 (s, 1H, OH). <sup>13</sup>C NMR (126 MHz, CDCl<sub>3</sub>) δ 29.75 (C(CH<sub>3</sub>)<sub>3</sub>), 31.77 (C(CH<sub>3</sub>)<sub>3</sub>), 34.52 (C(CH<sub>3</sub>)<sub>3</sub>), 35.47 (C(CH<sub>3</sub>)<sub>3</sub>), 47.99 (benzyl-CH<sub>2</sub>), 111.79, 116.88, 118.29, 118.63, 121.42, 121.56, 123.50, 126.41, 127.01, 127.08, 128.71, 130.52, 130.61, 137.79, 139.12, 139.54, 140.26, 146.02, 156.18, 156.20, 158.35 (aryl-C). HRMS (FAB+) *m/z*: calcd for C<sub>32</sub>H<sub>36</sub>ON<sub>2</sub> [M]<sup>+</sup> 464.2828; found 464.2817.

**<sup>Ad</sup>NNO-MOM 11-MOM.** Followed the same procedure as **5-MOM** starting from *N*-Adamant-1-yl-2-bromoaniline. Precipitate forms while stirring overnight. Crude yield: 62% golden foamy oil; some impurities were subsequently removed following deprotection. <sup>1</sup>H NMR (500 MHz, CDCl<sub>3</sub>) δ 1.35 (s, 9H, C(CH<sub>3</sub>)<sub>3</sub>), 1.51

(s, 9H, C(CH<sub>3</sub>)<sub>3</sub>), 1.57 – 1.75 (m, 6H, Ad-CH<sub>2</sub>), 1.90 (dd, *J* = 7.1, 2.9 Hz, 6H, Ad-CH<sub>2</sub>), 1.99 – 2.16 (m, 3H, Ad-CH), 3.30 (s, 3H, CH<sub>2</sub>OCH<sub>3</sub>), 4.56 (s, 2H, CH<sub>2</sub>OCH<sub>3</sub>), 7.12 – 7.19 (m, 1H, aryl-CH), 7.22 (ddd, *J* = 8.6, 7.0, 1.7 Hz, 1H, aryl-CH), 7.34 – 7.42 (m, 1H, aryl-CH), 7.45 (d, *J* = 2.5 Hz, 1H, aryl-CH), 7.48 (d, *J* = 2.6 Hz, 1H), 7.56 (dd, *J* = 7.7, 0.9 Hz, 1H, aryl-CH), 7.61 (ddd, *J* = 6.8, 5.1, 1.3 Hz, 2H, aryl-CH), 7.78 (t, *J* = 7.9 Hz, 1H, aryl-CH), 8.35 (s, 1H, NH). <sup>13</sup>C NMR (126 MHz, CDCl<sub>3</sub>) δ 29.77 (Ad-CH), 31.03 (C(CH<sub>3</sub>)<sub>3</sub>), 31.69 (C(CH<sub>3</sub>)<sub>3</sub>), 34.79 (C(CH<sub>3</sub>)<sub>3</sub>), 35.58 (C(CH<sub>3</sub>)<sub>3</sub>), 36.66 (Ad-CH<sub>2</sub>), 43.01 (Ad-CH<sub>2</sub>), 51.89 (Ad-quat), 57.56 (CH<sub>2</sub>OCH<sub>3</sub>), 99.61 (CH<sub>2</sub>OCH<sub>3</sub>), 119.35, 120.76, 122.31, 124.86, 126.34, 127.43, 128.86, 129.35, 130.12, 133.97, 136.87, 142.29, 145.82, 151.47, 156.17, 158.29, 159.93 (aryl-C). HRMS (FAB+) *m/z*: calcd for C<sub>37</sub>H<sub>49</sub>N<sub>2</sub>O<sub>2</sub> [M + H]<sup>+</sup> 553.3794; found 553.3790.

**Ad<sup>d</sup>NNO-H<sub>2</sub> 11-H<sub>2</sub>**. Followed the same procedure as **10-H<sub>2</sub>** except used diethyl ether as the eluent through the SiO<sub>2</sub> plug instead of dichloromethane. An off-white powder precipitated from a hot hexanes solution cooled in the freezer. Yield: 42% off-white powder. <sup>1</sup>H NMR (500 MHz, CDCl<sub>3</sub>) δ 1.39 (s, 9H, C(CH<sub>3</sub>)<sub>3</sub>), 1.49 (s, 9H, C(CH<sub>3</sub>)<sub>3</sub>), 1.62 – 1.70 (m, 6H, Ad-CH<sub>2</sub>), 1.98 (d, *J* = 3.0 Hz, 6H, Ad-CH<sub>2</sub>), 2.07 (s, 3H, Ad-CH), 5.44 (s, 1H, NH), 6.74 (td, *J* = 7.4, 1.1 Hz, 1H, aryl-CH), 7.12 (dd, *J* = 8.5, 1.2 Hz, 1H, aryl-CH), 7.22 – 7.26 (m, 1H, aryl-CH), 7.30 (dd, *J* = 7.6, 1.7 Hz, 1H, aryl-CH), 7.39 (dd, *J* = 7.7, 1.0 Hz, 1H, aryl-CH), 7.42 (d, *J* = 2.4 Hz, 1H, aryl-CH), 7.71 (d, *J* = 2.4 Hz, 1H, aryl-CH), 7.86 (d, *J* = 7.6 Hz,

1H, aryl-CH), 7.91 (dd,  $J = 8.2, 7.6$  Hz, 1H, aryl-CH), 13.96 (s, 1H, OH).  $^{13}\text{C}$  NMR (126 MHz,  $\text{CDCl}_3$ )  $\delta$  29.82 (Ad-CH), 29.87 ( $\text{C}(\text{CH}_3)_3$ ), 31.79 ( $\text{C}(\text{CH}_3)_3$ ), 34.52 ( $\text{C}(\text{CH}_3)_3$ ), 35.45 ( $\text{C}(\text{CH}_3)_3$ ), 36.60 (Ad-CH<sub>2</sub>), 42.57 (Ad-CH<sub>2</sub>), 51.87 (Ad-quat), 115.33, 116.22, 117.82, 118.15, 121.24, 121.90, 124.88, 126.38, 129.69, 131.21, 137.80, 138.93, 139.90, 144.59, 156.49, 156.62, 158.12 (aryl-C). HRMS (FAB+)  $m/z$ : calcd for  $\text{C}_{35}\text{H}_{44}\text{ON}_2$   $[\text{M}]^+$  508.3454; found 508.3441.

**2-bromo-N-methoxyethylaniline 12.** Copper (I) iodide (2.38 g, 0.0125 mol) and potassium phosphate (12.81 g, 0.0603 mol) were placed in a round bottom bomb charged with a stir bar. The bomb was sealed with a septum and placed under vacuum, then backfilled with Ar and isopropanol (30.0 ml), ethylene glycol (4.0 mL, 0.0717 mol), 2-methoxyethylamine (3.2 mL, 0.0368 mol) and 2-bromiodobenzene (3.9 mL, 0.0304 mol) were added via syringe. The flask was sealed with a Kontes valve and the reaction vessel was placed in a 90 °C oil bath to give a yellow suspension, which then turned green-blue within 30 min. The reaction was kept at 90 °C for 2 d then allowed to cool to room temperature and 30 mL of diethyl ether and 30 mL of water were added to the reaction mixture. The organic layer was extracted with diethyl ether (3 × 100 mL) and the combined organic phases were washed with water and brine until the aqueous layer was colorless (the first washes with water were teal). The combined organics were dried over sodium sulfate and the solvent was removed by rotary evaporation to give a brown oil. The oil was further purified by column

chromatography on silica gel using 10% ethyl acetate/hexanes ( $R_f = 0.33$ ). 2.273 g brown oil (0.00989 mol, Yield: 33% yield).  $^1\text{H}$  NMR (500 MHz,  $\text{CDCl}_3$ )  $\delta$  3.34 (t,  $J = 5.3$  Hz, 2H,  $\text{CH}_2\text{CH}_2\text{OCH}_3$ ), 3.42 (s, 3H,  $\text{CH}_2\text{CH}_2\text{OCH}_3$ ), 3.65 (dd,  $J = 5.7, 5.0$  Hz, 2H,  $\text{CH}_2\text{CH}_2\text{OCH}_3$ ), 4.65 (s, 1H, *NH*), 6.58 (ddd,  $J = 7.9, 7.4, 1.5$  Hz, 1H, aryl-*CH*), 6.65 (dd,  $J = 8.1, 1.5$  Hz, 1H, aryl-*CH*), 7.18 (ddd,  $J = 8.1, 7.3, 1.5$  Hz, 1H, aryl-*CH*), 7.43 (dd,  $J = 7.9, 1.5$  Hz, 1H, aryl-*CH*).  $^{13}\text{C}$  NMR (126 MHz,  $\text{CDCl}_3$ )  $\delta$  43.54 ( $\text{CH}_2\text{CH}_2\text{OCH}_3$ ), 58.99 ( $\text{CH}_2\text{CH}_2\text{OCH}_3$ ), 70.87 ( $\text{CH}_2\text{CH}_2\text{OCH}_3$ ), 110.13, 111.49, 118.02, 128.54, 132.57, 145.11 (aryl-*C*). HRMS (FAB+)  $m/z$ : calcd for  $\text{C}_9\text{H}_{12}\text{ONBr}$   $[\text{M}]^+$  229.0102; found 229.0110.

**MeOEt<sup>NO-MOM</sup> 13-MOM**. Followed the same procedure as **5-MOM** starting from 2-bromo-*N*-methoxyethylaniline **12**. Estimated yield: 81% brown oil.  $^1\text{H}$  NMR (500 MHz,  $\text{CDCl}_3$ )  $\delta$  1.34 (s, 9H,  $\text{C}(\text{CH}_3)_3$ ), 1.51 (s, 9H,  $\text{C}(\text{CH}_3)_3$ ), 3.06 (s, 3H,  $\text{CH}_2\text{CH}_2\text{OCH}_3$ ), 3.28 (s, 3H,  $\text{OCH}_2\text{OCH}_3$ ), 3.40 – 3.43 (m, 2H,  $\text{CH}_2\text{CH}_2\text{OCH}_3$ ), 3.51 – 3.55 (m, 2H,  $\text{CH}_2\text{CH}_2\text{OCH}_3$ ), 4.57 (s, 2H,  $\text{OCH}_2\text{OCH}_3$ ), 6.74 (td,  $J = 7.5, 1.1$  Hz, 1H, aryl-*CH*), 6.79 (dd,  $J = 8.3, 1.1$  Hz, 1H, aryl-*CH*), 7.27 – 7.31 (m, 1H, aryl-*CH*), 7.40 (d,  $J = 2.5$  Hz, 1H, aryl-*CH*), 7.44 (d,  $J = 2.5$  Hz, 1H, aryl-*CH*), 7.50 (dd,  $J = 7.6, 0.9$  Hz, 1H, aryl-*CH*), 7.66 (ddd,  $J = 7.8, 3.2, 1.3$  Hz, 2H, aryl-*CH*), 7.80 (t,  $J = 7.9$  Hz, 1H, aryl-*CH*), 8.94 (t,  $J = 5.6$  Hz, 1H, *NH*).  $^{13}\text{C}$  NMR (126 MHz,  $\text{CDCl}_3$ )  $\delta$  31.06 ( $\text{C}(\text{CH}_3)_3$ ), 31.69 ( $\text{C}(\text{CH}_3)_3$ ), 34.76 ( $\text{C}(\text{CH}_3)_3$ ), 35.60 ( $\text{C}(\text{CH}_3)_3$ ), 43.02 ( $\text{CH}_2\text{CH}_2\text{OCH}_3$ ), 57.62 ( $\text{OCH}_2\text{OCH}_3$ ), 58.59 ( $\text{CH}_2\text{CH}_2\text{OCH}_3$ ), 71.31 ( $\text{CH}_2\text{CH}_2\text{OCH}_3$ ), 99.88 ( $\text{OCH}_2\text{OCH}_3$ ), 111.43, 115.66, 119.94, 121.03,

121.73, 124.78, 126.42, 129.35, 129.42, 130.51, 137.09, 142.32, 145.89, 148.23, 151.77, 156.48, 159.47 (aryl-C). HRMS (FAB+)  $m/z$ : calcd for  $C_{30}H_{41}O_3N_2$  [M + H]<sup>+</sup> 477.3117; found 477.3115.

**MeOEt** **NNO-H<sub>2</sub> 13-H<sub>2</sub>**. 1.4004 g of **13-MOM** was placed in a 100 mL round bottom flask charged with a stir bar, and 50-mL of THF was added to give a brown solution. The flask was cooled to 0 °C using a water-ice bath; a 50 mL solution of 4:1 v/v conc. HCl/THF was added dropwise; the reaction mixture was stirred for 30 minutes at 0 °C, then removed from the ice bath and allowed to reach room temperature while stirring was continued overnight. The reaction was quenched with a 2 M aq. NaOH solution to give a solution with neutral pH. The organic layer was extracted with Et<sub>2</sub>O (3 × 50 mL) and the combined organics were dried over magnesium sulfate and rotovapped to yield a yellow-white solid, which was redissolved and passed through a SiO<sub>2</sub> plug, using 3:2 dichloromethane/hexanes as an eluent, to give a yellow crystalline solid. (428.6 mg, 0.991 mol, yield: 34%).  
<sup>1</sup>H NMR (500 MHz, CDCl<sub>3</sub>) δ 1.38 (s, 9H, C(CH<sub>3</sub>)<sub>3</sub>), 1.49 (s, 9H, C(CH<sub>3</sub>)<sub>3</sub>), 3.16 (s, 3H, CH<sub>2</sub>CH<sub>2</sub>OCH<sub>3</sub>), 3.38 (d,  $J = 5.7$  Hz, 2H, CH<sub>2</sub>CH<sub>2</sub>OCH<sub>3</sub>), 3.60 (t,  $J = 5.8$  Hz, 2H, CH<sub>2</sub>CH<sub>2</sub>OCH<sub>3</sub>), 5.80 (s, 1H, NH), 6.77 – 6.85 (m, 2H, aryl-CH), 7.30 – 7.35 (m, 1H, aryl-CH), 7.40 (dd,  $J = 7.9, 1.6$  Hz, 1H, aryl-CH), 7.42 (d,  $J = 2.4$  Hz, 1H, aryl-CH), 7.45 (dd,  $J = 7.8, 0.9$  Hz, 1H, aryl-CH), 7.68 (d,  $J = 2.3$  Hz, 1H, aryl-CH), 7.82 (d,  $J = 8.1$  Hz, 1H, aryl-CH), 7.92 (t,  $J = 7.9$  Hz, 1H, aryl-CH), 13.69 (s, 1H, OH). <sup>13</sup>C NMR (126 MHz, CDCl<sub>3</sub>) δ 29.78 (C(CH<sub>3</sub>)<sub>3</sub>), 31.77 (C(CH<sub>3</sub>)<sub>3</sub>), 34.50

(C(CH<sub>3</sub>)<sub>3</sub>), 35.43 (C(CH<sub>3</sub>)<sub>3</sub>), 43.24 (CH<sub>2</sub>CH<sub>2</sub>OCH<sub>3</sub>), 58.72 (CH<sub>2</sub>CH<sub>2</sub>OCH<sub>3</sub>), 71.01 (CH<sub>2</sub>CH<sub>2</sub>OCH<sub>3</sub>), 111.41, 116.85, 118.21, 118.75, 121.44, 121.49, 123.57, 126.22, 130.57, 130.60, 137.57, 138.91, 140.16, 146.15, 156.02, 156.12, 158.34 (aryl-C). HRMS (FAB+) *m/z*: calcd for C<sub>28</sub>H<sub>37</sub>O<sub>2</sub>N<sub>2</sub> [M + H]<sup>+</sup> 433.2855; found 433.2869.

**(10)ZrBn<sub>2</sub> 14.** A 2 mL benzene solution of **10-H<sub>2</sub>** (66.5 mg, 0.143 mmol) was added to a 2 mL benzene solution of ZrBn<sub>4</sub> (65.0 mg, 0.143 mmol) and stirred for ten minutes under inert atmosphere in the glovebox. Benzene was removed in vacuo from the resulting yellow solution to yield a yellow oil, which was redissolved in pentane and pumped dry several times to remove residual toluene to reveal a yellow powder. (90.8 mg, 0.123 mmol, yield: 86%). <sup>1</sup>H NMR (500 MHz, toluene-*d*<sub>8</sub>) δ 1.40 (s, 9H, C(CH<sub>3</sub>)<sub>3</sub>), 1.64 (s, 9H, C(CH<sub>3</sub>)<sub>3</sub>), 2.06 (d, *J* = 10.2 Hz, 2H, Zr-CH<sub>2</sub>), 2.22 (d, *J* = 10.3 Hz, 2H, Zr-CH<sub>2</sub>), 4.85 (s, 2H, NCH<sub>2</sub>Ph), 6.64 – 6.74 (m, 7H, aryl-CH), 6.77 – 6.81 (m, 1H, aryl-CH), 6.80 – 6.89 (m, 11H, aryl-CH), 7.07 (dd, *J* = 7.9, 1.6 Hz, 1H, aryl-CH), 7.25 (ddd, *J* = 8.5, 7.1, 1.6 Hz, 1H, aryl-CH), 7.35 (dd, *J* = 8.2, 1.2 Hz, 1H, aryl-CH), 7.40 (d, *J* = 2.3 Hz, 1H, aryl-CH), 7.60 (d, *J* = 2.2 Hz, 1H, aryl-CH). <sup>13</sup>C NMR (126 MHz, toluene-*d*<sub>8</sub>) δ 30.90 (C(CH<sub>3</sub>)<sub>3</sub>), 32.24 (C(CH<sub>3</sub>)<sub>3</sub>), 34.97 (C(CH<sub>3</sub>)<sub>3</sub>), 36.14 (C(CH<sub>3</sub>)<sub>3</sub>), 55.96 (NCH<sub>2</sub>), 65.65 (ZrCH<sub>2</sub>), 121.70, 121.92, 122.33, 122.38, 123.75, 124.91, 125.00, 126.94, 127.35, 127.58, 127.92, 128.08, 128.67, 129.59, 131.74, 133.00, 138.49, 138.96, 140.76, 141.64, 142.29, 143.84, 156.24, 156.30, 157.26 (aryl-C). Anal. Calcd for

$C_{46}H_{48}N_2OZr$  (%): C, 75.06; H, 6.57; N, 3.81. Found (1): C, 68.19; H, 6.23; N, 3.79. (2) C, 66.65; H, 6.08; N, 4.24. (This compound is air- and moisture-sensitive and despite repeated attempts satisfactory analysis could not be obtained.)

**(10)TiCl<sub>2</sub> 15.** A 3 mL benzene solution of **10-H<sub>2</sub>** (60.4 mg, 0.130 mmol) was added to a 3 mL benzene solution of TiCl<sub>2</sub>(NMe<sub>2</sub>)<sub>2</sub> (26.9 mg, 0.131 mmol) and stirred for ten minutes under inert atmosphere in the glovebox. Benzene was removed in vacuo from the resulting dark red solution to yield a deep purple solid, which was triturated several times with pentane to remove free dimethylamine (77.6 mg, 0.133 mmol, quantitative yield). <sup>1</sup>H NMR (300 MHz, C<sub>6</sub>H<sub>5</sub>Cl) δ 1.30 (s, 9H, C(CH<sub>3</sub>)<sub>3</sub>), 1.66 (s, 9H, C(CH<sub>3</sub>)<sub>3</sub>), 4.95 (s, 1H, NCH<sub>2</sub>), 6.12 (s, 1H, NCH<sub>2</sub>), 6.60 – 6.85 (m, 6H, aryl-CH), 7.02 – 7.12 (m, 2H, aryl-CH), 7.17 (dd, *J* = 7.8, 1.0 Hz, 1H, aryl-CH), 7.25 – 7.34 (m, 1H, aryl-CH), 7.48 (t, *J* = 8.0 Hz, 1H, aryl-CH), 7.56 (dd, *J* = 8.0, 1.5 Hz, 1H, aryl-CH), 7.63 – 7.72 (m, 3H, aryl-CH). <sup>13</sup>C NMR (126 MHz, C<sub>6</sub>D<sub>5</sub>Cl, –15 °C) δ 31.41 C(CH<sub>3</sub>)<sub>3</sub>, 32.45 (C(CH<sub>3</sub>)<sub>3</sub>), 35.69 (C(CH<sub>3</sub>)<sub>3</sub>), 36.63 C(CH<sub>3</sub>)<sub>3</sub>, 117.29, 123.11, 123.98, 126.02, 128.18, 129.55, 130.64, 132.98, 138.48, 139.58, 139.67, 145.83, 153.52, 155.43, 159.48 (aryl-C). Anal. Calcd for C<sub>32</sub>H<sub>34</sub>Cl<sub>2</sub>N<sub>2</sub>OTi (%): C, 66.11; H, 5.89; N, 4.82. Found: C, 65.98; H, 6.06; N, 4.87.

**(11)TiCl<sub>2</sub> 16.** A 3 mL benzene solution of **11-H<sub>2</sub>** (67.6 mg, 0.133 mmol) was added to a 3 mL benzene solution of TiCl<sub>2</sub>(NMe<sub>2</sub>)<sub>2</sub> (27.5 mg, 0.133 mmol) and stirred for ten minutes under inert atmosphere in the glovebox. Benzene was removed in vacuo from the resulting dark red solution to yield a light orange solid, which was triturated several times with pentane to remove free dimethylamine (86.4 mg, 0.134 mmol, quantitative yield). <sup>1</sup>H NMR (500 MHz, C<sub>6</sub>D<sub>5</sub>Cl) δ 1.30 (s, 9H, C(CH<sub>3</sub>)<sub>3</sub>), 1.33 – 1.39 (m, Ad-CH<sub>2</sub>, 6H), 1.63 – 1.71 (m, 6H, Ad-CH<sub>2</sub>), 1.78 (s, 9H, C(CH<sub>3</sub>)<sub>3</sub>), 1.79 (br s, 3H, Ad-CH), 7.24 (dd, *J* = 7.7, 1.0 Hz, 1H, aryl-CH), 7.36 – 7.43 (m, 2H, aryl-CH), 7.48 – 7.55 (m, 2H, aryl-CH), 7.58 – 7.62 (m, 1H, aryl-CH), 7.71 (q, *J* = 2.4 Hz, 2H, aryl-CH), 7.77 (dd, *J* = 8.3, 1.1 Hz, 1H, aryl-CH). <sup>13</sup>C NMR (126 MHz, C<sub>6</sub>D<sub>5</sub>Cl) δ 29.93 (Ad-CH), 30.36 (C(CH<sub>3</sub>)<sub>3</sub>), 31.31 (C(CH<sub>3</sub>)<sub>3</sub>), 34.60 (C(CH<sub>3</sub>)<sub>3</sub>), 35.69 (C(CH<sub>3</sub>)<sub>3</sub>), 35.87 (Ad-CH<sub>2</sub>), 42.62 (Ad-CH<sub>2</sub>), 69.51 (Ad-quat), 122.09, 122.25, 123.34, 123.72, 127.83, 128.65, 130.31, 131.13, 132.03, 133.17, 134.16, 137.90, 139.15, 144.77, 152.18, 153.39, 158.07 (aryl-C). Anal. Calcd for C<sub>35</sub>H<sub>42</sub>Cl<sub>2</sub>N<sub>2</sub>OTi (%): C, 67.21; H, 6.77; N, 4.48. Found (1): C, 66.53; H, 6.80; N, 4.20. (2) C, 66.37; H, 6.73; N, 4.36. (This compound is air- and moisture-sensitive and despite repeated attempts satisfactory %C analysis could not be obtained.)

**(13)ZrBn<sub>2</sub> 17.** A 2 mL benzene solution of **13-H<sub>2</sub>** (62.2 mg, 0.143 mmol) was added to a 2 mL benzene solution of ZrBn<sub>4</sub> (65.5 mg, 0.143 mmol) and stirred for ten minutes under inert atmosphere in the glovebox. Benzene was removed in

vacuo from the resulting yellow solution to yield a yellow oil, which was redissolved in pentane and pumped dry several times to remove residual toluene to reveal a yellow powder. (100.7 mg, 0.143 mmol, quantitative yield: 86%). This complex is fluxional at rt. Upon cooling, the pendant L-donor appears to coordinate irreversibly to Zr leading to a  $C_1$  complex with diastereotopic benzyl and ethyl protons.  $^1\text{H}$  NMR (500 MHz, toluene- $d_8$ ,  $-40\text{ }^\circ\text{C}$ )  $\delta$  1.44 (s, 9H,  $\text{C}(\text{CH}_3)_3$ ), 1.60 (s, 9H,  $\text{C}(\text{CH}_3)_3$ ), 2.11 – 2.16 (m, 1H, ethyl- $\text{CH}_2$ ), 2.32 (d,  $J = 9.5$  Hz, 1H, Zr- $\text{CH}_2$ ), 2.39 (d,  $J = 10.4$  Hz, 1H, Zr- $\text{CH}_2$ ), 2.58 (t,  $J = 7.1$  Hz, 2H, ethyl- $\text{CH}_2$ , Zr- $\text{CH}_2$ ), 2.77 (td,  $J = 11.6, 5.3$  Hz, 1H, ethyl- $\text{CH}_2$ ), 2.82 – 2.92 (m, 2H, ethyl- $\text{CH}_2$ , Zr- $\text{CH}_2$ ), 3.30 (s, 3H,  $\text{OCH}_3$ ), 6.48 (d,  $J = 7.5$  Hz, 2H, aryl- $\text{CH}$ ), 6.54 (dd,  $J = 8.3, 1.2$  Hz, 1H, aryl- $\text{CH}$ ), 6.70 (t,  $J = 7.3$  Hz, 1H, aryl- $\text{CH}$ ), 6.74 (dd,  $J = 7.8, 1.1$  Hz, 1H, aryl- $\text{CH}$ ), 6.84 (t,  $J = 7.4$  Hz, 2H, aryl- $\text{CH}$ ), 6.88 (d,  $J = 9.5$  Hz, 1H, aryl- $\text{CH}$ ), 6.90 (t,  $J = 8.8$  Hz, 1H, aryl- $\text{CH}$ ), 7.07 (s, 1H, aryl- $\text{CH}$ ), 7.20 (dd,  $J = 8.0, 1.2$  Hz, 1H, aryl- $\text{CH}$ ), 7.26 (d,  $J = 2.4$  Hz, 1H, aryl- $\text{CH}$ ), 7.40 (t,  $J = 7.4$  Hz, 3H, aryl- $\text{CH}$ ), 7.71 (d,  $J = 2.5$  Hz, 1H, aryl- $\text{CH}$ ).

**2-(3,5-di-*t*-butyl-2-(methoxymethoxy)phenyl)-6-(*o*-tolyl)pyridine CNO-MOM**

**18-MOM.** An oven-dried 25 mL Schlenk bomb was charged with a stirbar, evacuated and refilled with Ar. Under positive Ar pressure, 0.750 g of **2**, 0.251 g of *o*-tolyl-boronic acid, 0.107 g of  $\text{Pd}(\text{PPh}_3)_4$  and 0.784 g of  $\text{K}_3\text{PO}_4$  crushed with a mortar and pestle were added and the vessel was sealed with a septum. The vessel was evacuated and refilled with Ar three times, and then 5 mL of dry

toluene was added via syringe and the vessel was sealed with a Kontes valve. The reaction mixture was stirred at room temperature for 10 min, then the vessel was placed in a 100 °C oil bath for 18 h, then cooled to room temperature, and the suspension filtered through celite with the aid of Et<sub>2</sub>O. Solvent was removed in vacuo and the resulting residue was redissolved in dichloromethane and passed through a SiO<sub>2</sub> plug using 1:9 Et<sub>2</sub>O/hexanes as the eluent. 0.742 g (96% crude yield). <sup>1</sup>H NMR (500 MHz, CDCl<sub>3</sub>) δ 1.35 (s, 9H, C(CH<sub>3</sub>)<sub>3</sub>), 1.50 (s, 9H, C(CH<sub>3</sub>)<sub>3</sub>), 2.53 (s, 3H, tolyl-CH<sub>3</sub>), 3.37 (s, 3H, CH<sub>2</sub>OCH<sub>3</sub>), 4.61 (s, 2H, CH<sub>2</sub>OCH<sub>3</sub>), 7.28 – 7.34 (m, 3H, aryl-CH), 7.38 (dd, *J* = 7.7, 1.0 Hz, 1H, aryl-CH), 7.44 (d, *J* = 2.6 Hz, 1H, aryl-CH), 7.48 – 7.52 (m, 1H, aryl-CH), 7.52 (dd, *J* = 2.6, 0.8 Hz, 1H, aryl-CH), 7.69 (dd, *J* = 7.9, 0.9 Hz, 1H, aryl-CH), 7.79 (t, *J* = 7.7 Hz, 1H, aryl-CH). <sup>13</sup>C NMR (126 MHz, CDCl<sub>3</sub>) δ 20.87 (tolyl-CH<sub>3</sub>), 31.03 (C(CH<sub>3</sub>)<sub>3</sub>), 31.61 (C(CH<sub>3</sub>)<sub>3</sub>), 34.73 (C(CH<sub>3</sub>)<sub>3</sub>), 35.55 (C(CH<sub>3</sub>)<sub>3</sub>), 57.52 (CH<sub>2</sub>OCH<sub>3</sub>), 99.60 (CH<sub>2</sub>OCH<sub>3</sub>), 122.05, 123.03, 124.96, 125.99, 126.65, 128.35, 129.89, 131.02, 134.23, 136.19, 136.33, 140.54, 142.34, 146.00, 151.36, 157.76, 160.16 (aryl-C). HRMS (FAB+) *m/z*: calcd for C<sub>28</sub>H<sub>36</sub>O<sub>2</sub>N [M + H]<sup>+</sup> 418.2746; found 418.2726.

**2,4-di-*t*-butyl-6-(6-(*o*-tolyl)pyridin-2-yl)phenol CNO-H<sub>2</sub> 18-H<sub>2</sub>.** 0.355 g of **18-MOM** was placed in a 50 mL round bottom flask charged with a stirbar and 20 mL of THF was added to give a colorless solution. The flask was cooled to 0 °C with a water-ice bath; a 15 mL solution of 1:1 THF/conc. HCl was added dropwise. The reaction was stirred for 30 min at 0 °C, then removed from the ice

bath and allowed to reach room temperature while stirring, which resulted in the reaction solution turning pale translucent yellow. Stirring was continued overnight, and then the solution was quenched with 2 M aq. NaOH to give a solution with neutral pH. The organic layer was extracted with diethyl ether (3 × 30 mL) and the combined organics were dried over magnesium sulfate and rotovapped to reveal a yellow oil, which was precipitated from hot hexanes followed by cooling in the freezer to give a pale yellow powder. 0.173 g (54% yield). <sup>1</sup>H NMR (500 MHz, CDCl<sub>3</sub>) δ 1.39 (s, 9H, C(CH<sub>3</sub>)<sub>3</sub>), 1.48 (s, 9H, C(CH<sub>3</sub>)<sub>3</sub>), 2.42 (s, 3H, tolyl-CH<sub>3</sub>), 7.29 – 7.41 (m, 4H, aryl-CH), 7.43 (d, *J* = 2.4 Hz, 1H, aryl-CH), 7.46 (dt, *J* = 7.0, 1.4 Hz, 1H, aryl-CH), 7.74 (d, *J* = 2.4 Hz, 1H, aryl-CH), 7.87 – 7.94 (m, 2H, aryl-CH), 14.67 (s, 1H, OH). <sup>13</sup>C NMR (126 MHz, CDCl<sub>3</sub>) δ 20.59 (tolyl-CH<sub>3</sub>), 29.71 (C(CH<sub>3</sub>)<sub>3</sub>), 31.79 (C(CH<sub>3</sub>)<sub>3</sub>), 34.51 (C(CH<sub>3</sub>)<sub>3</sub>), 35.45 (C(CH<sub>3</sub>)<sub>3</sub>), 117.75, 117.95, 120.99, 121.68, 126.18, 126.36, 128.81, 129.73, 131.13, 136.07, 137.80, 137.90, 139.35, 139.79, 156.42, 157.16, 158.55 (aryl-C). HRMS (FAB+) *m/z*: calcd for C<sub>26</sub>H<sub>31</sub>ON [M]<sup>+</sup> 373.2406; found 373.2424.

**(18)TiBn<sub>2</sub> 19.** To a stirring slurry of **18-H<sub>2</sub>** (30.2 mg, 0.081 mmol) in 5:1 pentane/ether was added to a 3 mL solution of TiBn<sub>4</sub> (33.4 mg, 0.081 mmol) and the resulting red solution was stirred for ten minutes under inert atmosphere in the glovebox. The reaction solution was passed through a pad of celite to remove impurities and with 5:1 pentane/ether, then solvent was removed in vacuo to yield a dark red solid, which was triturated several times with pentane before being

redissolved in 5:1 pentane/ether and recrystallized by cooling in the freezer. (30.2 mg, 0.050 mmol, 62% yield).  $^1\text{H}$  NMR (300 MHz, toluene- $d_8$ )  $\delta$  1.37 (s, 9H,  $\text{C}(\text{CH}_3)_3$ ), 1.85 (s, 9H,  $\text{C}(\text{CH}_3)_3$ ), 2.21 (s, 3H, Ar- $\text{CH}_3$ ), 3.88 (d,  $J = 8.3$  Hz, 2H, Ti- $\text{CH}_2$ ), 4.15 (d,  $J = 8.3$  Hz, 2H, Ti- $\text{CH}_2$ ), 6.33 – 6.44 (m, 2H, aryl- $\text{CH}$ ), 6.54 (t,  $J = 7.7$  Hz, 4H, aryl- $\text{CH}$ ), 6.63 – 6.71 (m, 4H, aryl- $\text{CH}$ ), 6.82 (d,  $J = 4.7$  Hz, 2H, aryl- $\text{CH}$ ), 7.13 (d,  $J = 5.4$  Hz, 1H, aryl- $\text{CH}$ ), 7.23 (t,  $J = 7.1$  Hz, 1H, aryl- $\text{CH}$ ), 7.37 (d,  $J = 2.4$  Hz, 1H, aryl- $\text{CH}$ ), 7.69 (d,  $J = 2.4$  Hz, 1H, aryl- $\text{CH}$ ), 8.51 (d,  $J = 6.9$  Hz, 1H, aryl- $\text{CH}$ ).  $^{13}\text{C}$  NMR (126 MHz,  $\text{C}_6\text{D}_6$ )  $\delta$  23.59 (tolyl- $\text{CH}_3$ ), 30.99 ( $\text{C}(\text{CH}_3)_3$ ), 31.84 ( $\text{C}(\text{CH}_3)_3$ ), 34.66 ( $\text{C}(\text{CH}_3)_3$ ), 35.80 ( $\text{C}(\text{CH}_3)_3$ ), 92.42 (Ti- $\text{CH}_2$ ), 119.61, 121.77, 123.32, 124.72, 125.70, 126.58, 127.75, 128.57, 129.33, 131.13, 132.54, 132.65, 133.00, 136.76, 137.81, 138.66, 142.08, 157.60, 158.15, 165.17, 204.42 (aryl-C). Anal. Calcd for  $\text{C}_{40}\text{H}_{43}\text{NOTi}$  (%): C, 79.85; H, 7.20; N, 2.33. Found (1): C, 74.91; H, 6.99; N, 2.33. (2) C, 74.74; H, 6.86; N, 2.32. (This compound is air- and moisture-sensitive and despite repeated attempts satisfactory %C analysis could not be obtained.)

**Recovery of Ligand 5 from Small Scale Polymerization Reaction with 8 and 1-Hexene.** To a 20 mL vial in the glovebox was added 1 mL of 1-hexene and 50 equiv (0.193 g) of dry MAO. The 1-hexene/MAO solution was stirred for 5 min, then a solution of **8** dissolved in 1 mL of PhCl was added to the vial and the reaction was stirred for 25 min at room temperature. The vial was then removed from the glovebox and 2 mL of  $\text{D}_2\text{O}$  were added slowly, followed by 5 drops of

conc. HCl, and 4 mL of D<sub>2</sub>O, which resulted in de-colorization of the dark red solution. The organic layer was extracted with hexanes (3 × 4 mL) and the combined organics were dried over magnesium sulfate and solvent removed *in vacuo* to reveal a pale yellow solid. 44.9 mg (5-D<sub>2</sub> and poly-1-hexene). MS (FAB+) *m/z*: calcd for C<sub>33</sub>H<sub>38</sub>ON<sub>2</sub> [M]<sup>+</sup> 478.2984; found 478.3524.

**2-(3,5-di-*t*-butyl-2-(methoxymethoxy)phenyl)-6-(3,5-di-*t*-butylphenyl)pyridine**

**ArNO-MOM 20-MOM.** An oven-dried 50 mL Schlenk bomb was charged with a stirbar, evacuated and refilled with Ar. Under positive Ar pressure, 0.501 g of 2-bromo-6-(3,5-di-*t*-butylphenyl)pyridine, 0.547 g of **1**, 67.8 mg of Pd<sub>2</sub>dba<sub>3</sub>, 62.2 mg SPhos and 0.624 g of K<sub>3</sub>PO<sub>4</sub> crushed with a mortar and pestle were added and the vessel was sealed with a septum. The vessel was evacuated and refilled with Ar three times, and then 10 mL of dry toluene was added via syringe and the vessel was sealed with a Kontes valve. The reaction mixture was stirred at room temperature for 10 min, then the vessel was placed in a 100 °C oil bath for 42 h, then cooled to room temperature, and the suspension filtered through celite with the aid of Et<sub>2</sub>O. Solvent was removed *in vacuo* and the resulting residue was redissolved in dichloromethane and passed through a SiO<sub>2</sub> plug using 1:9 Et<sub>2</sub>O/hexanes as the eluent. 0.749 g (quantitative crude yield). <sup>1</sup>H NMR (500 MHz, CDCl<sub>3</sub>) δ 1.39 (s, 9H, C(CH<sub>3</sub>)<sub>3</sub>), 1.42 (s, 18H, C(CH<sub>3</sub>)<sub>3</sub>), 1.53 (s, 9H, C(CH<sub>3</sub>)<sub>3</sub>), 3.42 (s, 3H, CH<sub>2</sub>OCH<sub>3</sub>), 4.65 (s, 2H, CH<sub>2</sub>OCH<sub>3</sub>), 7.46 (d, *J* = 2.6 Hz, 1H, aryl-CH), 7.53 (t, *J* = 1.8 Hz, 1H, aryl-CH), 7.69 (dd, *J* = 7.5, 1.3 Hz, 1H, aryl-CH), 7.73 (d,

$J = 2.6$  Hz, 1H, aryl-CH), 7.75 (dd,  $J = 7.8, 1.4$  Hz, 1H, aryl-CH), 7.78 (d,  $J = 7.6$  Hz, 1H, aryl-CH), 7.98 (d,  $J = 1.8$  Hz, 2H, aryl-CH).  $^{13}\text{C}$  NMR (126 MHz,  $\text{CDCl}_3$ )  $\delta$  31.04 ( $\text{C}(\text{CH}_3)_3$ ), 31.63 ( $\text{C}(\text{CH}_3)_3$ ), 31.65 ( $\text{C}(\text{CH}_3)_3$ ), 34.77 ( $\text{C}(\text{CH}_3)_3$ ), 35.15 ( $\text{C}(\text{CH}_3)_3$ ), 35.60 ( $\text{C}(\text{CH}_3)_3$ ), 57.59 ( $\text{CH}_2\text{OCH}_3$ ), 99.53 ( $\text{CH}_2\text{OCH}_3$ ), 118.65, 121.50, 122.92, 123.31, 124.91, 127.08, 128.54, 129.11, 134.05, 136.66, 139.06, 142.38, 145.91, 151.14, 151.49, 157.72, 158.21 (aryl-C). HRMS (FAB+)  $m/z$ : calcd for  $\text{C}_{35}\text{H}_{50}\text{O}_2\text{N}$   $[\text{M} + \text{H}]^+$  516.3842; found 516.3836.

**2,4-di-*t*-butyl-6-(6-(3,5-di-*t*-butylphenyl)pyridin-2-yl)phenol ArNO-H 20-H.**

Followed the same procedure as **18-H<sub>2</sub>**. A yellow powder precipitated from a hot hexanes solution cooled in the freezer. Yield: 53% yellow powder.  $^1\text{H}$  NMR (500 MHz,  $\text{CDCl}_3$ )  $\delta$  1.39 (s, 9H,  $\text{C}(\text{CH}_3)_3$ ), 1.43 (s, 18H,  $\text{C}(\text{CH}_3)_3$ ), 1.52 (s, 9H,  $\text{C}(\text{CH}_3)_3$ ), 7.44 (d,  $J = 2.4$  Hz, 1H, aryl-CH), 7.57 (t,  $J = 1.8$  Hz, 1H, aryl-CH), 7.65 (dd,  $J = 7.0, 1.5$  Hz, 1H, aryl-CH), 7.73 (d,  $J = 2.3$  Hz, 1H, aryl-CH), 7.85 – 7.93 (m, 4H, aryl-CH), 15.19 (s, 1H, OH).  $^{13}\text{C}$  NMR (126 MHz,  $\text{CDCl}_3$ )  $\delta$  29.70 ( $\text{C}(\text{CH}_3)_3$ ), 31.60 ( $\text{C}(\text{CH}_3)_3$ ), 31.81 ( $\text{C}(\text{CH}_3)_3$ ), 34.51 ( $\text{C}(\text{CH}_3)_3$ ), 35.24 ( $\text{C}(\text{CH}_3)_3$ ), 35.52 ( $\text{C}(\text{CH}_3)_3$ ), 117.77, 118.00, 118.11, 120.95, 121.57, 123.80, 126.29, 137.62, 137.89, 138.40, 139.71, 151.69, 155.16, 157.37, 158.87 (aryl-C). HRMS (FAB+)  $m/z$ : calcd for  $\text{C}_{33}\text{H}_{45}\text{ON}$   $[\text{M}]^+$  471.3501; found 471.3508.

**6-(3,5-di-*t*-butyl-2-(methoxymethoxy)phenyl)picolinaldehyde.** A 100 mL Schlenk bomb was charged with a stirbar and 1.24 g (6.65 mmol) 6-

bromopyridine-2-carboxaldehyde, 2.50 g (6.65 mmol) 2-(3,5-di-*tert*-butyl-2-(methoxymethoxy)phenyl)-4,4,5,5-tetramethyl-1,3,2-dioxaborolane, and 0.385 g (0.333 mmol) Pd(PPh<sub>3</sub>)<sub>4</sub> were added and the vessel was sealed with a septum. The bomb was evacuated and refilled with argon three times. 25 mL of dry toluene and 10 mL of 2 M Na<sub>2</sub>CO<sub>3</sub> were injected into the vessel with a syringe, and the vessel was sealed with a Kontes valve. The reaction mixture was placed in an oil bath at 100°C and was stirred overnight. The organic layer was extracted using methylene chloride (4 x 30 mL), and the combined organics were dried with magnesium sulfate and rotovapped. The product, a white powder, was purified by chromatography on SiO<sub>2</sub> using 1:10 ethyl acetate/hexane. (2.1412 g, 6.0236 mmol, 91% yield). <sup>1</sup>H NMR (500 MHz, CDCl<sub>3</sub>) δ 1.35 (s, 9H, C(CH<sub>3</sub>)<sub>3</sub>), 1.48 (s, 9H, C(CH<sub>3</sub>)<sub>3</sub>), 3.25 (s, 3H, CH<sub>2</sub>OCH<sub>3</sub>), 4.55 (s, 2H, CH<sub>2</sub>OCH<sub>3</sub>), 7.48 (s, 2H, aryl-CH), 7.68 – 8.03 (m, 3H, aryl-CH), 10.17 (s, CHO). <sup>13</sup>C NMR (126 MHz, CDCl<sub>3</sub>) δ 31.08 (C(CH<sub>3</sub>)<sub>3</sub>), 31.60 (C(CH<sub>3</sub>)<sub>3</sub>), 34.83 (C(CH<sub>3</sub>)<sub>3</sub>), 35.60 (C(CH<sub>3</sub>)<sub>3</sub>), 57.40 (CH<sub>2</sub>OCH<sub>3</sub>), 100.02 (CH<sub>2</sub>OCH<sub>3</sub>), 119.67, 125.80, 126.34, 129.75, 133.17, 136.90, 142.83, 146.62, 151.63, 152.98, 159.41 (aryl-C), 194.00 (CHO).

**Amido(pyridine)phenoxide N-((6-(3,5-di-*t*-butyl-2-(methoxymethoxy)phenyl)pyridin-2-yl)methyl)-1-phenylethanamine 21-MOM.** To a 100 mL round-bottom flask charged with a stirbar was added a 1.00 g (2.81 mmol) slurry of 6-(3,5-di-*tert*-butyl-2-(methoxymethoxy)phenyl)picolinaldehyde in 15 mL of acetonitrile, and 363 μL of DL- $\alpha$ -methylbenzylamine (2.81 mmol) was added via syringe.

The reaction mixture was stirred for 30 minutes, then 0.924 g of NaHB(OAc)<sub>3</sub> was added and stirring was continued for one hour. The reaction was then quenched with 60 mL saturated sodium bicarbonate solution, and the organic layer was extracted with ether (3 x 50 mL). The combined organics were dried over magnesium sulfate and rotovapped to yield a colorless oil. (1.0947 g, 2.3764 mmol, 85% yield). <sup>1</sup>H NMR (500 MHz, CDCl<sub>3</sub>) δ 1.36 (s, 9H, C(CH<sub>3</sub>)<sub>3</sub>), 1.47 (d, *J* = 6.5 Hz, 3H, CH(CH<sub>3</sub>)), 1.50 (s, 9H, C(CH<sub>3</sub>)<sub>3</sub>), 2.34 (s, 1H, NH), 3.33 (s, 3H, CH<sub>2</sub>OCH<sub>3</sub>), 3.86 (s, 1H, CH<sub>2</sub>), 3.91 (q, *J* = 6.6 Hz, 1H, CH(CH<sub>3</sub>)), 4.55 (s, 2H, CH<sub>2</sub>OCH<sub>3</sub>), 7.17 (dd, *J* = 7.6, 1.0 Hz, 1H, aryl-CH), 7.22 – 7.30 (m, 1H, aryl-CH), 7.36 (t, *J* = 7.6 Hz, 2H, aryl-CH), 7.38 – 7.48 (m, 4H, aryl-CH), 7.58 (dd, *J* = 7.8, 1.1 Hz, 1H, aryl-CH), 7.66 (t, *J* = 7.7 Hz, 1H, aryl-CH). <sup>13</sup>C NMR (126 MHz, CDCl<sub>3</sub>) δ 24.44 (CH(CH<sub>3</sub>)), 31.03 (C(CH<sub>3</sub>)<sub>3</sub>), 31.63 (C(CH<sub>3</sub>)<sub>3</sub>), 34.77 (C(CH<sub>3</sub>)<sub>3</sub>), 35.58 (C(CH<sub>3</sub>)<sub>3</sub>), 53.04 (CH<sub>2</sub>), 57.46 (CH<sub>2</sub>OCH<sub>3</sub>), 58.09 (CH(CH<sub>3</sub>)), 99.52 (CH<sub>2</sub>OCH<sub>3</sub>), 120.51, 123.40, 125.10, 126.46, 127.00, 127.16, 128.62, 133.99, 136.46, 142.49, 145.33, 146.07, 151.41, 158.06, 159.52 (aryl-C). HRMS (FAB+) *m/z*: calcd for C<sub>30</sub>H<sub>41</sub>N<sub>2</sub>O<sub>2</sub> [M + H]<sup>+</sup> 461.3168; found 461.3161.

**Amido(pyridine)phenoxide 2,4-di-tert-butyl-6-(6-(((1-phenylethyl)amino)-methyl)pyridin-2-yl)phenol 21-H<sub>2</sub>.** To a 250 mL round-bottom flask charged with a stirbar was added 1.0947 g (0.00263 mol) of N-((6-(3,5-di-tert-butyl-2-(methoxymethoxy)phenyl)pyridin-2-yl)methyl)-1-phenylethylamine and 10.5 mL of THF. To the stirring solution was added 10.5 mL of a 2:1 conc. HCl/THF

solution, and stirring was continued at room temperature overnight. Solvent was removed in vacuo to yield the hydrochloride salt, which was washed with ether. The salt was then dissolved in 10 mL methylene chloride and a saturated sodium bicarbonate solution was added until the aqueous layer reached a neutral pH. The organic layer was extracted with methylene chloride (4 x 20 mL) and the combined organics were dried over magnesium sulfate and solvent was removed in vacuo to yield a yellow oil. (0.9700 g, 2.3284 mmol, 88% yield)  $^1\text{H}$  NMR (500 MHz,  $\text{CD}_2\text{Cl}_2$ )  $\delta$  1.44 (s, 9H,  $\text{C}(\text{CH}_3)_3$ ), 1.45 (d,  $J = 6.8$  Hz, 3H,  $\text{CH}(\text{CH}_3)$ ), 1.58 (s, 9H,  $\text{C}(\text{CH}_3)_3$ ), 1.96 (s, 1H,  $\text{NH}$ ), 3.80 – 3.95 (m, 3H,  $\text{CH}(\text{CH}_3)$ ,  $\text{CH}_2$ ), 7.28 (d,  $J = 8.0$  Hz, 1H, aryl- $\text{CH}$ ), 7.31 (d,  $J = 7.2$  Hz, 1H, aryl- $\text{CH}$ ), 7.37 – 7.42 (m, 2H, aryl- $\text{CH}$ ), 7.43 – 7.47 (m, 2H, aryl- $\text{CH}$ ), 7.49 (d,  $J = 2.4$  Hz, 1H, aryl- $\text{CH}$ ), 7.76 (d,  $J = 2.4$  Hz, 1H, aryl- $\text{CH}$ ), 7.81 (t,  $J = 7.9$  Hz, 1H, aryl- $\text{CH}$ ), 7.87 (d,  $J = 8.1$  Hz, 1H, aryl- $\text{CH}$ ), 14.83 (s, 1H,  $\text{OH}$ ).  $^{13}\text{C}$  NMR (126 MHz,  $\text{CD}_2\text{Cl}_2$ )  $\delta$  24.98 ( $\text{CH}(\text{CH}_3)$ ), 30.08 ( $\text{C}(\text{CH}_3)_3$ ), 32.07 ( $\text{C}(\text{CH}_3)_3$ ), 34.91 ( $\text{C}(\text{CH}_3)_3$ ), 35.87 ( $\text{C}(\text{CH}_3)_3$ ), 52.83 ( $\text{CH}(\text{CH}_3)$ ), 58.16 ( $\text{CH}_2$ ), 118.36, 118.56, 120.22, 121.58, 126.67, 127.40, 127.58, 129.08, 138.07, 138.70, 140.44, 146.14, 157.51, 157.88, 159.03, 171.28 (aryl-C). HRMS (FAB+)  $m/z$ : calcd for  $\text{C}_{33}\text{H}_{38}\text{N}_2\text{O}$   $[\text{M}]^+$  446.3297; found 446.3286.

**(21)TiBn<sub>2</sub> 22.** A solution of 11.3 mg (0.0274 mmol) of  $\text{TiBn}_4$  in  $\text{C}_6\text{D}_6$  was added to a solution of 11.4 mg (0.0274 mmol) of **21-H<sub>2</sub>** in  $\text{C}_6\text{D}_6$  in the glovebox to produce the deep-red complex. The identity of the complex was confirmed by  $^1\text{H}$  NMR spectroscopy.  $^1\text{H}$  NMR (300 MHz,  $\text{C}_6\text{D}_6$ )  $\delta$  1.38 (s, 9H), 1.74 (d,  $J = 6.8$  Hz, 3H),

2.00 (s, 9H), 3.32 (d,  $J = 9.6$  Hz, 1H), 3.35 (d,  $J = 8.5$  Hz, 1H), 3.53 (d,  $J = 9.1$  Hz, 1H), 3.60 (d,  $J = 8.5$  Hz, 1H), 4.37 (d,  $J = 20.9$  Hz, 1H), 4.54 (d,  $J = 21.0$  Hz, 1H), 6.21 (d,  $J = 7.6$  Hz, 1H), 6.33 (t,  $J = 7.1$  Hz, 1H), 6.39 – 6.45 (m, 2H), 6.48 – 6.61 (m, 2H), 6.79 (td,  $J = 7.8, 3.6$  Hz, 4H), 7.22 (t,  $J = 7.5$  Hz, 3H), 7.41 – 7.51 (m, 3H), 7.60 (d,  $J = 2.4$  Hz, 1H), 7.81 (d,  $J = 2.4$  Hz, 1H).

**(21)HfBn<sub>2</sub> 23.** A solution of 21.6 mg (0.0398 mmol) HfBn<sub>4</sub> in C<sub>6</sub>D<sub>6</sub> was added to a solution of 16.6 mg (0.0398 mmol) **21-H<sub>2</sub>** in C<sub>6</sub>D<sub>6</sub> in the glovebox to yield a gold-colored solution. The identity of the metal complex was confirmed by <sup>1</sup>H NMR spectroscopy.

**(21)TiCl<sub>2</sub> 24.** A solution of 52.00 mg (0.051 mmol) TiCl<sub>2</sub>(NMe<sub>2</sub>)<sub>2</sub> in C<sub>6</sub>D<sub>6</sub> was added to a solution of 21.2 mg (0.051 mmol) **21-H<sub>2</sub>** in C<sub>6</sub>D<sub>6</sub> in the glovebox to produce the deep purple solution. Solvents were removed in vacuo. (137.6 mg, quantitative yields). 15 mg of the compound were recrystallized in THF/DCM. The identity of the resulting metal complex was confirmed by X-ray crystallography and <sup>1</sup>H NMR spectroscopy.

**Polymerization of 8 at KFUPM.** To the new glass reactor of the new computer controlled polymerization instrument was added 50 mL of dry toluene, 1 mL triisobutylaluminum, and 24.2 mL 10 wt% MAO in toluene (1000 equiv) at about 10 °C. The temperature was adjusted to 10 °C and the nitrogen was replaced

with propylene (2 bar). A 30  $\mu\text{mol}$  (18 mg) sample of catalyst **8** was transferred to a small vial in the Ar-filled glovebox and capped with a septum. The sample was dissolved in 10 mL of toluene and transferred to the reactor against a propylene flow at 10 °C. The reactor was closed, and propylene was rapidly added to give a total volume of approximately 150 mL at 10 °C, whereupon the temperature increased to approx. 20 °C and pressure to approx. 6 bar. Propylene addition was stopped, and stirring increased to 800 rpm, T = 25 °C and p = 7.2 bar (8.2 atm). The reaction was run for 30 min to give approx. 2:1 liquid propylene:toluene. The reactor was vented and opened when most liquid propylene had evaporated. A film of polymer formed on evaporation from the stainless steel pan that we decanted the toluene and polymer solution into. A solid polymer formed on addition of a couple of mL of methanol. Air drying overnight yielded crude weight of PP of about 14 g. Crude polymer was dissolved in toluene, washed with HCl/methanol (about 1:10) and placed in a separatory funnel. Toluene layer was placed in flask and reduced by half in volume, then transferred to stainless steel pan to evaporate remaining toluene. The polymer did not crystallize. Transferred with some toluene to flask and pumped mostly dry. Gave oily uncrystalline product.

**Polymerization of 8 at Dow Chemical. Reactor Procedures:** Propylene polymerizations were conducted in a 1.8 L SS batch reactor. This reactor was manufactured by Buchi AG and sold by Mettler, and is heated/cooled via the

vessel jacket and reactor head. Syltherm™ 800 is the heat transfer fluid used and is controlled by a separate heating/cooling skid. Both the reactor and the heating/cooling system are controlled and monitored by a Camile TG process computer. The bottom of the reactor is fitted with a large orifice bottom dump valve, which empties the reactor contents into a 6 L SS dump pot. The dump pot is vented to a 30 gal. blowdown tank, with both the pot and the tank N<sub>2</sub> purged. All chemicals used for polymerization or catalyst makeup are run through purification columns, to remove any impurities that may affect polymerization. The propylene and toluene were passed through 2 columns, the first containing A2 alumina, the second containing Q5 reactant. The N<sub>2</sub> was passed through a single Q5 reactant column. The reactor was cooled to 50°C for chemical additions. The Camile then controlled the addition of 700 g. of IsoparE, using a micro-motion flowmeter to add accurately the desired amount. The 150 g. of propylene was then added through the micro-motion flowmeter. The reactor is then preloaded with MMAO to scavenge any impurities in the feeds. After the chemicals are in the reactor, the reactor was heated up to 70°C for polymerization. The catalyst solution (0.005 M in toluene) is mixed with the desired activator and transferred into the catalyst shot tank. This is followed by 3 rinses of toluene, 5 mL each. Immediately after catalyst addition to the reactor, the run timer begins. For successful polymerizations, exotherm and pressure drops were observed. These polymerizations were run for 15 min., then the agitator was stopped, the reactor pressured up to ~500 psi with N<sub>2</sub>, and the

bottom dump valve opened to empty reactor contents to the dump pot. The dump pot contents are poured into trays that are set in a vacuum oven, where they are heated up to 140°C under vacuum to remove any remaining solvent. After the trays cool to ambient temperature, the polymers are weighed for yields and submitted for polymer testing.

**Procedure for GPC Analysis performed by Dow Chemical.** Molecular weight distribution ( $M_w$ ,  $M_n$ ) information was determined by analysis on a custom Dow-built Robotic-Assisted Dilution High-Temperature Gel Permeation Chromatographer (RAD-GPC). Polymer samples were dissolved for 90 minutes at 160°C at a concentration of 30mg/mL in 1,2,4-trichlorobenzene (TCB) stabilized by 300ppm BHT, while capped and with stirring. They were then diluted to 1mg/mL immediately before a 400 $\mu$ L aliquot of the sample was injected. The GPC utilized two (2) Polymer Labs PLgel 10 $\mu$ m MIXED-B columns (300x10mm) at a flow rate of 2.0mL/minute at 150°C. Sample detection was performed using a PolyChar IR4 detector in concentration mode. A conventional calibration of narrow Polystyrene (PS) standards was utilized, with apparent units adjusted to homo-polyethylene (PE) using known Mark-Houwink coefficients for PS and PE in TCB at this temperature. Absolute  $M_w$  information was calculated using a PDI static low-angle light scatter detector.

**Procedure for DSC Analysis performed by Dow Chemical.** Melting and crystallization temperatures of polymers were measured by differential scanning calorimetry (DSC 2910, TA Instruments, Inc.). Samples were first heated from room temperature to 210 °C at 10°C /min. After being held at this temperature for 4 min, the samples were cooled to -40 °C at 10/min and were then heated to 215 °C at 10/min after being held at -40°C for 4 min.

**Table 3.4** Crystal data and structure refinement for **8**, **14**, and **16**.

	<b>8</b>	<b>14</b>	<b>16</b>
CCDC Number	877737		
Empirical formula	C <sub>33</sub> H <sub>36</sub> Cl <sub>2</sub> N <sub>2</sub> OTi	C <sub>46</sub> H <sub>48</sub> N <sub>2</sub> OZr	C <sub>36.83</sub> H <sub>46.32</sub> Cl <sub>2.34</sub> N <sub>2</sub> OTi
Formula weight	595.44	736.08	663.77
T (K)	100(2)	100(2)	100(2)
a, Å	9.955(2)	11.0188(4)	10.387(2)
b, Å	11.603(3)	13.6909(5)	15.918(4)
c, Å	25.865(5)	15.0870(6)	21.740(5)
α, deg	90	64.169(2)	76.406(5)
β, deg	96.160(9)	68.942(2)	79.036(5)
γ, deg	90	75.522(2)	87.948(5)
Volume, Å <sup>3</sup>	2970.6(11)	1899.90(13)	3429.9(14)
Z	4	2	4
Crystal system	Monoclinic	Triclinic	Triclinic
Space group	P2 <sub>1</sub> /n	P -1	P -1
<i>d</i> <sub>calc</sub> , g/cm <sup>3</sup>	1.331	1.287	1.285
θ range, deg	1.58 to 24.71	2.0 to 39.6	1.447 to 30.637
Abs. coefficient, mm <sup>-1</sup>	0.497	0.33	0.463
Abs. correction	None	Semi Emp.	Semi Emp.
GOF	1.057	1.25	1.026
<i>R</i> <sub>1</sub> , <i>wR</i> <sub>2</sub> [ <i>I</i> >2σ( <i>I</i> )]	0.0384, 0.1052	0.0379, 0.0764	0.0387, 0.0950

**Table 3.5** Crystal data and structure refinement for **7** and **24**(THF).

	<b>17</b>	<b>24</b> (THF)
CCDC Number		
Empirical formula	C <sub>40</sub> H <sub>43</sub> NO <sub>3</sub> Ti	C <sub>39.67</sub> H <sub>57.34</sub> Cl <sub>2</sub> N <sub>2</sub> O <sub>3.92</sub> Ti
Formula weight	601.65	743.73
T (K)	100(2)	100(2)
a, Å	10.5475(6)	11.0051(7)
b, Å	11.5064(6)	12.9025(9)
c, Å	14.7987(8)	14.9598(10)
α, deg	67.224(2)	70.820(3)
β, deg	86.953(3)	77.256(3)
γ, deg	76.102(3)	85.136(3)
Volume, Å <sup>3</sup>	1605.91(15)	1956.7(2)
Z	2	2
Crystal system	Triclinic	Triclinic
Space group	P -1	P -1
<i>d</i> <sub>calc</sub> , g/cm <sup>3</sup>	1.244	1.262
θ range, deg	2.44 to 41.64	1.9 to 26.2
Abs. coefficient, mm <sup>-1</sup>	0.30	0.40
Abs. correction	Semi Emp.	Semi Emp.
GOF	1.71	1.63
<i>R</i> <sub>1</sub> , <i>wR</i> <sub>2</sub> [ <i>I</i> > 2σ( <i>I</i> )]	0.0415, 0.1014	0.0642, 0.1328

## References

1. Hustad, P. D. *Science* **2009**, *325*, 704-707.
2. Natta, G.; Pino, P.; Corradini, P.; Danusso, F.; Mantica, E.; Mazzanti, G.; Moraglio, G. *J. Am. Chem. Soc.* **1955**, *77*, 1708-1710.
3. Gibson, V. C.; Spitzmesser, S. K. *Chem. Rev.* **2003**, *103*, 283-315.
4. (a) Brintzinger, H. H.; Fischer, D.; Mülhaupt, R.; Rieger, B.; Waymouth, R. M. *Angew. Chem. Int. Ed.* **1995**, *34*, 1143-1170. (b) Coates, G. W. *Chem. Rev.* **2000**, *100*, 1223-1252. (c) Resconi, L.; Cavallo, L.; Fait, A.; Piemontesi, F. *Chem. Rev.* **2000**, *100*, 1253-1346.
5. (a) Domski, G. J.; Rose, J. M.; Coates, G. W.; Bolig, A. D.; Brookhart, M. *Prog. Polym. Sci.* **2007**, *32*, 30-92. (b) Anderson-Wile, A. M.; Edson, J. B.; Coates, G. W. In *Complex Macromolecular Architectures*; John Wiley & Sons (Asia) Pte Ltd: Singapore, 2011, p 267-316.
6. Arriola, D. J.; Carnahan, E. M.; Hustad, P. D.; Kuhlman, R. L.; Wenzel, T. T. *Science* **2006**, *312*, 714-719.
7. (a) Agapie, T.; Henling, L. M.; DiPasquale, A. G.; Rheingold, A. L.; Bercaw, J. E. *Organometallics* **2008**, *27*, 6245-6256. (b) Golisz, S. R.; Bercaw, J. E. *Macromolecules* **2009**, *42*, 8751-8762.
8. Tonks, I. A.; Tofan, D.; Weintrob, E. C.; Agapie, T.; Bercaw, J. E. *Organometallics* **2012**, *31*, 1965-1974.
9. Alfa Aesar, H34478 2-Bromo-6-iodopyridine, 97%, 2013. <http://www.alfa.com/en/GP100W.pgm?DSSTK=H34478&rnd=060431362> (accessed June 25, 2013).
10. Alfa Aesar, A15397 2,6-Dibromopyridine, 98%, 2013. <http://www.alfa.com/en/GP100W.pgm?DSSTK=A15397&rnd=1911298042> (accessed June 25, 2013).
11. Alfa Aesar, H26961 2-Bromo-6-chloropyridine, 95%, 2013. <http://www.alfa.com/en/GP100W.pgm?DSSTK=H26961&rnd=664437533> (accessed June 25, 2013).
12. (a) Snégaroff, K.; Nguyen, T. T.; Marquise, N.; Halauko, Y. S.; Harford, P. J.; Roisnel, T.; Matulis, V. E.; Ivashkevich, O. A.; Chevallier, F.; Wheatley, A. E. *Chem. Eur. J.* **2011**, *17*, 13284-13297. (b) Chau, N. T. T.; Meyer, M.; Komagawa, S.; Chevallier, F.; Fort, Y.; Uchiyama, M.; Mongin, F.; Gros, P. C. *Chem. Eur. J.* **2010**, *16*, 12425-12433.
13. Zhang, H.; Tse, M. K.; Chan, K. S. *Synth. Commun.* **2001**, *31*, 1129-1139.
14. Agapie, T.; Bercaw, J. E. *Organometallics* **2007**, *26*, 2957-2959.

15. Rivas, F. M.; Riaz, U.; Giessert, A.; Smulik, J. A.; Diver, S. T. *Org. Lett.* **2001**, *3*, 2673-2676.
16. (a) Rebstock, A. S.; Mongin, F.; Trécourt, F.; Quéguiner, G. *Org. Biomol. Chem.* **2003**, *1*, 3064-3068. (b) Baudoin, O.; Guénard, D.; Guéritte, F. *J. Org. Chem.* **2000**, *65*, 9268-9271.
17. Tsukahara, T.; Swenson, D. C.; Jordan, R. F. *Organometallics* **1997**, *16*, 3303-3313.
18. (a) Xu, T.; Liu, J.; Wu, G.-P.; Lu, X.-B. *Inorg. Chem.* **2011**, *50*, 10884-10892.
19. See for example: (a) Boussie, T. R.; Diamond, G. M.; Goh, C.; Hall, K. A.; LaPointe, A. M.; Leclerc, M.; Lund, C.; Murphy, V.; Shoemaker, J. A. W.; Tracht, U.; Turner, H.; Zhang, J.; Uno, T.; Rosen, R. K.; Stevens, J. C. *J. Am. Chem. Soc.* **2003**, *125*, 4306-4317. (b) Frazier, K. A.; Froese, R. D.; He, Y.; Klosin, J.; Theriault, C. N.; Vosejka, P. C.; Zhou, Z.; Abboud, K. A. *Organometallics* **2011**, *30*, 3318-3329.
20. Passaglia, E.; Kevorkian, H. K. *J. Appl. Phys.* **1963**, *34*, 90-97.
21. For  $^{13}\text{C}$  NMR assignment of 2,1-insertions see: (a) Asakura, T.; Nishiyama, Y.; Doi, Y. *Macromolecules* **1987**, *20*, 616-620. (b) Grassi, A.; Zambelli, A.; Resconi, L.; Albizzati, E.; Mazzocchi, R. *Macromolecules* **1988**, *21*, 617-622. (c) Cheng, H. N.; Ewen, J. A. *Makromol. Chem.* **1989**, *190*, 1931-1943. (d) Asakura, T.; Nakayama, N.; Demura, M.; Asano, A. *Macromolecules* **1992**, *25*, 4876-4881. (e) Zhou, Z.; Stevens, J. C.; Klosin, J.; Kummerle, R.; Qiu, X. H.; Redwine, D.; Cong, R. J.; Taha, A.; Mason, J.; Winniford, B.; Chauvel, P.; Montanez, N. *Macromolecules* **2009**, *42*, 2291-2294.
22. Busico, V.; Cipullo, R.; Chadwick, J. C.; Modder, J. F.; Sudmeijer, O. *Macromolecules* **1994**, *27*, 7538-7543.
23. Hustad, P. D.; Tian, J.; Coates, G. W. *J. Am. Chem. Soc.* **2002**, *124*, 3614-3621.
24. Resconi has reported a zirconocene catalyst that polymerizes propylene with 2,1-insertions on the order of 3 mol%: Resconi, L.; Camurati, I.; Sudmeijer, O. *Top. Catal.* **1999**, *7*, 145-163. A Ti thio(bisphenoxy) complex has been reported by Miyatake et al. that gives a regioirregular polypropylene (the mol% of 2,1-insertions was not reported): Miyatake, T.; Mizunuma, K.; Kakugo, M. *Makromol. Chem., Macromol. Symp.* **1993**, *66*, 203-214.
25. For exemplary  $^{13}\text{C}$  NMR of polypropylene from a late-metal catalyst see: McCord, E. F.; McLain, S. J.; Nelson, L. T. J.; Arthur, S. D.; Coughlin, E. B.; Ittel, S. D.; Johnson, L. K.; Tempel, D.; Killian, C. M.; Brookhart, M. *Macromolecules* **2001**, *34*, 362-371.

26. Ewart, S. W.; Sarsfield, M. J.; Jeremic, D.; Tremblay, T. L.; Williams, E. F.; Baird, M. C. *Organometallics* **1998**, *17*, 1502-1510.
27. Würtz, S.; Lohre, C.; Fröhlich, R.; Bergander, K.; Glorius, F. *J. Am. Chem. Soc.* **2009**, *131*, 8344-8345.
28. Aluri, B. R.; Kindermann, M. K.; Jones, P. G.; Dix, I.; Heinicke, J. *Inorg. Chem.* **2008**, *47*, 6900-6912.
29. (a) Tshuva, E. Y.; Goldberg, I.; Kol, M.; Weitman, H.; Goldschmidt, Z. *Chem. Commun.* **2000**, 379-380. (b) Tshuva, E. Y.; Goldberg, I.; Kol, M.; Goldschmidt, Z. *Organometallics* **2001**, *20*, 3017-3028. (c) Tshuva, E. Y.; Groysman, S.; Goldberg, I.; Kol, M.; Goldschmidt, Z. *Organometallics* **2002**, *21*, 662-670.
30. (a) Segal, S.; Goldberg, I.; Kol, M. *Organometallics* **2005**, *24*, 200-202. (b) Yeori, A.; Goldberg, I.; Shuster, M.; Kol, M. *J. Am. Chem. Soc.* **2006**, *128*, 13062-13063.
31. Tshuva, E. Y.; Goldberg, I.; Kol, M. *J. Am. Chem. Soc.* **2000**, *122*, 10706-10707.
32. Kwong, F. Y.; Klapars, A.; Buchwald, S. L. *Org. Lett.* **2002**, *4*, 581-584.
33. Bassi, I.; Allegra, G.; Scordamaglia, R.; Chioccola, G. *J. Am. Chem. Soc.* **1971**, *93*, 3787-3788.
34. Giesbrecht, G. R.; Whitener, G. D.; Arnold, J. *Organometallics* **2000**, *19*, 2809-2812.
35. (a) Chan, M. C.; Kui, S. C.; Cole, J. M.; McIntyre, G. J.; Matsui, S.; Zhu, N.; Tam, K. H. *Chem. Eur. J.* **2006**, *12*, 2607-2619. (b) Tam, K.-H.; Lo, J. C.; Guo, Z.; Chan, M. C. *J. Organomet. Chem.* **2007**, *692*, 4750-4759. (c) Tam, K.-H.; Chan, M. C.; Kaneyoshi, H.; Makio, H.; Zhu, N. *Organometallics* **2009**, *28*, 5877-5882. (d) Liu, C.-C.; So, L.-C.; Lo, J. C.; Chan, M. C.; Kaneyoshi, H.; Makio, H. *Organometallics* **2012**, *31*, 5274-5281. (e) Lo, J. C.; Chan, M. C.; Lo, P.-K.; Lau, K.-C.; Ochiai, T.; Makio, H. *Organometallics* **2013**, *32*, 449-459.
36. Murray, M. C.; Baird, M. C. *Can. J. Chem.* **2001**, *79*, 1012-1018.
37. (a) Boussie, T. R.; Diamond, G. M.; Goh, C.; Hall, K. A.; LaPointe, A. M.; Leclerc, M. K.; Murphy, V.; Shoemaker, J. A.; Turner, H.; Rosen, R. K. *Angew. Chem. Int. Ed.* **2006**, *45*, 3278-3283. (b) Froese, R. D.; Hustad, P. D.; Kuhlman, R. L.; Wenzel, T. T. *J. Am. Chem. Soc.* **2007**, *129*, 7831-7840.
38. Hintermann, L.; Dang, T. T.; Labonne, A.; Kribber, T.; Xiao, L.; Naumov, P. *Chem. Eur. J.* **2009**, *15*, 7167-7179.
39. Diamond, G. M.; Hall, K. A.; LaPointe, A. M.; Leclerc, M. K.; Longmire, J.; Shoemaker, J. A.; Sun, P. *ACS Catalysis* **2011**, *1*, 887-900.

40. Davies, C. J.; Gregory, A.; Griffith, P.; Perkins, T.; Singh, K.; Solan, G. A. *Tetrahedron* **2008**, *64*, 9857-9864.
41. (a) Resconi, L.; Bossi, S.; Abis, L. *Macromolecules* **1990**, *23*, 4489-4491. (b) Chien, J. C. W.; Wang, B. P. *J. Polym. Sci., A: Polym. Chem.* **1988**, *26*, 3089-3102. (c) Chien, J. C. W.; Razavi, A. *J. Polym. Sci., A: Polym. Chem.* **1988**, *26*, 2369-2380. (d) Chien, J. C. W.; Wang, B. P. *J. Polym. Sci., A: Polym. Chem.* **1990**, *28*, 15-38.
42. Busico, V.; Cipullo, R.; Pellicchia, R.; Rongo, L.; Talarico, G.; Macchioni, A.; Zuccaccia, C.; Froese, R. D. J.; Hustad, P. D. *Macromolecules* **2009**, *42*, 4369-4373.
43. Pangborn, A. B.; Giardello, M. A.; Grubbs, R. H.; Rosen, R. K.; Timmers, F. J. *Organometallics* **1996**, *15*, 1518-1520.
44. Benzing, E.; Kornicker, W. *Chem. Ber.* **1961**, *94*, 2263-2267.
45. Felten, J. J.; Anderson, W. P. *J. Organomet. Chem.* **1972**, *36*, 87-92.

